

THE INTERACTION OF ELECTROMAGNETIC  
WAVES WITH SOME NATURAL SURFACES

DISSERTATION

Presented in Partial Fulfillment of the Requirements for  
the Degree Doctor of Philosophy in the Graduate  
School of The Ohio State University

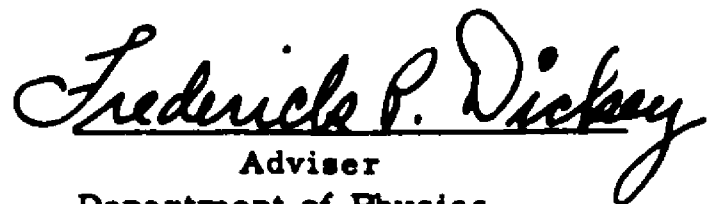
By

WILLIAM HELLER PEAKE, B.S., M.A.

\* \* \* \* \*

The Ohio State University  
1959

Approved by:



Adviser

Department of Physics  
and Astronomy

## ACKNOWLEDGEMENTS

I would like to thank my adviser, Professor Dickey, and my colleagues in the Antenna Laboratory, particularly Professor R. L. Cosgriff and Mr. R. C. Taylor, for their encouragement and advice during the past several years.

Some of the measurements of complex dielectric constant reported in Chapter II were made by Mr. Tet Pang, and some of the correlation functions were computed by Mr. Byron Potts.

A part of the work described in this dissertation was sponsored by the Air Research and Development Command, Wright Air Development Center, Wright Patterson Air Force Base, Ohio, under contracts AF 33(616)-3649 and AF 33(616)-6158.

# TABLE OF CONTENTS

	<u>Page</u>
<b>CHAPTER I - THE PROBLEM OF SCATTERING BY NON-UNIFORM SURFACES</b>	<b>1</b>
A. <u>Introduction</u>	1
B. <u>The Taxonomic Problem and the Scattering         Problem</u>	1
C. <u>The Role of Models</u>	3
D. <u>General Approach</u>	4
<b>CHAPTER II - THE SCATTERING COEFFICIENTS</b>	<b>6</b>
A. <u>Introduction</u>	6
B. <u>The Slightly Rough Surface</u>	12
C. <u>The Surface of Long, Thin Lossy Cylinders</u>	21
<b>CHAPTER III - THE BACK-SCATTERING COEFFICIENTS, WITH APPLICATIONS TO THE RADAR RETURN FROM TERRAIN</b>	<b>34</b>
A. <u>Introduction</u>	34
B. <u>Models with Undetermined Parameters</u>	34
C. <u>The Slightly Rough Surface</u>	38
D. <u>Surfaces Covered with Vegetation in the Form         of Long Thin Lossy Cylinders</u>	43
E. <u>Other Theoretical Models</u>	48
<b>CHAPTER IV - APPLICATIONS TO THE RADIOMETRIC PROPERTIES OF TERRAIN</b>	<b>62</b>
A. <u>Introduction - Kirchhoff's Law</u>	62

B. <u>Apparent Surface Temperatures</u>	68
C. <u>Point Source Effects</u>	75
D. <u>Application to the Apparent Temperature of Some Natural Surfaces</u>	77
<b>CHAPTER V - CONCLUSIONS</b>	<b>86</b>
<b>REFERENCES</b>	<b>88</b>
<b>APPENDIX I</b>	<b>93</b>
<b>APPENDIX II</b>	<b>98</b>

## LIST OF FIGURES

	<u>Page</u>
Fig. 1. Geometry of the scattering problem.	7
Fig. 2. Scattering from a slightly rough surface.	13
Fig. 3. Scattering by a cylinder.	23
Fig. 4. Back-scattering from a vegetation covered surface (15" grass in head) illustrating Eq. (51).	36
Fig. 5. Back-scattering from a vegetation covered surface (short grass) illustrating Eq. (52).	37
Fig. 6. Correlation functions for 3 asphalt surfaces.	40
Fig. 7. Correlation functions for 2 concrete surfaces.	40
Fig. 8. Effect of dielectric constant on return from a slightly rough surface (horizontal polarization).	41
Fig. 9. Effect of dielectric constant on return from a slightly rough surface (vertical polarization).	41
Fig. 10. Calculated and measured return from a slightly rough asphalt surface (vertical polarization).	50
Fig. 11. Calculated and measured return from a slightly rough asphalt surface (horizontal polarization).	50
Fig. 12. Calculated and measured return from a slightly rough asphalt surface (vertical polarization).	51
Fig. 13. Calculated and measured return from a slightly rough asphalt surface (horizontal polarization).	51
Fig. 14. Calculated and measured return from a slightly rough asphalt surface (vertical polarization).	52
Fig. 15. Calculated and measured return from a slightly rough asphalt surface (horizontal polarization).	52

Fig. 16.	Calculated and measured return from a slightly rough concrete surface (vertical polarization).	53
Fig. 17.	Calculated and measured return from a slightly rough concrete surface (horizontal polarization).	53
Fig. 18.	Calculated and measured return from a slightly rough concrete surface (vertical polarization).	54
Fig. 19.	Calculated and measured return from a slightly rough concrete surface (horizontal polarization).	54
Fig. 20.	Calculated and measured return from vegetation at 8.6 mm wavelength. Dependence on water content.	55
Fig. 21.	Calculated and measured return from vegetation at 3 cm wavelength. Dependence on water content.	55
Fig. 22.	Calculated and measured return from vegetation at 8.6 mm wavelength. Dependence on water content.	56
Fig. 23.	Calculated and measured return from vegetation at 3 cm wavelength. Dependence on water content.	56
Fig. 24.	Calculated and measured return from vegetation at 8.6 mm wavelength. Dependence on AN.	57
Fig. 25.	Calculated and measured return from vegetation at 3 cm wavelength. Dependence on AN.	57
Fig. 26.	Calculated and measured return from vegetation at 8.6 mm wavelength. Dependence on AN.	58
Fig. 27.	Calculated and measured return from vegetation at 3 cm wavelength. Dependence on AN.	58
Fig. 28.	Calculated return from vegetation at $K_a$ -band. Ratio of return for vertical polarization to return for horizontal polarization for two values of water content and various densities of vegetation.	59

Fig. 29.	Calculated return from vegetation at X-band. Ratio of return for vertical polarization to return for horizontal polarization for two values of water content and various densities of vegetation.	60
Fig. 30.	Calculated and measured wavelength dependence of the return from vegetation, at $45^{\circ}$ incidence angle.	61
Fig. 31.	Geometry for derivation of Kirchhoff's law.	64
Fig. 32.	Contributions to the apparent temperature of a surface.	70
Fig. 33.	Measured and calculated apparent temperature of an asphalt surface.	79
Fig. 34.	The functions $F_1(r)$ and $F_2(r)$ vs $r$ .	82
Fig. 35.	Measured and calculated apparent temperature of a vegetation covered surface.	84
Fig. 36.	Measured and calculated apparent temperature of a vegetation covered surface.	84
Fig. 37.	Measured and calculated apparent temperature of a vegetation covered surface.	85
Fig. 38.	Geometry for reciprocity theorem.	99

## CHAPTER I

### THE PROBLEM OF SCATTERING BY NON-UNIFORM SURFACES

#### A. Introduction

One of the major unsolved problems of electromagnetic theory is that of the interaction of electromagnetic radiation with non-uniform surfaces, particularly those natural surfaces that constitute the surface of the earth. Apart from its intrinsic interest, a general solution of this problem would have many applications, both scientific and technical. A complete solution for all frequencies and classes of surface is out of the question at the present time. However, there exist certain general relations between the properties of the surface and those of the radiation in interaction with it. There are also certain restricted wavelength intervals and classes of surface for which detailed solutions of the scattering problem may be obtained. It is the purpose of this study to derive some of these general relations, and to carry out the detailed solution for two special surfaces of practical interest in the microwave region.

#### B. The Taxonomic Problem and the Scattering Problem

There are two major difficulties that face the investigator of such problems. The first is that of solving the electromagnetic scattering problem for any particular, properly specified non-uniform surface. Unfortunately, present theories of scattering from



irregular surfaces are not sufficiently well developed to permit an exact solution of the scattering problem except in a few special cases. Thus approximate solutions must be used.

The second, and in some respects the more difficult, problem is that of describing the surfaces of interest, or at least of classifying them into categories that are significant for the scattering problem. These categories may be chosen intuitively, on the basis of the appearance of the surface; experimentally, on the basis of the observed characteristics of the interaction of the surface with radiation; or on theoretical grounds, on the basis of the kind of model used to represent the surface when formulating the scattering problem. It is clear that in any useful taxonomy, all three approaches should lead to the same grouping or association of terrains.

A good idea of the rather primitive state of the classification problem as it applies to the interaction of light waves with natural surfaces may be had from Penndorf's review<sup>1</sup> of Krinov's reflectivity data.<sup>2</sup> At microwave frequencies, the situation is similar.<sup>15</sup> Indeed even the relatively simple problem of describing the surface of the sea is only now,<sup>3</sup> after several decades of intensive research, approaching a state that is suitable for the solution of scattering problems.

### C. The Role of Models

As a consequence of these two difficulties, it has been customary to approach the problem of calculating the interaction of electromagnetic radiation with such surfaces by the use of models. That is, use has been made of idealized surfaces which are more or less amenable to theoretical treatment, and more or less representative of the category of natural surface under consideration. Not all surfaces can be represented in this way at the present time, but for those which can, the specification of a few basic parameters of the surface (which may be chosen on the basis of theoretical convenience or experimental evidence) will allow one to estimate the interaction of the surface with radiation.

In the past, most surface models have fallen into one of two classes, depending on which of these two principal difficulties their authors have wished to confront. In the first group<sup>4, 5, 6</sup> the models have been chosen so as to avoid the difficulties of the scattering problem, by representing the surface with assemblies of objects of known scattering properties (spheres, point scatterers, facets, etc.). The number, size, etc., of these scatterers have provided the parameters of the models, to be fitted by recourse to experiment. Insofar as it has been the aim of such models to predict the statistical properties of the scattered radiation, and to provide empirical formulas

for its angular dependence, they have been quite successful. However, it is often rather difficult to relate the parameters of the model to directly observable properties of the surface.

The second group of models<sup>7-16</sup> have been aimed at providing detailed solutions of certain well defined scattering problems, usually of the boundary-value type, and are often of great theoretical interest. However, the lack of any real resemblance between the model surface and those encountered in practice have made it difficult to apply them directly.

#### D. General Approach

In contrast to such models, an effort has been made here to develop "complete" models which, while simple enough to permit the scattering problem to be solved with reasonable accuracy, still bear a close resemblance to the actual surface under consideration. Thus the parameters of the model, and consequently the characteristics of the scattered radiation, may be calculated from the surface properties alone. Conversely, once a model has been validated by scattering measurements, its parameters may be used to classify the surface in a rational and quantitative way.

In the next chapter (Chapter II) the scattering coefficients are defined for a general surface. The relation between them and several parameters of particular interest (the back-scattering coefficient,

the absorption coefficient, the albedo) are derived. The scattering coefficients for two "complete" model surfaces are then worked out in detail. One of the models is applicable to slightly rough, continuous surfaces, and the other to surfaces covered with vegetation in the form of long, thin lossy cylinders. In Chapter III the results are applied to the interpretation of the radar return from terrain (back-scattering).

In Chapter IV, the reciprocity properties of the scattering coefficients are used to derive Kirchhoff's radiation law in a form which takes account of the angular dependence of the emitted radiation, and the polarization properties of the surface. The results are then applied to the interpretation of measurements of the apparent temperatures of some natural surfaces.

## CHAPTER II

### THE SCATTERING COEFFICIENTS

#### A. Introduction

An analysis of the interaction of electromagnetic waves with natural surfaces may most conveniently be carried out in terms of the differential scattering coefficients of the surface. It is the purpose of this chapter to derive these coefficients for two particular surface models. Before doing so, it is necessary to define them. Although many different definitions have been used in the past (differing chiefly in the manner in which normalization with respect to surface area and solid angle was carried out) the coefficient to be used here is a generalization of one frequently used in radar-return work.<sup>17</sup> Consider an infinite surface, forming, on the average, a plane, although over small regions it may have any complexity of structure (see Fig. 1). If radiation of intensity  $I_0$  (watts/meter<sup>2</sup>) falls at an angle of incidence  $\theta_0$  and azimuth  $\phi_0$  on a given element of surface area  $S$ , and the intensity of the scattered radiation in the direction  $\theta_s \phi_s$  at a distance  $R$  from  $S$  is  $I_s$ , then the scattering parameter  $\gamma(\theta_0 \phi_0; \theta_s \phi_s)$  is defined by the equation

$$(1) \quad I_0 \gamma(\theta_0 \phi_0; \theta_s \phi_s) S \cos \theta_0 = 4\pi R^2 I_s$$

or

$$(2) \quad \gamma(\theta_0\phi_0; \theta_s\phi_s) = (4\pi R^2 I_s) / (I_0 S \cos \theta_0) .$$

In this second expression, the numerator is the total power which would be scattered by  $S$  if it scattered isotropically into  $4\pi$  steradians with the same intensity as it does in the scattering direction; the denominator is the power incident on  $S$ ; and  $\gamma$  is their ratio.

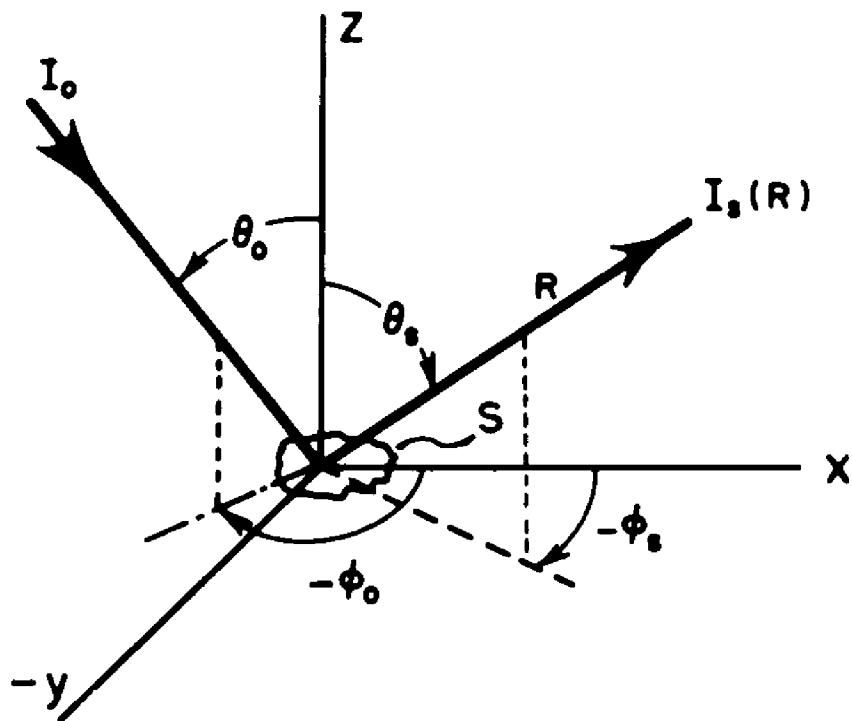


Fig. 1. Geometry of the scattering problem.

For the types of random surface of interest, it will be assumed that  $I_s$  is proportional to  $S$ , and inversely proportional to  $R^2$  at sufficiently large distances from  $S$ ; under these conditions  $\gamma$  becomes independent of  $R$  and  $S$ , and is a characteristic of the surface. It is clear that  $S$ , and thus the projected area of the

illuminating beam of radiation, must be much larger than any significant structural features of the surface if  $\gamma$  is also to be independent of the particular area at which the illumination is directed.

It is clear that for the general surface,  $\gamma$  should refer to, and is a function of, the specific state of polarization of both the incident and the scattered radiation. Any two orthogonal polarization states may be used for this purpose. In this study, the conventions and terminology of engineering usage have been chosen, although they are somewhat ambiguous. These polarization states are indicated via the notation:

	<u>Incident Wave</u>	<u>Scattered Wave</u>
$\gamma_{vv}$	Vertically Polarized	Vertically Polarized
$\gamma_{hh}$	Horizontally Polarized	Horizontally Polarized
$\gamma_{vh}$	Vertically Polarized	Horizontally Polarized
$\gamma_{hv}$	Horizontally Polarized	Vertically Polarized

The words "vertically polarized" refer to a wave with its electric vector in the plane of incidence (parallel polarization); the words "horizontally polarized" refer to a wave with its electric vector in the plane of the surface (perpendicular polarization).

There are certain general relationships between these four scattering coefficients that are consequences of the electromagnetic reciprocity theorem.<sup>20, 21</sup> For example, consider first the situation

in which the incident radiation is horizontally polarized, comes from the direction  $\theta_0\phi_0$ , has intensity  $I_0$  at the surface, and has a horizontal component of scattered intensity  $I_s$  in the direction  $\theta_s\phi_s$  at distance  $R$  from  $S$ . Then, from Eq. (2),

$$(3) \quad \cos \theta_0 \gamma_{hh}(\theta_0\phi_0; \theta_s\phi_s) = 4\pi R^2 I_s / (S I_0) .$$

Next consider the reverse situation in which horizontally polarized radiation is incident from the direction  $\theta_s\phi_s$ , has intensity  $I_0$  at the surface, and produces scattered radiation with horizontal component of scattered intensity  $I'_s$  in the direction  $\theta_0\phi_0$  at distance  $R$  from  $S$ . Then from Eq. (2),

$$(4) \quad \cos \theta_s \gamma_{hh}(\theta_s\phi_s; \theta_0\phi_0) = 4\pi R^2 I'_s / (S I_0) .$$

Now, from the reciprocity theorem,  $I_s = I'_s$ .<sup>\*</sup> Thus, from (3) and

(4) one obtains

$$(5a) \quad \cos \theta_0 \gamma_{hh}(\theta_0\phi_0; \theta_s\phi_s) = \cos \theta_s \gamma_{hh}(\theta_s\phi_s; \theta_0\phi_0) .$$

Similarly, for the other polarization states,

$$(5b) \quad \cos \theta_0 \gamma_{hv}(\theta_0\phi_0; \theta_s\phi_s) = \cos \theta_s \gamma_{vh}(\theta_s\phi_s; \theta_0\phi_0)$$

$$(5c) \quad \cos \theta_0 \gamma_{vh}(\theta_0\phi_0; \theta_s\phi_s) = \cos \theta_s \gamma_{hv}(\theta_s\phi_s; \theta_0\phi_0)$$

$$(5d) \quad \cos \theta_0 \gamma_{vv}(\theta_0\phi_0; \theta_s\phi_s) = \cos \theta_s \gamma_{vv}(\theta_s\phi_s; \theta_0\phi_0) .$$

---

<sup>\*</sup>See Appendix II.



In what follows, the coefficients will often be written in the form  $\gamma(o, s)$  or  $\gamma(s, o)$ . Here  $(o)$  refers to the direction  $\theta_o \phi_o$  and  $(s)$  refers to the direction  $\theta_s \phi_s$ ; the first letter or pair of angles within the brackets refers to the direction from which the radiation is incident, and the second letter or pair of angles refers to the direction into which the radiation is scattered.

It is often convenient to account for specular reflection (as from a plane surface or a grating), by introducing  $\gamma$ 's with the properties of delta-functions. This representation may easily be obtained by integrating Eq. (1) over scattering angles in the vicinity of the specular beam,

$$\frac{I_o \cos \theta_o S}{4\pi} \int \gamma(o, s) d\Omega_s = \int R^2 I_s d\Omega_s$$

where  $d\Omega_s$  is the element of solid angle. Now the right hand side represents the total power in the specularly reflected beam, which may be written as  $\rho(o, s) I_o S \cos \theta_o$ , where  $\rho(o, s)$ , the reflection coefficient, is just the fraction of power in the incident beam that appears in the specularly reflected beam. Thus if  $\gamma(o, s)$  has the form of a constant multiplied by  $\delta(\theta_s - \theta_{sp}) \delta(\phi_s - \phi_{sp})$ , where  $\theta_{sp}$ ,  $\phi_{sp}$  define the specular direction, then

$$(6) \quad \gamma(o, s) = \frac{4\pi \rho(o, s)}{\sin \theta_{sp}} \delta(\theta_s - \theta_{sp}) \delta(\phi_s - \phi_{sp}) .$$

Appropriate subscripts must be supplied for the four polarization states.

As an example of the use of this representation, one may consider a perfectly flat surface, where  $\theta_{sp} = \theta_0$  and  $\phi_{sp} = \phi_0 + \pi$ . The reflection coefficients are  $\rho_{hh} = |R_h|^2$ ;  $\rho_{vv} = |R_v|^2$ ;  $\rho_{vh} = \rho_{hv} = 0$ ; here  $R_h$  and  $R_v$  are the Fresnel coefficients (see Eq. (80)).

To conclude this section, certain commonly used parameters will be expressed in terms of the  $\gamma$ 's. The first, the "radar cross-section per unit area of terrain", designated in the literature<sup>21</sup> by  $\sigma_0$ , is found from

$$\sigma_0(\theta_0) = \cos \theta_0 \gamma(\theta_0 \phi_0; \theta_0 \phi_0)$$

and may refer to any of the four polarization combinations.

The albedo of a surface usually refers to the fraction of incident radiation of random polarization rescattered by the surface for a band of frequencies in the optical region. Here the albedo  $A$  is defined as the fraction of the power incident on the surface from the direction  $\theta_0 \phi_0$  (at a specific polarization and frequency) that is rescattered. With this definition the albedo is

$$A(\theta_0, \phi_0) = \int \frac{I_s R^2 d\Omega_s}{S I_0 \cos \theta_0}$$

so that, from Eq. (1), taking account of the polarization properties of the surface, the albedo  $A_v(\theta_o\phi_o)$  for vertically polarized incident radiation is

$$(7a) \quad A_v(\theta_o\phi_o) = (4\pi)^{-1} \int [\gamma_{vv}(o, s) + \gamma_{vh}(o, s)] d\Omega_s.$$

There is a corresponding expression for horizontally polarized incident radiation

$$(7b) \quad A_h(\theta_o\phi_o) = (4\pi)^{-1} \int [\gamma_{hh}(o, s) + \gamma_{hv}(o, s)] d\Omega_s.$$

Another surface parameter of interest is the absorption coefficient ( $a$ ), defined here as the fraction of power (of a given polarization and frequency) incident on the surface from the direction  $\theta_o\phi_o$  that is absorbed by the surface. Clearly, for the types of surfaces considered here, which are assumed to be thick enough so that no energy is transmitted through the body they define, the absorption coefficient is just unity minus the albedo,

$$(8a) \quad a_h(\theta_o\phi_o) = 1 - A_h(\theta_o\phi_o)$$

$$(8b) \quad a_v(\theta_o\phi_o) = 1 - A_v(\theta_o\phi_o) .$$

## B. The Slightly Rough Surface

The first surface model for which the scattering coefficients will be calculated in detail is one that may be called the "slightly

rough surface." This is a practically plane surface in which the slope is everywhere much less than unity, and for which the maximum height above the mean plane surface is much less than a wavelength. The surface may be described formally by giving its elevation  $z = f(xy)$  at every point in the  $x$ - $y$  plane (see Fig. 2).

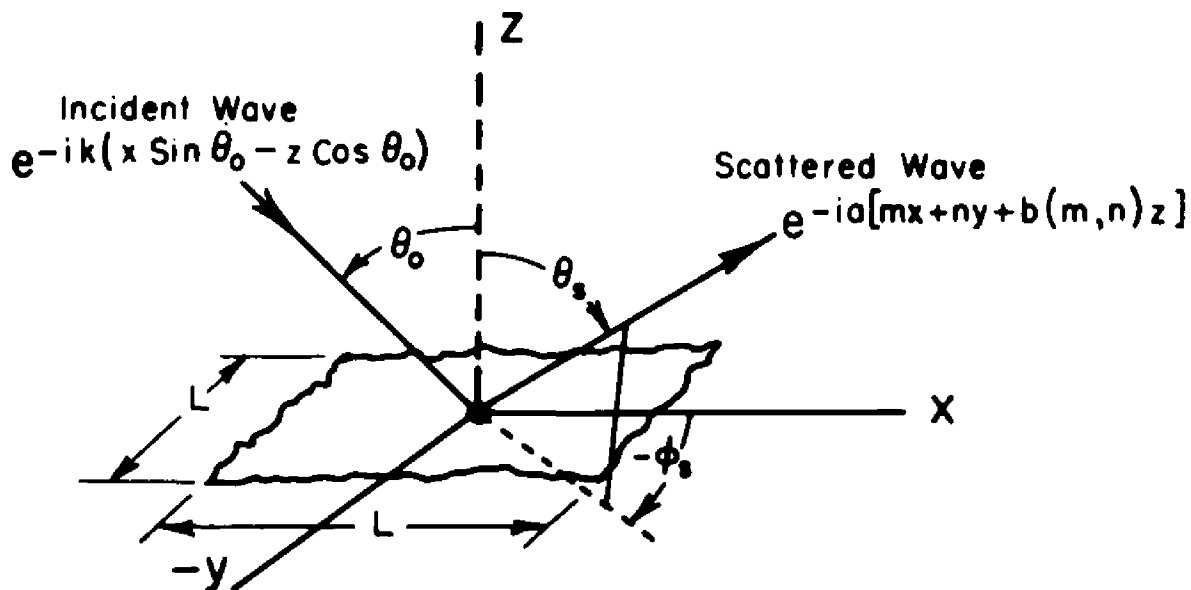


Fig. 2. Scattering from a slightly rough surface.

Now if attention is confined to a large square of side  $L$ , the altitude may be expanded in a Fourier series

$$(9) \quad z = f(x, y) = \sum_{-\infty}^{\infty} \sum_{-\infty}^{\infty} P(m, n) \exp[-ia(mx+ny)] ,$$

$$a = 2\pi/L \quad m, n \text{ integers}$$

where, because  $f$  is real,  $P(m, n) = P^*(-m, -n)$ . The interest here is not in regular surfaces of a periodic type,<sup>12</sup> but rather in randomly rough surfaces; the Fourier decomposition permits a straightforward

definition of what is meant by randomness. According to S. O. Rice,<sup>16</sup> the surface is considered a random one if an average, designated by  $\langle \rangle$ , over an infinite set of such elements of side  $L$  leads to the following properties of the coefficients;

$$(10) \quad \langle P(m, n) \rangle = 0$$

which implies the randomness of the individual coefficients;

$$(11) \quad \langle P(m, n) P^*(m, n) \rangle = (\pi/L)^2 W(p, q)$$

$$p = 2\pi m/L \quad q = 2\pi n/L$$

which implies that the average exists, and defines the spectral density function  $W(p, q)$  for the surface; and finally

$$(12) \quad \langle P(m, n) P(u, v) \rangle = 0 \quad m \neq -u \quad n \neq -v,$$

which implies the independence of the individual coefficients. It is also convenient to define the mean square surface roughness,

$$(13) \quad \overline{z^2} \equiv \langle f^2(x, y) \rangle$$

it being assumed that the mean surface elevation is zero, i. e.,

$\langle f(x, y) \rangle = 0$ . The correlation function  $\rho(\xi, \eta)$  for the surface is

defined by

$$(14) \quad \overline{z^2} \rho(\xi, \eta) = \langle f(x+\xi, y+\eta) f(x, y) \rangle,$$

i. e.,  $\rho(0, 0) = 1$ . The functions  $\overline{z^2} \rho(\xi, \eta)$  and  $W(p, q)$  are the Fourier transforms of each other.

The scattering from such a surface is calculated by a perturbation method introduced by Rayleigh,<sup>18</sup> and extended to the electromagnetic case in detail by S. O. Rice<sup>16</sup> and others.<sup>15</sup> It is based upon an expansion of the scattered field into a series of plane waves  $E(m, n; z) e^{i\omega t}$ , where, in the notation of Rice, which will be followed as far as possible in what follows,

$$(15) \quad \begin{aligned} E(m, n; z) &= \exp[-ia(mx+ny) -ib(m, n)z] \\ b(m, n) &= \begin{cases} [K^2 - a^2m^2 - a^2n^2]^{\frac{1}{2}} & m^2+n^2 < K^2/a^2 \\ -i[a^2m^2 + a^2n^2 - K^2]^{\frac{1}{2}} & m^2+n^2 > K^2/a^2 \end{cases} \end{aligned}$$

In the simplest case, in which the surface is a perfect conductor, and the incident wave is horizontally polarized, the total electric fields in the region above the surface may be written

$$(16) \quad \begin{aligned} E_x &= \sum_{-\infty}^{\infty} A_{mn} E(m, n; z) \\ E_y &= 2i \sin(Kz \cos \theta_0) \exp(-iKx \sin \theta_0) + \sum B_{mn} E(m, n; z) \\ E_z &= \sum C_{mn} E(m, n; z) \end{aligned}$$

where the first term in  $E_y$  is just the sum of the incident and specularly reflected waves for a perfectly flat surface, and  $A_{mn}$ ,  $B_{mn}$ ,  $C_{mn}$  are the amplitudes of the scattered waves (relative to an incident wave of unit amplitude). The horizontal component of the

scattered field  $E_h^s$  in the direction specified by the integers  $m, n$ , is then

$$(17) \quad E_h^s(m, n) = (-A_{mn} \sin \phi_s + B_{mn} \cos \phi_s) E(m, n; z);$$

the corresponding vertical component of the scattered field is

$$(18) \quad E_v^s(m, n) = (-A_{mn} \cos \theta_s \cos \phi_s - B_{mn} \cos \theta_s \sin \phi_s + C_{mn} \sin \theta_s) E(m, n; z) .$$

To evaluate the scattering cross-sections for the surface it is convenient to average over a small range of solid angles. By comparing equivalent expressions for a plane wave specified by the integers  $(m, n)$  or the scattering angles  $(\theta_s, \phi_s)$ , one finds that  $am = K \sin \theta_s \cos \phi_s$ ;  $an = K \sin \theta_s \sin \phi_s$ . Consequently the differential unit of solid angle may be found by evaluating the Jacobian of the transformation, to give

$$(19) \quad d\Omega_s = \sin \theta_s d\theta_s d\phi_s = \left[ \cos \theta_s \right]^{-1} d(am/K) d(an/K),$$

where the differentials  $d(am/K)$  are small in the limit  $L \rightarrow \infty$ . Thus the power  $P^s$  scattered by the surface per unit solid angle in the direction  $\theta_s, \phi_s$  is, for horizontal polarization,

$$(20) \quad P_h^s = \frac{z_0}{2} |E_h^s(m, n)|^2 \frac{\Delta m \Delta n}{d\Omega_s} L^2 \cos \theta_s \\ = \frac{z_0}{2} (K/a)^2 \cos^2 \theta_s |-A_{mn} \sin \phi_s + B_{mn} \cos \phi_s|^2 L^2$$

where  $z_0$  is the impedance of free space and where the summation of the  $A_{mn}$  and  $B_{mn}$  over a small range  $\Delta m \Delta n$  of  $m$  and  $n$  has been approximated by their mean values multiplied by the intervals. Keeping in mind the definition of  $\gamma$  and  $P_h^s$ , and the fact that the incident wave had unit field strength, (or intensity  $z_0/2$ ), one finds

$$(21) \quad Y_{hh}(0, s) = \frac{4\pi P_h^s}{(z_0/2) \cos \theta_0 L^2}$$

or

$$(22) \quad Y_{hh}(\theta_0, 0; \theta_s \phi_s) = 4\pi \left( \frac{\cos^2 \theta_s}{\cos \theta_0} \right) (K/a)^2 |B_{mn} \cos \phi_s - A_{mn} \sin \phi_s|^2$$

and similarly

$$(23) \quad Y_{hv}(\theta_0, 0; \theta_s \phi_s) = 4\pi \left( \frac{\cos^2 \theta_s}{\cos \theta_0} \right) (K/a)^2 \left| \begin{array}{l} -A_{mn} \cos \theta_s \cos \phi_s \\ -B_{mn} \cos \theta_s \sin \phi_s \\ +C_{mn} \sin \theta_s \end{array} \right|^2$$

where, of course, the values of  $m$  and  $n$  are those appropriate to the scattering direction  $\theta_s \phi_s$ .

Now for surfaces such that  $|f| \ll \lambda$  and  $|\partial f/\partial x|; |\partial f/\partial y| \ll 1$ , i.e., for surfaces which have everywhere an elevation much less than a wavelength, and a slope much less than unity, one can obtain the coefficients  $A_{mn} B_{mn} C_{mn}$  by a perturbation calculation. For a surface of arbitrary conductivity and dielectric constant, and for a horizontally polarized incident wave, the coefficients have been worked out by Rice.<sup>16</sup> To the first order in  $(f/\lambda)$  they are given by



$$\begin{aligned}
 A_{mn} &= 2iU(a^2 mn) P(m-\nu, n) (Dd)^{-1} \\
 (24) \quad B_{mn} &= 2iU(-a^2 m^2 - bc) P(m-\nu, n) (Dd)^{-1} \\
 C_{mn} &= 2iU(anc) P(m-\nu, n) (Dd)^{-1}
 \end{aligned}$$

where

$$\begin{aligned}
 U &= (\sigma^2 - \tau^2) \left[ 1 + (\tau \cos \theta'_0) (\sigma \cos \theta_0)^{-1} \right]^{-1} \\
 a\nu &= K \sin \theta_0
 \end{aligned}$$

$$K = 2\pi/\lambda$$

$\lambda$  = free space wavelength

$$\sigma = iK$$

$$\tau = \sigma(\epsilon_1 - i\epsilon_2)^{\frac{1}{2}}$$

$\epsilon_1$  = relative dielectric constant of surface material

$$\epsilon_2 = g/(\omega\epsilon_0)$$

$g$  = conductivity of surface material

$\epsilon_0$  = permittivity of free space

$$\cos \theta'_0 = \left[ 1 - (\sigma/\tau)^2 \sin^2 \theta_0 \right]^{\frac{1}{2}}$$

$$d = b + c$$

$$ib = \left[ \sigma^2 + a^2(m^2 + n^2) \right]^{\frac{1}{2}}$$

$$ic = \left[ \tau^2 + a^2(m^2 + n^2) \right]^{\frac{1}{2}}$$

$$D = a^2 m^2 + a^2 n^2 + bc$$

and the  $P(m-\nu, n)$  are to be found from Eq. (9). When all the algebraic reductions are carried out, one finds that for a slightly rough surface with arbitrary complex dielectric constant  $\epsilon' = \epsilon_1 - i\epsilon_2$ , the

scattering parameters for horizontal incidence are given by

$$Y_{hh}(\theta_0, 0; \theta_s, \phi_s) = \frac{4}{\pi} \overline{z^2} K^4 \cos \theta_0 \cos^2 \theta_s T_{hh} I \quad (25)$$

$$Y_{hv}(\theta_0, 0; \theta_s, \phi_s) = \frac{4}{\pi} \overline{z^2} K^4 \cos \theta_0 \cos^2 \theta_s T_{hv} I$$

where

$$T_{hh} = \left| \frac{(\epsilon' - 1) \cos \phi_s}{\left[ \cos \theta_0 + \sqrt{\epsilon' - \sin^2 \theta_0} \right] \left[ \cos \theta_s + \sqrt{\epsilon' - \sin^2 \theta_s} \right]} \right|^2$$

$$T_{hv} = \left| \frac{-\sin \phi_s \sqrt{\epsilon' - \sin^2 \theta_s} (\epsilon' - 1)}{\left[ \cos \theta_0 + \sqrt{\epsilon' - \sin^2 \theta_0} \right] \left[ \epsilon' \cos \theta_s + \sqrt{\epsilon' - \sin^2 \theta_s} \right]} \right|^2$$

$$I = \int_{-\infty}^{\infty} \int_{-\infty}^{\infty} e^{ig(\xi, \eta)} \rho(\xi, \eta) d\xi d\eta$$

$$g(\xi, \eta) = K\xi (\sin \theta_s \cos \phi_s - \sin \theta_0) + K\eta \sin \theta_s \sin \phi_s .$$

In deriving the expression I, use was made of the fact that the correlation function  $\overline{z^2} \rho(\xi, \eta)$  is the Fourier transform of the power spectral density  $W(p, q)$  for the surface.

The corresponding results for vertically polarized incident radiation may be found in an entirely similar way by utilizing the corresponding coefficients (ABC) for that case. Since these were not given by Rice, they are worked out in the Appendix. They lead to the formulas

$$Y_{vv}(\theta_0, 0; \theta_s, \phi_s) = \frac{4}{\pi} \overline{z^2} K^4 \cos \theta_0 \cos^2 \theta_s T_{vv} I$$

(26)

$$Y_{vh}(\theta_0, 0; \theta_s, \phi_s) = \frac{4}{\pi} \overline{z^2} K^4 \cos \theta_0 \cos^2 \theta_s T_{vh} I$$

where

$$T_{vv} = \left| \frac{(\epsilon' - 1) [\epsilon' \sin \theta_0 \sin \theta_s - \cos \phi_s \sqrt{\epsilon' - \sin^2 \theta_0} \sqrt{\epsilon' - \sin^2 \theta_s}]}{[\epsilon' \cos \theta_0 + \sqrt{\epsilon' - \sin^2 \theta_0}] [\epsilon' \cos \theta_s + \sqrt{\epsilon' - \sin^2 \theta_s}]} \right|^2$$

$$T_{vh} = \left| \frac{-(\epsilon' - 1) \sin \phi_s \sqrt{\epsilon' - \sin^2 \theta_0}}{[\epsilon' \cos \theta_0 + \sqrt{\epsilon' - \sin^2 \theta_0}] [\cos \theta_s + \sqrt{\epsilon' - \sin^2 \theta_s}]} \right|^2 .$$

If the surface is isotropic, i. e., if the correlation function  $\rho(\xi, \eta)$  has the property  $\rho(\xi, \eta) = \rho(\sqrt{\xi^2 + \eta^2})$ , then one may introduce polar coordinates

$$\xi = r \cos \psi \quad \eta = r \sin \psi$$

and, by integrating over the polar angle, obtain

$$(27) \quad I = 2\pi \int_0^{\infty} r \rho(r) J_0 \left[ Kr (\sin^2 \theta_0 + \sin^2 \theta_s - 2 \sin \theta_0 \sin \theta_s \cos \phi_s)^{\frac{1}{2}} \right] dr.$$

The scattering coefficients have an interesting property. They show that in the approximation to which they are correct, the scattering from a slightly rough surface is the product of two factors, one of which (I) involves only the surface structure, but is independent of the material. The other ( $T_{hh}$  etc.) depends on the complex dielectric constant but is independent of the structure of the surface.

The results obtained above will be used in Chapter III to calculate the back scattering of microwaves from asphalt and concrete surfaces. It may be of interest to note here these results can also be used to calculate the "diffusion" of light waves by very highly polished glass or metal surfaces. Maréchal<sup>38</sup> has shown, in a much less detailed calculation, that the total diffuse scattering from such a surface is proportional to the mean square surface roughness ( $\overline{z^2}$ ), as is also obviously predicted by Eqs. (26) and (27). These equations should also predict the dependence of the "diffused" light on polarization, dielectric constant, scattering and incidence angles, etc.

### C. The Surface of Long, Thin Lossy Cylinders

The second surface model for which the scattering coefficients will be calculated in detail is one which, it is hoped, can represent terrain surfaces covered with vegetation in the form of long, thin lossy cylinders. It is assumed that the cylinders are placed at random over the surface, and are far enough apart (a few wavelengths, see Reference 35) so that the single scattering approximation may be used. However, in order to account for the attenuation of the incident radiation as it penetrates the scattering layer, it is supposed that the incident field is equal to the free space field multiplied by an exponential attenuation factor. The reason for this

assumption is to bring the single scattering approximation into at least qualitative agreement with the physical facts of the situation. It is clear that the incident wave must be attenuated as it penetrates a surface of infinitely long, lossy cylinders. The single scattering approximation (in the strict sense, where the incident field is taken equal to the free space field in the absence of scatterers), entirely fails to account for this attenuation. Moreover, the scattered radiation in that approximation is a function of the length of the cylinders, which is also unreasonable physically.

The assumption of an exponentially attenuated incident wave is equivalent to assigning an imaginary part to the propagation constant, that is to say, it is an approximation in the same spirit as the conventional "multiple scattering" approximation.<sup>19, 35</sup> The latter also assigns to the medium an effective propagation constant which may be calculated in terms of the number of particles per unit volume of the medium and the forward scattering amplitude. The relation between the two approximations is discussed at the end of this chapter.

The scattering from a single cylinder, due to the incident field just described, will first be calculated. The cylinder is taken with one end, its upper end, at the origin of coordinates (see Fig. 3), and with its axis specified by the unit vector  $\vec{n}$  and the angles  $\theta, \phi$ .

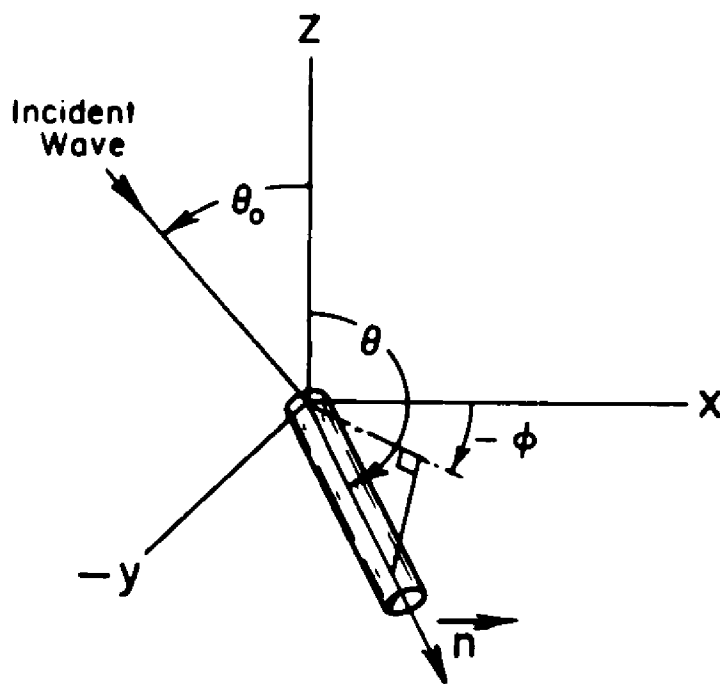


Fig. 3. Scattering by a cylinder.

It is supposed that the cylinder extends downwards from the plane  $z = 0$ , i. e.,  $\pi/2 < \theta < \pi$ . The assumed incident fields for vertical and horizontal polarization are then

$$(28a) \quad \vec{E}_h^i = -\vec{j} E_0 \psi$$

$$(28b) \quad \vec{E}_v^i = (\vec{i} \cos \theta_0 + \vec{k} \sin \theta_0) E_0 \psi$$

$$(28c) \quad \psi = \exp \left[ -iK(x \sin \theta_0 - z \cos \theta_0) + \alpha z \right] \quad z < 0$$

where  $\vec{i}$   $\vec{j}$   $\vec{k}$  are unit vectors along the three coordinate axes;  $E_0$  is the amplitude of the incident field at the plane  $z = 0$ ; and  $\alpha$  is the assumed attenuation rate of the incident field strength. Now if  $\vec{E}_t$ ,  $\vec{H}_t$  are the total electric and magnetic fields in the presence of the

scatterer,  $\vec{E}^i, \vec{H}^i$  are the assumed incident fields in the absence of the scatterer, and  $\vec{E}_s, \vec{H}_s$  are the scattered fields, defined by

$$\vec{E}_s = \vec{E}_t - \vec{E}^i$$

$$\vec{H}_s = \vec{H}_t - \vec{H}^i$$

then, within the scatterer

$$\nabla \times \vec{H}_t = (g + i\omega\epsilon_0\epsilon_1) \vec{E}_t$$

where  $g$  and  $\epsilon_1$  are the conductivity and relative dielectric constant of the cylinder material.

The incident field satisfies

$$\nabla \times \vec{H}^i = i\omega\epsilon_0 \vec{E}^i .$$

Subtracting, it is found that the scattered field satisfies

$$(29) \quad \nabla \times \vec{H}_s = i\omega\epsilon_0 \vec{E}_s + [g + i\omega\epsilon_0(\epsilon_1 - 1)] \vec{E}_t .$$

Thus the scattered field is generated by the effective current density

$$(30) \quad \vec{J}_s = [g + i\omega\epsilon_0(\epsilon_1 - 1)] \vec{E}_t = i\omega\epsilon_0(\epsilon' - 1) \vec{E}_t .$$

It is still necessary to calculate  $E_t$ , which will only be done approximately. For this purpose, the incident field is resolved into two parts, one parallel to the cylinder axis and the other perpendicular

to it. It is assumed that for a scatterer much less than a wavelength in diameter, the parallel component of the electric field inside is equal to the parallel component of the incident field (continuity of tangential electric field). The perpendicular component of the electric field within the scatterer is taken equal to  $(t)$  times the perpendicular component of the incident field (static approximation). For a non-conducting dielectric circular cylinder, for example,  $t = 2 / (1 + \epsilon_1)$ . However for cylinders of arbitrary cross-section and conductivity,  $t$  is a tensor function of the angle between the perpendicular component of the incident field and some axis which specifies the orientation of the cylinder cross-section. For example, if the cylinder were of elliptical cross-section, both the magnitude and the direction of the internal field are functions of the angle between the external field and the major axis of the ellipse. Thus, strictly speaking,  $t$  has a simple interpretation only for circular cylinders; in the general case it may be regarded as a parameter having some effective value. With these assumptions, the total field within the cylinder is

$$\vec{E}_t = (\vec{E}^i \cdot \vec{n})\vec{n} + t[\vec{E}^i - (\vec{E}^i \cdot \vec{n})\vec{n}]$$

(31)

$$\vec{n} = \vec{i} \sin \theta \cos \phi + \vec{j} \sin \theta \sin \phi + \vec{k} \cos \theta$$

from which the current may be found by using Eq. (30). The



scattered fields due to such a current distribution may be found by standard methods (Reference 20, p. 89) to be, at a great distance  $R$  from the scatterer,

$$\mathbf{E}_v^s = \frac{-i\omega\mu}{4\pi R} e^{-iKR} \int (\vec{J}_s \cdot \vec{i}_{\theta_s}) e^{iK\vec{\rho} \cdot \vec{R}_1} dV \quad (32)$$

$$\mathbf{E}_h^s = \frac{-i\omega\mu}{4\pi R} e^{-iKR} \int (\vec{J}_s \cdot \vec{i}_{\phi_s}) e^{iK\vec{\rho} \cdot \vec{R}_1} dV$$

where  $\mu$  is the permeability of free space,  $\vec{\rho}$  is the vector which specifies the position of  $dV$ ,  $\vec{R}_1$  is a unit vector in the scattering direction

$$(33) \quad \vec{R}_1 = \vec{i} \sin \theta_s \cos \phi_s + \vec{j} \sin \theta_s \sin \phi_s + \vec{k} \cos \theta_s$$

and  $\vec{i}_{\phi_s}$ ,  $\vec{i}_{\theta_s}$  are unit vectors in the "horizontal" and "vertical" polarization directions, respectively:

$$(34) \quad \vec{i}_{\theta_s} = -\vec{i} \cos \theta_s \cos \phi_s - \vec{j} \cos \theta_s \sin \phi_s + \vec{k} \sin \theta_s$$

$$(35) \quad \vec{i}_{\phi_s} = -\vec{i} \sin \phi_s + \vec{j} \cos \phi_s .$$

For a thin cylinder of cross-sectional area  $A$ , the integration over the cylinder volume may be replaced by an integration over a length coordinate  $s$  along the cylinder, with  $dV \triangleq A ds$  and  $\vec{\rho} \triangleq s\vec{n}$ . With this final approximation the integrals of Eq. (32) may be evaluated. To save space only the case where both incident and scattered fields are horizontally polarized will be carried out in detail. When

Eqs. (28a), (28c), (30), (31), (33) and (35) are substituted into Eq. (32b), the expression for the scattered field becomes

$$(36) \quad E_{hh}^s = \frac{E_0 A K^2 (\epsilon' - 1)}{4\pi R} e^{-iKR} \left[ t \cos \phi_s + (1-t) \sin^2 \theta \sin \phi \sin(\phi - \phi_s) \right] \cdot \int_0^\infty e^{SM} ds$$

where

$$M = \alpha \cos \theta - iK(\sin \theta \sin \theta_0 \cos \phi - \cos \theta \cos \theta_0) + iK(\sin \theta \sin \theta_s \cos(\phi - \phi_s) + \cos \theta \cos \theta_s) .$$

The integral is just  $M^{-1} \exp(SM)$  which has the value  $M^{-1}$  at the lower limit and the value zero at the upper limit, since  $\cos \theta$  is always negative and  $\alpha$  is positive. Thus

$$(37) \quad \left| \frac{E_{hh}^s}{E_0} \right|^2 = \frac{A^2 K^4 |\epsilon' - 1|^2}{(4\pi R)^2 |M|^2} \left[ (1-t) \sin^2 \theta \sin \phi \sin(\phi_s - \phi) + t \cos \phi_s \right]^2 .$$

It is now necessary to average over the distribution of cylinder orientations to obtain the average power scattered by a single cylinder. It will be assumed that the cylinder axes are oriented at random. However, the probability that the axis of a given cylinder lies in the element of solid angle  $d\Omega$  in the direction  $\vec{n}$ , will be assumed to be proportional to  $\cos^2 \theta d\Omega$ . Thus the average value (designated by  $\overline{(\quad)}$ ) of any function  $F$  of  $\theta, \phi$  will be defined by

$$(38) \quad \overline{F(\theta, \phi)} = \frac{\int F(\theta, \phi) \cos^2 \theta d\Omega}{\int \cos^2 \theta d\Omega} .$$

This choice of averaging function maintains symmetry about the vertical axis, gives a slight preference to the vertical direction, and makes certain integrals easier to evaluate. Nevertheless it has not been possible to carry out the average of Eq. (37) correctly. Instead the numerator and denominator have been averaged separately, and their ratio taken, i.e., it has been assumed that the following equation

$$(39) \quad \frac{\left[ t \cos \phi_s + (1-t) \sin^2 \theta \sin \phi \sin(\phi - \phi_s) \right]^2}{|M|^2} = \frac{\left[ t \cos \phi_s + (1-t) \sin^2 \theta \sin \phi \sin(\phi - \phi_s) \right]^2}{|M|^2}$$

is true at least approximately. If there are  $N$  cylinders per unit area of surface then the scattering coefficients, from Eq. (1), are given by

$$(40) \quad \gamma = 4\pi R^2 N \sec \theta_0 \left| \tilde{E}^s / E_0 \right|^2.$$

Substituting (38) into (40) and making use of (39), the coefficients are

$$(41a) \quad \gamma_{hh}(0, s) = B \left[ (3 - 2 \sin^2 \phi_s) + t(8 - 10 \sin^2 \phi_s) + t^2(24 - 23 \sin^2 \phi_s) \right]$$

$$(41b) \quad \gamma_{hv}(0, s) = B \left[ (1 + 2 \sin^2 \theta_s + 2 \cos^2 \theta_s \sin^2 \phi_s) \right. \\ \left. + t(-2 - 4 \sin^2 \theta_s + 10 \cos^2 \theta_s \sin^2 \phi_s) \right. \\ \left. + t^2(1 + 2 \sin^2 \theta_s + 23 \cos^2 \theta_s \sin^2 \phi_s) \right]$$

$$(41c) \quad Y_{vh}(o, s) = B \left[ (1 + 2 \sin^2 \theta_o + 2 \cos^2 \theta_o \sin^2 \phi_s) \right. \\ \left. + t(-2 - 4 \sin^2 \theta_o + 10 \cos^2 \theta_o \sin^2 \phi_s) \right. \\ \left. + t^2 (1 + 2 \sin^2 \theta_o + 23 \cos^2 \theta_o \sin^2 \phi_s) \right]$$

$$(41d) \quad Y_{vv}(o, s) = B \left[ (1-t)^2 (3 - 2 \cos^2 \theta_s \cos^2 \theta_o \sin^2 \phi_s) \right. \\ \left. + (\sin \theta_s \sin \theta_o - \cos \theta_s \cos \theta_o \cos \phi_s) Q \right]$$

where

$$(42) \quad B = \frac{(AN)(AK^2) \left[ (\epsilon_1 - 1)^2 + \epsilon_2^2 \right]}{28\pi \cos \theta_o \left[ 3/5(\alpha/K)^2 + 3(\cos \theta_o + \cos \theta_s)^2 \right. \\ \left. + (\sin^2 \theta_o + \sin^2 \theta_s - 2 \sin \theta_o \sin \theta_s \cos \phi_s) \right]}$$

$$Q = 12(1-t)^2 \sin \theta_s \sin \theta_o + 14t(1-t) (3 \sin \theta_o \sin \theta_s - \cos \theta_o \cos \theta_s \cos \phi_s) \\ + 35t^2 (\sin \theta_o \sin \theta_s - \cos \theta_o \cos \theta_s \cos \phi_s) .$$

The attenuation factor may, together with  $t$ , be regarded as parameters of the theory. However, that part of the attenuation due to absorption (i.e., due to the imaginary component  $i\epsilon_2$  of the dielectric constant of the cylinders) may be calculated from the model. To do so, one may start with an expression for the average power per unit volume dissipated in the cylinder material,

$$(43) \quad \frac{dP}{dV} = (g/2) \vec{E}_t \cdot \vec{E}_t^*$$

Thus the total power  $dP$  absorbed in a vertical increment  $dz$ , or volume  $A(\cos \theta)^{-1} dz$  of the cylinder material, is

$$(44) \quad dP = \frac{dP}{dV} A dz (\cos \theta)^{-1} .$$

But the average incident power  $P$  at that level associated with a single cylinder is just the power density in the incident beam multiplied by the effective area  $N^{-1} \cos \theta_0$ ,

$$(45) \quad P = (z_0/2) \vec{E}_i \cdot \vec{E}_i^* (N^{-1} \cos \theta_0) .$$

Thus, averaging over the cylinder distribution and recalling that  $\alpha$  was defined as the attenuation rate for the field strength, there results

$$(46) \quad 2\alpha = \frac{1}{P} \frac{dP}{dz} = (g/z_0) \left( \frac{AN}{\cos \theta_0} \right) \left( \frac{\overline{E_t \cdot E_t^*}}{E_i \cdot E_i^* \cos \theta} \right) .$$

Upon carrying out the average according to (38), this gives

$$(47a) \quad \alpha_h/K = (3/16) AN\epsilon_2 \sec \theta_0 (1 + 3t^2) ,$$

for horizontally polarized incident radiation, and

$$(47b) \quad \alpha_v/K = (3/16) AN\epsilon_2 \sec \theta_0 \left[ (1+3t^2) + \sin^2 \theta_0 (1-t^2) \right]$$

for vertically polarized incident radiation.

Because the preceding calculations have the appearance of a typical single-scattering approximation, it might be supposed that one could dispense with the empirical attenuation factor  $\alpha$ , and calculate an effective propagation constant for the "medium" of the scatterers using standard methods.<sup>37</sup> This is not the case, because

of the hypothesis, supported (at certain frequencies) by experimental evidence to be given in Chapter III D, that the incident radiation is essentially extinguished in a depth much less than the length of the cylinders. The consequence is that only  $N$ , the number of cylinders per unit area of surface, has any significance for the model, whereas the standard calculation expresses the propagation constant in terms of the number of particles per unit volume. However, by comparing the results of the standard calculation with the one just given, a value may be inferred for the effective number of cylinders per unit volume, by considering the cylinders to be broken up into effective lengths which act independently. Not surprisingly, this effective length turns out to be of the same magnitude as  $1/\alpha$ , the penetration depth. To show this formally, suppose that the incident wave is not the expression (28) containing  $(\alpha)$ , but rather

$$(48) \quad \psi_0 = \exp[-iK_m(x \sin \theta_0 - z \cos \theta_0)]$$

where  $K_m$  is the desired (complex) propagation constant for the medium. If this is substituted into Eq. (35) and the forward scattering ( $\phi_s = 0$ ;  $\theta_s = \pi - \theta_0$ ) evaluated, one gets

$$\frac{E_{hh}^s(\theta_0, \pi; \pi - \theta_0, 0)}{E_0} = \frac{(\epsilon' - 1) AK^2 e^{-iKR}}{4\pi R(K_m - K)(\cos \theta \cos \theta_0 - \sin \theta \sin \theta_0 \cos \phi)}$$

where it is assumed that radiation takes place into free space. The average over cylinder orientations must now be carried out according to Eq. (38). For the simplest case of normal incidence this leads to the following value for  $\overline{S(\theta)}$ , the average forward scattering amplitude

$$\begin{aligned} \overline{S(\theta)} &\cong iKR e^{iKR} \left( \frac{E_{hh}^s}{E_0} \right) \\ &= \frac{3}{8} (1+3t) \left[ \frac{iAK^3(\epsilon'-1)}{4\pi(K_m-K)} \right] . \end{aligned}$$

From the forward scattering theorem (Reference 37, p. 33) one has, formally,

$$K_m/K = 1 - 2\pi n K^{-3} \overline{S(\theta)}$$

where  $n$  is the number of scatterers per unit volume. Thus, combining the last two equations,

$$(49) \quad (K_m - K)^2 = \frac{3}{16} nAK(\epsilon'-1)(1+3t) \theta_0 = 0 .$$

Now  $K_m$  may be written in the form  $K_m = K + \Delta K - iK_2$ , where  $\Delta K$  is the correction to the real part of the propagation constant (i.e.,  $1 + (\Delta K/K)$  is the refractive index) and  $K_2$  is the imaginary part of  $K_m$ .

To compare this result with Eq. (47) it is necessary to choose the parameters so that the assumptions of each derivation are

satisfied. The forward scattering method required  $|K_m - K| \ll K$ ; the calculation involving  $\alpha$ , which ignored the contribution of scattering to the extinction of the incident radiation, should be valid if  $\alpha/K \ll 1$  and  $\epsilon_2 \gg \epsilon_1 - 1$ . Under these conditions, (49) has the solution

$$\Delta K = K_2 = \left[ \frac{3}{32} n A K \epsilon_2 (1 + 3t) \right]^{\frac{1}{2}} \quad \begin{array}{l} \epsilon_2 \gg \epsilon_1 - 1 \\ \theta_0 = 0 \end{array}$$

whereas from (47),

$$\alpha/K = \frac{3}{8} A N \epsilon_2 (1 + 3t) .$$

By comparing the expressions (28) and (48) for the incident wave, it is clear that at normal incidence one should have  $\alpha = K_2$ , which requires that

$$n = 2NK_2 .$$

The effective length of the cylinders is thus  $(1/2K_2)$ , as might have been expected.



CHAPTER III  
THE BACK-SCATTERING COEFFICIENTS, WITH APPLICATIONS  
TO THE RADAR RETURN FROM TERRAIN

A. Introduction

The simplest special case of the formulas derived in the preceding chapter is that of back-scattering. Since this corresponds to predicting the radar return from terrain, some recently published experimental data<sup>17</sup> will allow a check on the formulas just derived. That is, it will permit one to determine whether the models are adequate to represent the more complex surfaces encountered in practice. To conform to engineering notation, in this section only the angle between the incoming propagation vector and the plane of the surface, called the "grazing angle" or "incidence angle," will be designated by  $\theta$ . Thus  $\theta + \theta_0 = \pi/2$ . The back scattering coefficient  $\gamma(\theta_0\phi_0; \theta_0\phi_0)$  will be designated simply by  $\gamma$ .

B. Models with Undetermined Parameters

Before discussing the models just mentioned, it may be of interest to describe briefly some of the more useful models with undetermined parameters, since these have often been used in radar design. In his study of radar ground return,<sup>4, 21</sup> R. E. Clapp proposed three simple models with which airborne measurements might be compared. His first model corresponded to a surface obeying

Lambert's law

$$(50) \quad \gamma = c \sin \theta \quad \sigma_0 = c \sin^2 \theta$$

where  $c$  is an undetermined parameter. Although such a law may have a certain validity at optical wavelengths, it was rejected by Clapp on the grounds that it did not fit his measurements, and that no easily visualized mechanism could account for scattered radiation that was independent of the direction of the incident radiation.

Clapp's second model was composed of a single layer of spheres,  $N$  per unit area, each with a scattering cross-section  $A_K$ , giving

$$(51) \quad \gamma = NA_K \operatorname{cosec} \theta; \quad \sigma_0 = NA_K .$$

Clapp rejected this model also, partly because he considered a single layer of spheres to be a poor representation of a three dimensional surface. However, the model might apply to certain types of vegetation, such as a field of oats in head, where the heads of grain represent essentially a single layer of rather large scatterers. An example of measured back-scattering in agreement with this model is given in Fig. 4. Here, and throughout this section, the ordinate, labelled " $\gamma$  in db", represents  $10 \log \gamma$ , and the experimental measurements of  $\gamma$  are due to R. C. Taylor.<sup>17</sup> The calculated curve in Fig. 4 is from Eq. (51) with the parameter  $(NA_K)$  chosen arbitrarily.

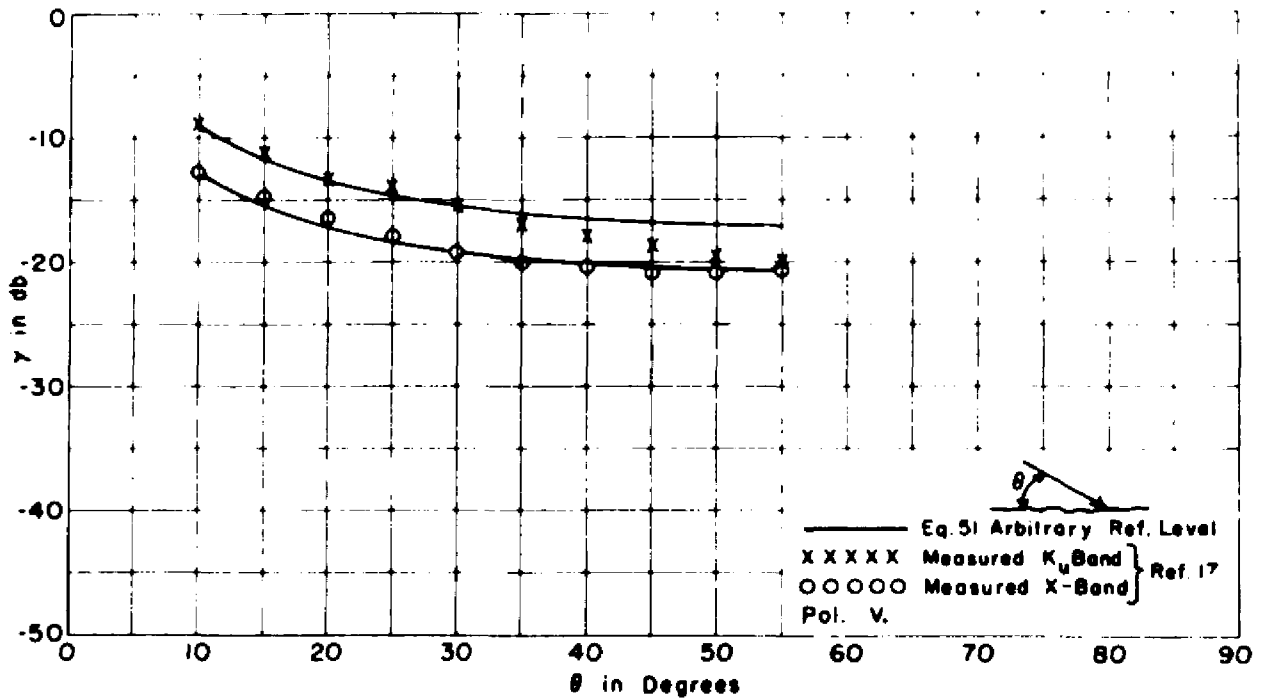


Fig. 4. Back scattering from a vegetation covered surface (15" grass in head) illustrating Eq. (51).

In the third model proposed by Clapp, the terrain surface was represented by many layers of spheres, each of which absorbed a fraction  $(1-\delta)$  of the energy falling on it, and reradiated the rest isotropically. Then

$$(52) \quad \gamma = \delta \quad \sigma_0 = \delta \sin \theta .$$

This model was in good agreement with Clapp's measurements and with many subsequent measurements of the radar return from vegetation covered surfaces. An excellent illustration of data fitted by this model may be found in Fig. 5. Here the experimental data follow almost exactly the horizontal straight line predicted by

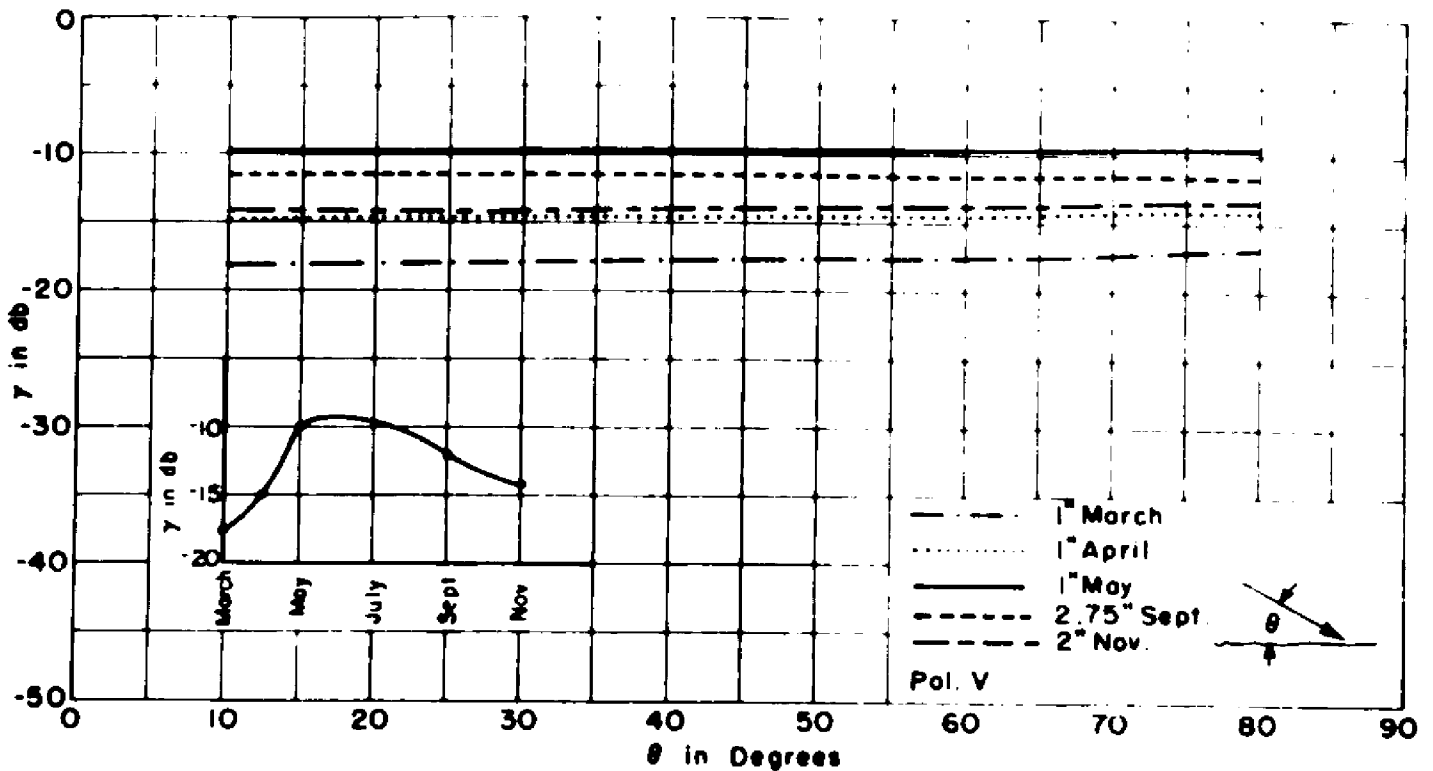


Fig. 5. Back scattering from a vegetation covered surface (short grass) illustrating Eq. (52).

Eq. (52). In connection with this model it may be mentioned that a paper by W.S. Ament<sup>8</sup> has sometimes been quoted as showing that no physical surface can have  $\sigma_0 = \delta \sin \theta$ , as predicted by Eq. (52). Insofar as Ament's proofs are correct, however, they show only that a surface cannot reradiate uniformly in all directions, and cannot have  $\gamma \rightarrow \text{constant}$  as  $\theta \rightarrow 0$ ; in no case do the proofs apply to the practical terrain return problem.

A somewhat more elaborate terrain model, which represents the terrain by arrays of facets, has been proposed by Katz and Spetner.<sup>5</sup> It has been used by its authors to fit data taken with airborne radars.

### C. The Slightly Rough Surface

The radar return from slightly rough surfaces, such as might be represented in practice by asphalt or concrete roadways, can be calculated from the results of Chapter IID. For back scattering, Eqs. (26) and (28) become

$$(53) \quad \gamma = 8 \sin^3 \theta T \overline{z^2} K^4 \int_0^{\infty} \rho(r) J_0(2Kr \cos \theta) r dr$$

where, for incident and back-scattered radiation both horizontally polarized,

$$(54a) \quad T_h = \left| \frac{\epsilon_1 - i\epsilon_2 - 1}{\left[ \sin \theta + (\epsilon_1 - i\epsilon_2 - \cos^2 \theta)^{\frac{1}{2}} \right]^2} \right|^2$$

and for incident and back-scattered radiation both vertically polarized,

$$(54b) \quad T_v = \left| \frac{(\epsilon_1 - i\epsilon_2 - 1) \left[ (\epsilon_1 - i\epsilon_2)(1 + \cos^2 \theta) - \cos^2 \theta \right]}{\left[ (\epsilon_1 - i\epsilon_2) \sin \theta + (\epsilon_1 - i\epsilon_2 - \cos^2 \theta)^{\frac{1}{2}} \right]^2} \right|^2 .$$

In order to compare the predictions of these equations with the measurements of Taylor<sup>17</sup> on a series of asphalt and concrete surfaces, it is necessary to know  $\overline{z^2}$ ,  $\rho(r)$ ,  $\epsilon_1$  and  $\epsilon_2$ . The parameters  $\overline{z^2}$  and  $\rho(r)$  were estimated by making a plaster cast of a representative area of each surface. These casts were then sliced into sections to expose typical surface profiles. The surface height was measured every 0.25 mm (in some cases every 0.1 mm) along the

profile using a comparator. A linear correction term was applied to the raw data to ensure zero average height and zero average slope, and the mean square roughness and correlation function computed by conventional methods. The results are shown in Figures 6 and 7, each point representing an average of some five or six sections of a given plaster-cast. Similar results for runway surfaces have been given in References 22 and 23.

It was not possible to measure the complex dielectric constant of these surface materials directly. Instead, representative samples of asphalt and concrete from other sources were measured using standard waveguide methods,<sup>24</sup> and were found to have the following values of complex dielectric constant:

- $\epsilon_1 - i\epsilon_2 = 6.5 - i1.5$  Concrete X-band ( $\lambda = 3.0$  cm)
- 5.5 - i0.5 Concrete K<sub>a</sub>-band ( $\lambda = 0.86$  cm)
- 4.3 - i0.1 Asphalt X-band
- 2.5 - i0.6 Asphalt K<sub>a</sub>-band.

No great significance should be placed on these values, since the measurements are not only rather inaccurate (especially for the asphalt surface) but the true value of  $\epsilon'$  depends on the state, composition, etc., of the particular sample.

The contributions of  $T_v$  and  $T_h$  to the overall return have been calculated for these particular dielectric constants and are shown in Figs. 8 and 9.

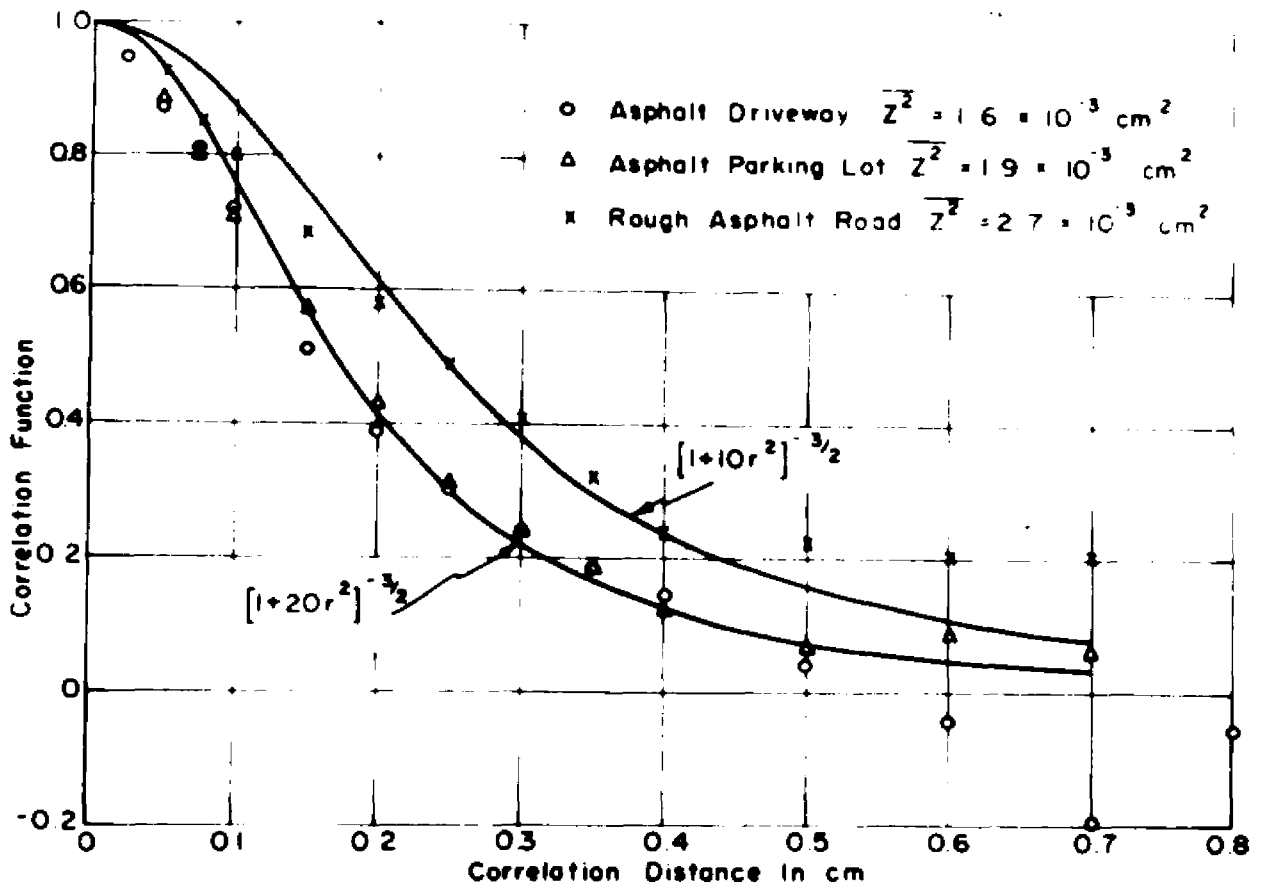


Fig. 6. Correlation functions for 3 asphalt surfaces.

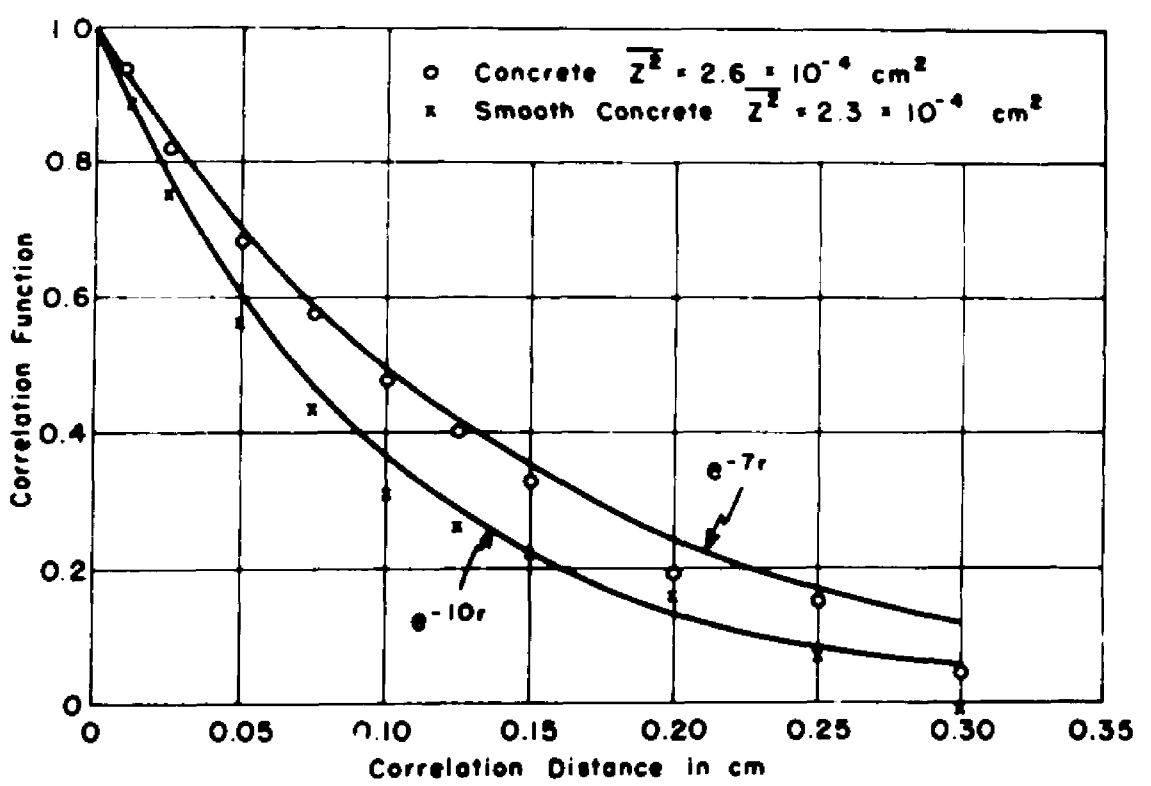


Fig. 7. Correlation functions for 2 concrete surfaces.

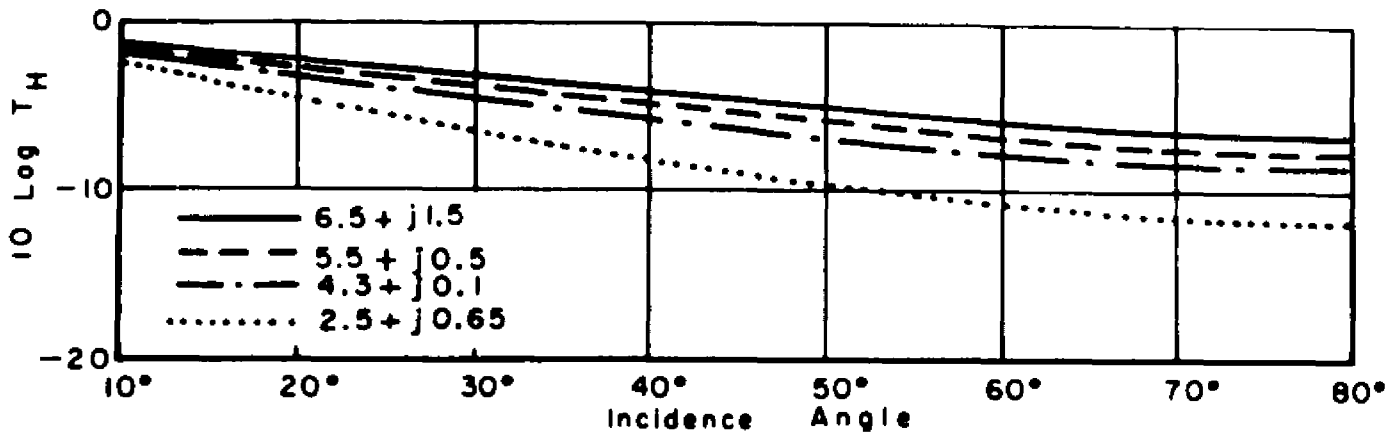


Fig. 8. Effect of dielectric constant on return from a slightly rough surface (horizontal polarization).

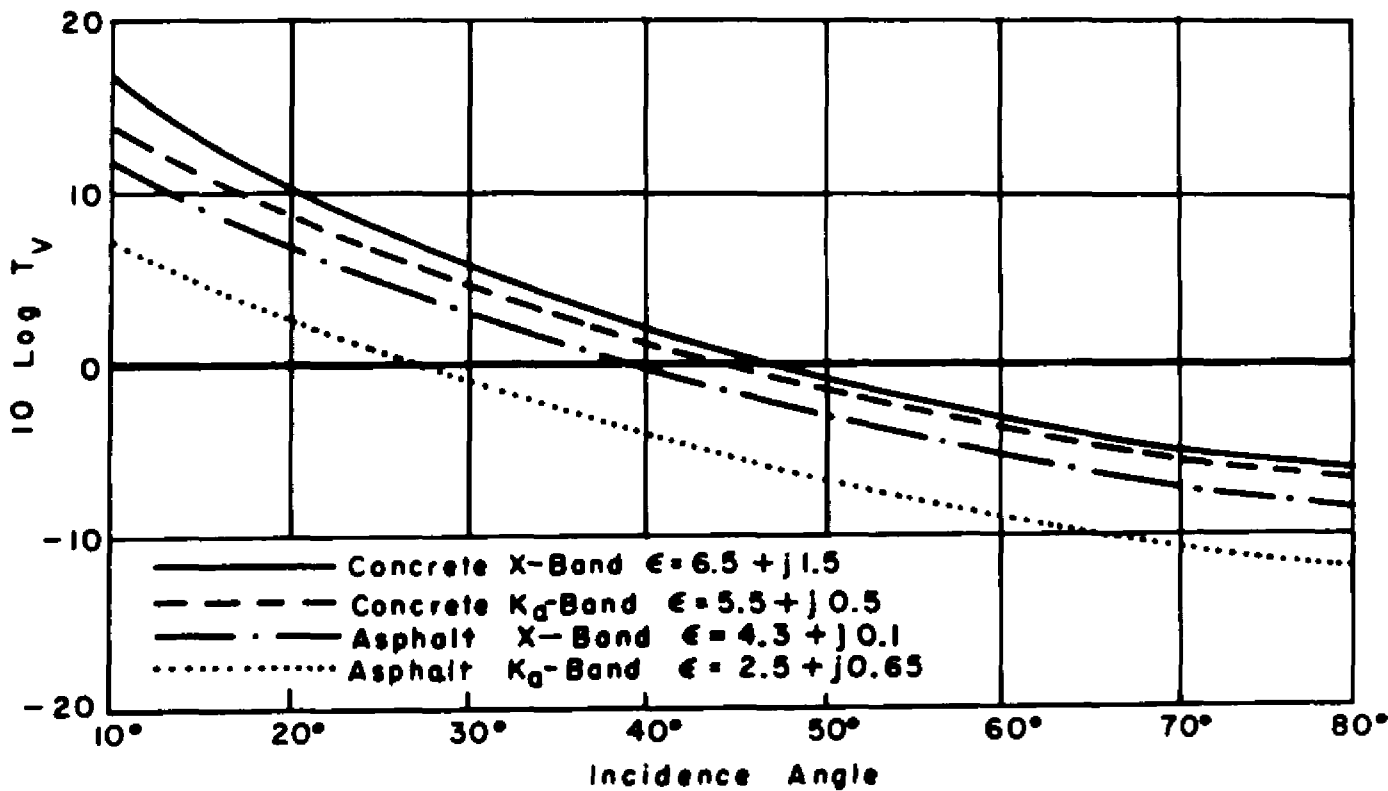


Fig. 9. Effect of dielectric constant on return from a slightly rough surface (vertical polarization).



The extent to which the perturbation theory, as given by Eq. (53), can actually predict the back-scattering from real terrain surfaces may be judged from Figs. 10 to 19. In these figures the ordinate is  $10 \log Y$  and the abscissa is incidence angle. In each case the measured points are due to Taylor,<sup>17</sup> and the calculated curves are based on the measured surface properties only. It is clear from these figures that the dependence of the back-scattered power on surface roughness, polarization, frequency and angle of incidence are very well represented by the theory. The differences between the measured and calculated return are due partly to the failure of the surface to satisfy the theoretical assumptions (e.g., slopes of order unity, inhomogeneous dielectric) and partly to the crudeness of the estimates of dielectric constants and correlation functions. In particular, the fact that the correlation functions were calculated only for correlation distances of less than a few millimeters, means that the tail of the actual correlation function may be considerably different from the assumed curves of Figs. 6 and 7. The calculated return is most sensitive to the shape of the tail at the longer wavelengths and at incidence angles towards normal. Since the discrepancy between theory and measurement is greatest under just these conditions, it is probable that more accurate values for  $\rho(r)$  would give better agreement. Nevertheless,

it is felt that for all practical purposes, the model may be used to calculate the return from such surfaces to within a few db. Conversely, the success of the model implies that an accurate prediction of the return from such surfaces requires specification of the surface roughness, correlation function, and complex dielectric constant.

**D. Surfaces Covered with Vegetation in the form of Long Thin Lossy Cylinders**

For surfaces covered with certain types of vegetation, such as grass, flags, etc., for which it may be assumed that the individual blades or stems scatter like long thin lossy cylinders distributed at random over the surface, the scattered return signal may be found from Eqs. (41). For back scattering, these reduce to

$$(55a) \quad \gamma_{hh} = \frac{A^2 NK^2 [(\epsilon_1 - 1)^2 + \epsilon_2^2] [3 + 8t + 16t^2]}{28\pi \sin \theta [3(\alpha_h / K)^2 + 4(1 + 2 \sin^2 \theta)]} ,$$

$$(55b) \quad \gamma_{vv} = \frac{A^2 NK^2 [(\epsilon_1 - 1)^2 + \epsilon_2^2] [3 + 8t + 16t^2 + \cos^2 \theta (12 + 4t - 16t^2)]}{28\pi \sin \theta [3(\alpha_v / K)^2 + 4(1 + 2 \sin^2 \theta)]} ,$$

$$(55c) \quad \gamma_x = \frac{A^2 NK^2 [(\epsilon_1 - 1)^2 + \epsilon_2^2] (1-t)^2 (1 + 2 \cos^2 \theta)}{28\pi \sin \theta [3(\alpha / K)^2 + 4(1 + 2 \sin^2 \theta)]} ,$$

$$(56a) \quad \alpha_h / K = (3/16) AN \epsilon_2 \operatorname{cosec} \theta (1 + 3t^2) ,$$

$$(56b) \quad \alpha_v / K = (3/16) AN \epsilon_2 \operatorname{cosec} \theta [1 + 3t^2 + \cos^2 \theta (1 - t^2)]$$

where  $\gamma_x$  is the cross polarized return ( $\gamma_{hv}$  or  $\gamma_{vh}$ ). The value of  $\alpha$  appropriate for the incident radiation must be used.

In deriving the above formulas, it was assumed that the cylinder axes were distributed according to Eq. (38). This slight preference for the vertical direction is not necessarily characteristic of actual vegetation. Thus the angular dependence, and more especially the polarization dependence, of the calculated return may not represent the measured dependence in all respects. Nevertheless, it is felt that this model may be used to explain some of the more prominent features of the radar return from certain types of vegetation covered surfaces.

The justification for using this particular model may be found in certain data taken by Taylor<sup>17</sup> which show that the return from grass, at  $K_a$ -band, is significantly greater than the return from the bare ground beneath. At the same time, the return is essentially independent of the length of the grass (after a certain minimum of vegetation cover has appeared). These two observations suggest that the incident radiation must be almost completely extinguished before reaching the ground underlying the vegetation. Thus the major assumption of the model of Chapter II C is satisfied (at least at  $K_a$ -band; the evidence at X-band is not so clear cut). Furthermore, Fig. 5 shows that there is also a marked seasonal dependence

of the return, with a large increase in the spring despite the fact that constant mowing kept the grass at essentially constant depth. This suggests that the water content and the number of blades per unit area may have a decided influence on the return, since both these parameters are known to increase during the spring growth, and to diminish slowly during the later summer, fall and winter. In order to determine whether, in fact, Eqs. (55) and (56) can account for the return from grass covered surfaces, it is only necessary to determine the parameters  $A$ ,  $N$ ,  $\epsilon_1$ ,  $\epsilon_2$  for the surfaces in question. It has not been possible to do this in detail, especially since some of the measurements were made before the theory was developed. However, some rough measurements for the ordinary lawn grass under consideration show that  $A \simeq 10^{-2} \text{ cm}^2$  and that the product  $AN$  lies in the range  $0.10 > AN > 0.01$ . The complex dielectric constant of a grass blade might also be measured, for example by cavity methods.<sup>26</sup> For the qualitative use of Eqs. (55) and (56), however, the effective dielectric constant of the blades, and its relation to their water content, has been estimated by the following procedure. It is assumed that for vegetation with a water content of  $100f$  % by weight, the dielectric constant is given by

$$(57) \quad \epsilon_1 - i\epsilon_2 = 2.5(1-f) + f\epsilon_w$$

where the first term is supposed to represent the contribution of the solid matter, and  $\epsilon_w$  is the dielectric constant of water, given by the usual relaxation formula<sup>24</sup>

$$(58) \quad \epsilon_w = 5 + \frac{75}{1 + i(1.85/\lambda)} ; (\lambda \text{ in cm}).$$

Such an estimate is admittedly rather crude, especially since it is known<sup>25, 26</sup> that absorbed or chemically bound water may not satisfy Eq. (58). Nevertheless, it is believed that the use of Eq. (58) will serve to illustrate the effect of season, frequency, etc., on the return. For this purpose, Figs. 20 to 27 have been prepared, based on Eqs. (55) to (58), with  $A = 1.3 \times 10^{-2} \text{ cm}^2$ , and the other parameters as specified on each figure. The value of  $t$  has been taken as  $2/(1 + \epsilon_1)$ . In each case, representative measurements by Taylor are included for comparison. Figures 20 to 23 show the effect of increasing the moisture content from 30%, representative of dried grass, to 90%, representative of very moist green grass.<sup>31</sup> It may be seen from these figures that such a change of moisture content is adequate to account for the observed seasonal dependence of the return. The general level of the return is also accounted for at both wavelengths (X- and  $K_a$ -bands) although the details of the angular dependence are not. Figures 24-27 show the dependence of the return on the parameter AN. Here the general level of the

observed return corresponds to choosing  $AN \approx 0.03$ , which is in reasonable agreement with the observed value of the parameter for grass covered surfaces. Figures 28 and 29 show the calculated polarization dependence of the return for several values of  $AN$  and  $f$ , together with some of Taylor's measurements. The measured polarization dependence is not always in good agreement with the predictions of the model, due partly to the fact that the calculated results are somewhat sensitive to the assumed choice of distribution for the orientation of the cylinder axes. However, the tendency for the drier and sparser vegetation to exhibit a greater vertically polarized return as the angle of incidence moves away from the normal is reproduced by the model. Finally, Fig. 30 shows the measured frequency dependence of a wide variety of vegetation surfaces, together with the predictions of the model just described. The line labelled "Dielectric Constant Independent of Wavelength" shows what would be obtained if the wavelength dependence of the dielectric constant were ignored. It is clear from this figure that the wavelength dependence of the dielectric constant, even though it may not be exactly as given in Eq. (58), must still play an important role in determining the overall wavelength dependence of the return.

The cross-polarized return from such surfaces has been reported by Campbell,<sup>35</sup> and is about 5 db below the horizontally polarized return. This is also in qualitative agreement with the prediction of Eq. (55).

Although the detailed agreement between the calculated and the measured return is not so good as it was for the slightly rough surfaces, it is found that the general level of the return, the frequency dependence, the seasonal dependence, and the statistical properties<sup>4, 21</sup> of the return can be accounted for qualitatively. This suggests that the model may be of use in predicting other features (e.g., albedo, bistatic scattering) of the interaction of electromagnetic radiation with vegetation surfaces, at least as to order of magnitude. Conversely, to the extent that the model is successful, it shows that the number of cylinders per unit area, their cross-sectional area, and their dielectric constant must be specified to describe the surface properly.

#### E. Other Theoretical Models

In addition to the simple models of Section IIIB, and the "complete" models of Sections IIIC and IIID, there is a third class of models for scattering from non-uniform surfaces. In this class, interest is concentrated more on the theoretical details of the scattering problem than on maintaining any particular

resemblance between the model surface and some actual terrain. For example, Twersky<sup>14</sup> has considered a surface of perfectly conducting hemispherical bosses distributed at random over a perfectly conducting plane; Ament<sup>8</sup> has considered a surface of perfectly conducting half-planes or wires; and Carlson and Heins<sup>10</sup> have considered the scattering from a regular array of plates. The bibliography (References 6 - 16) includes a representative sample of American, British and Russian literature on such models.



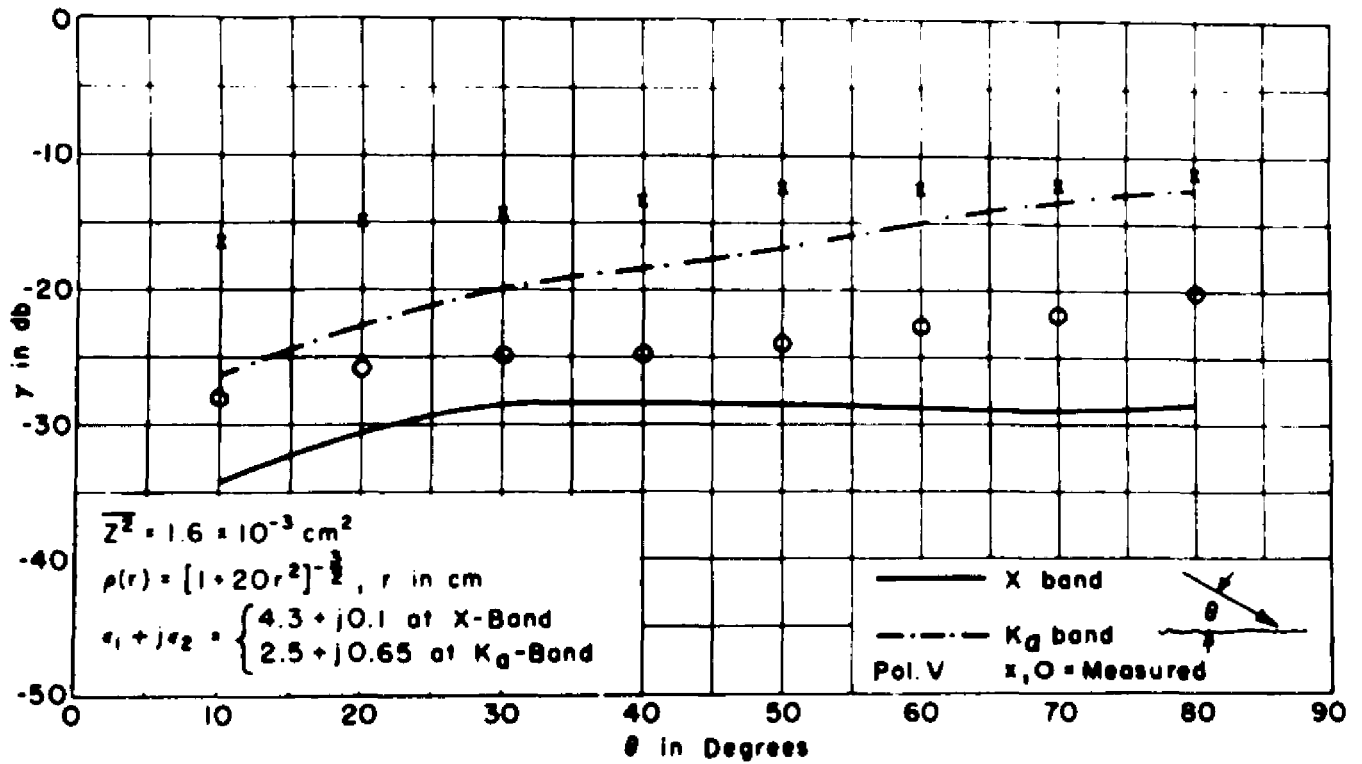


Fig. 10. Calculated and measured return from a slightly rough asphalt surface (vertical polarization).

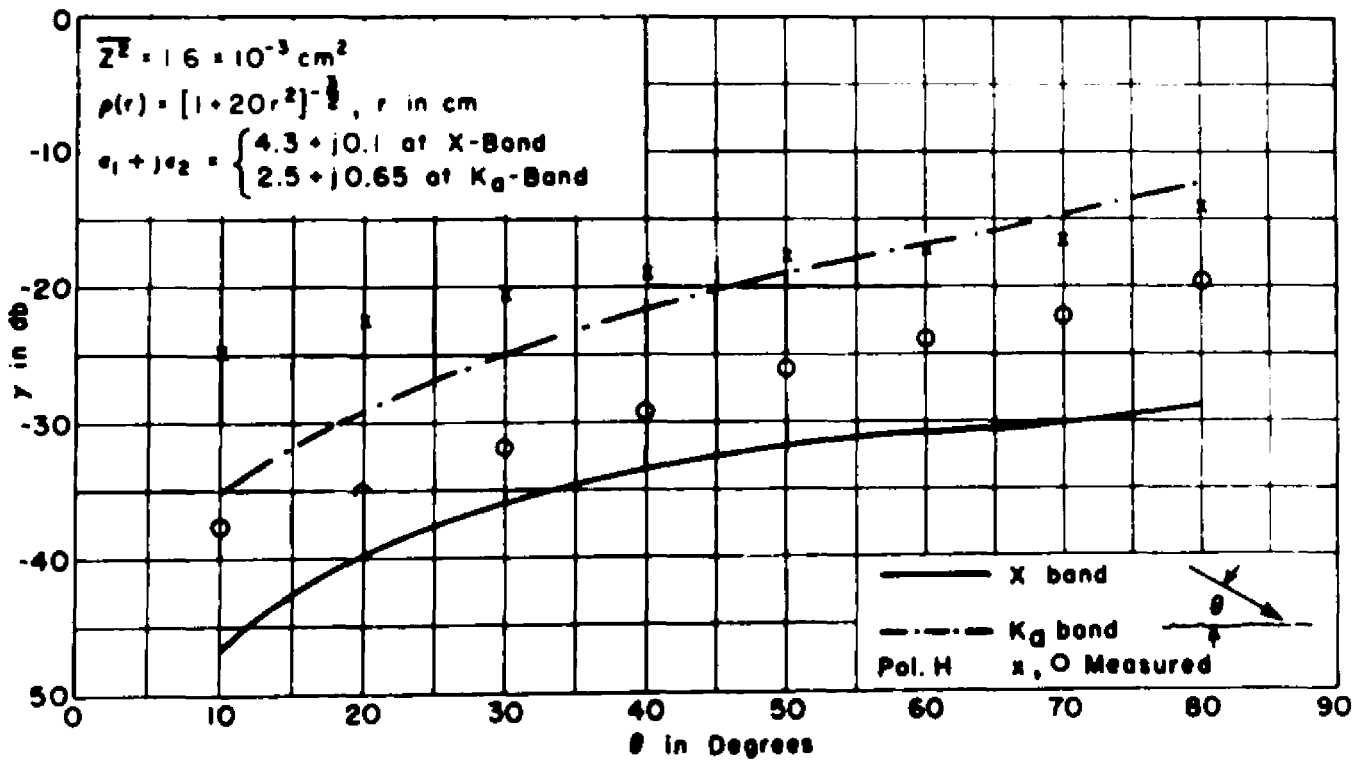


Fig. 11. Calculated and measured return from a slightly rough asphalt surface (horizontal polarization).

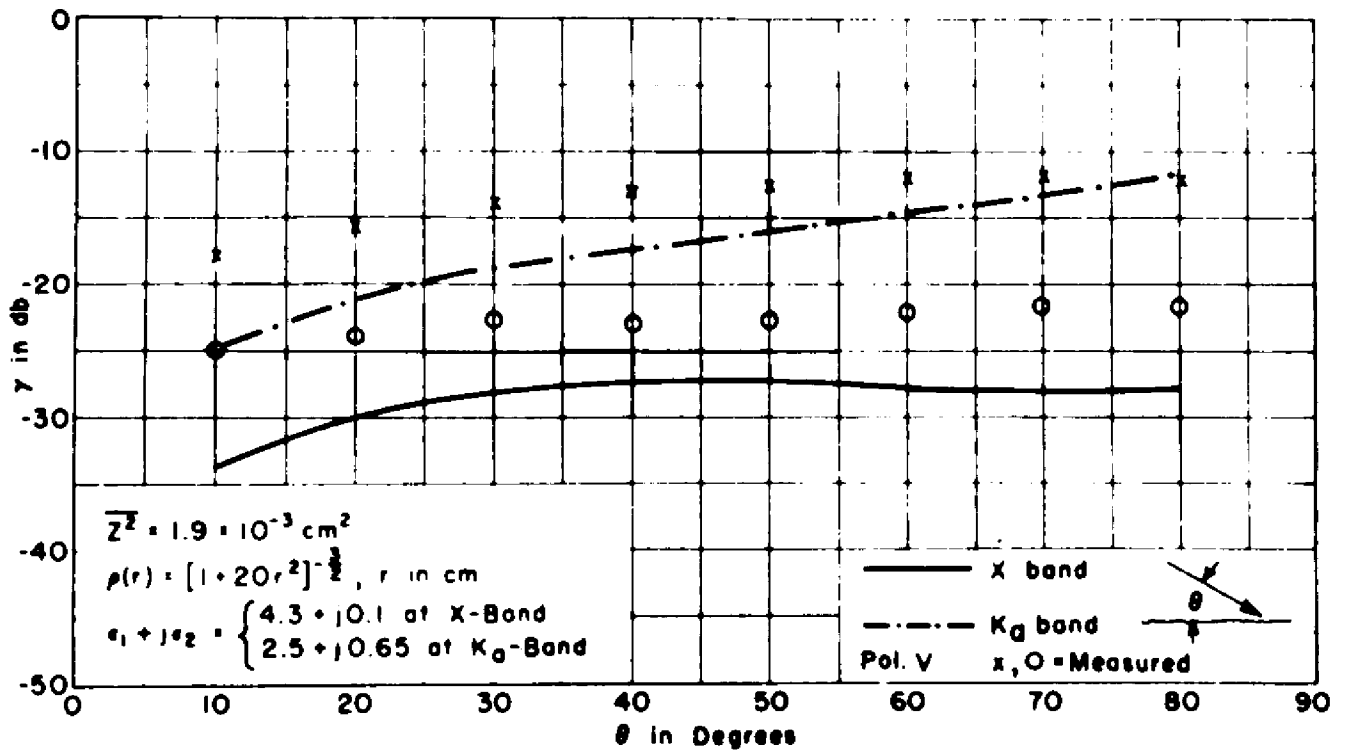


Fig. 12. Calculated and measured return from a slightly rough asphalt surface (vertical polarization).

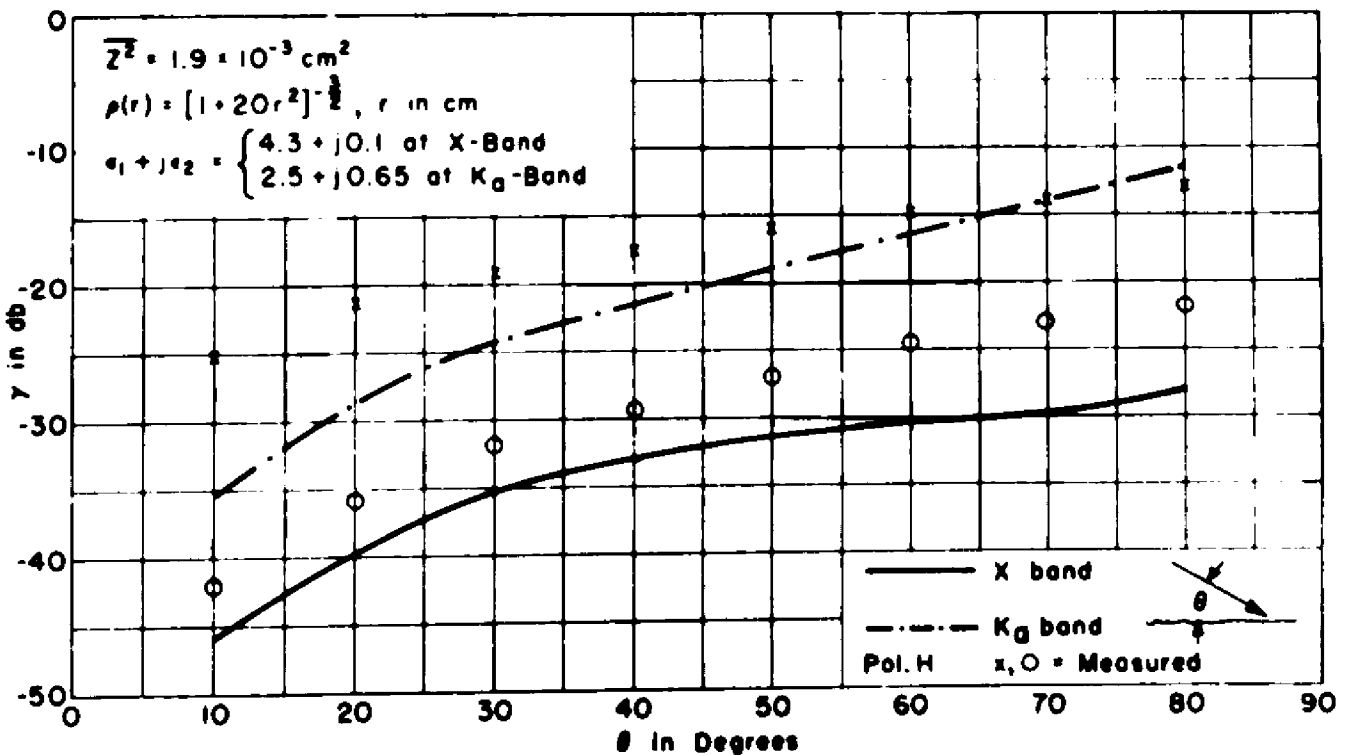


Fig. 13. Calculated and measured return from a slightly rough asphalt surface (horizontal polarization).

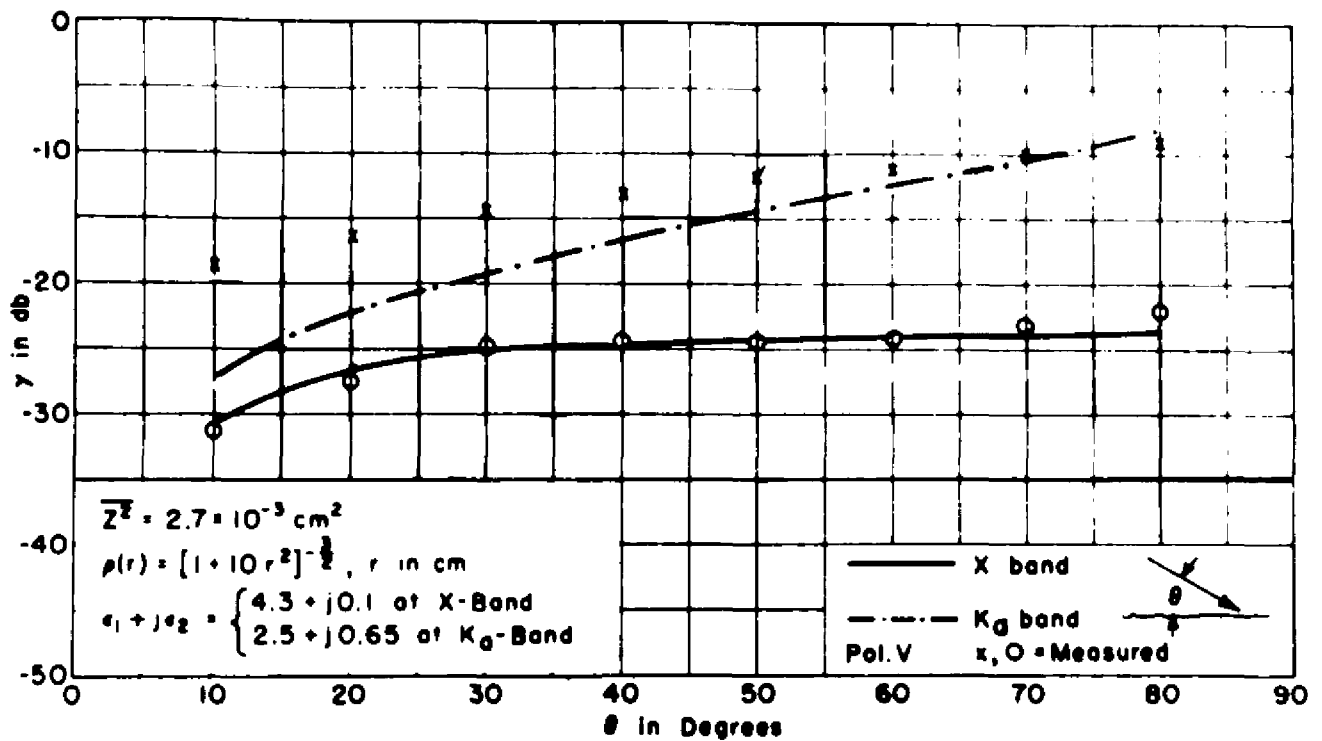


Fig. 14. Calculated and measured return from a slightly rough asphalt surface (vertical polarization).

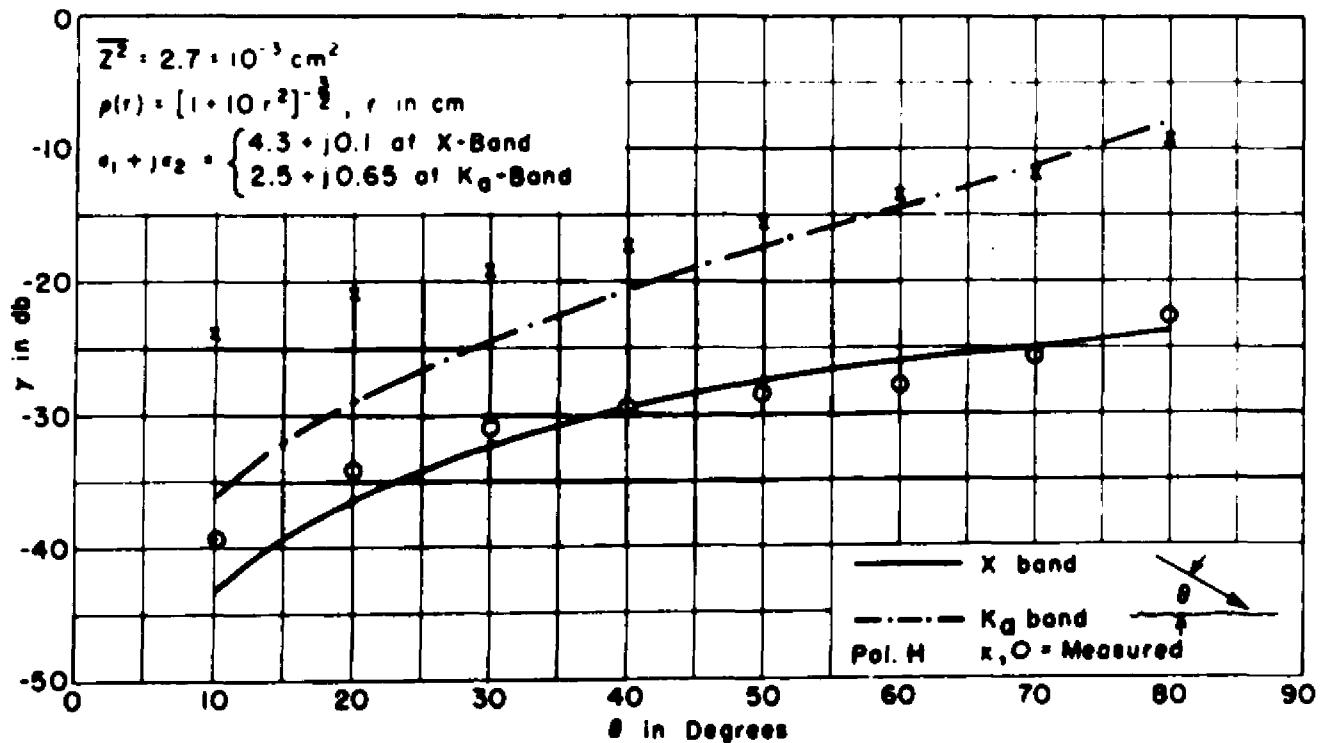


Fig. 15. Calculated and measured return from a slightly rough asphalt surface (horizontal polarization).

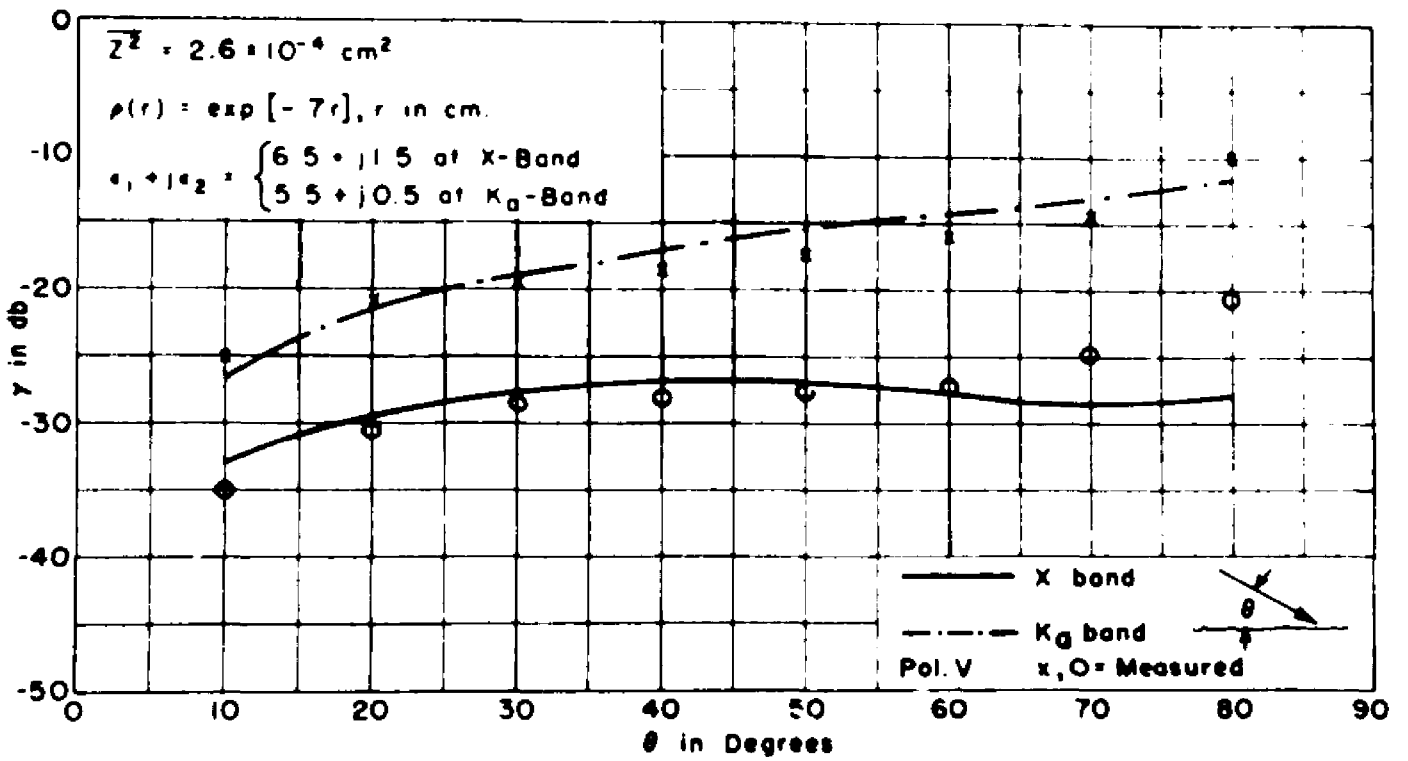


Fig. 16. Calculated and measured return from a slightly rough concrete surface (vertical polarization).

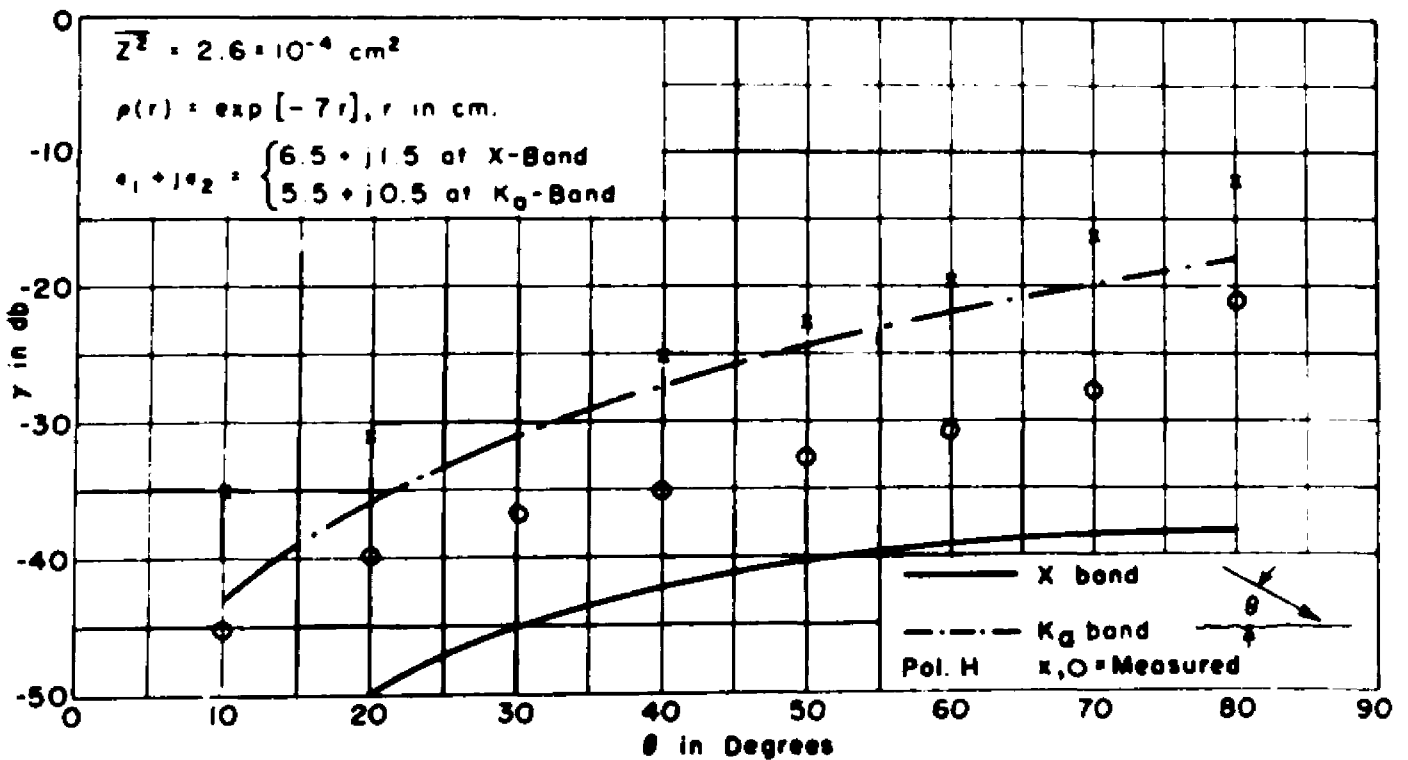


Fig. 17. Calculated and measured return from a slightly rough concrete surface (horizontal polarization).

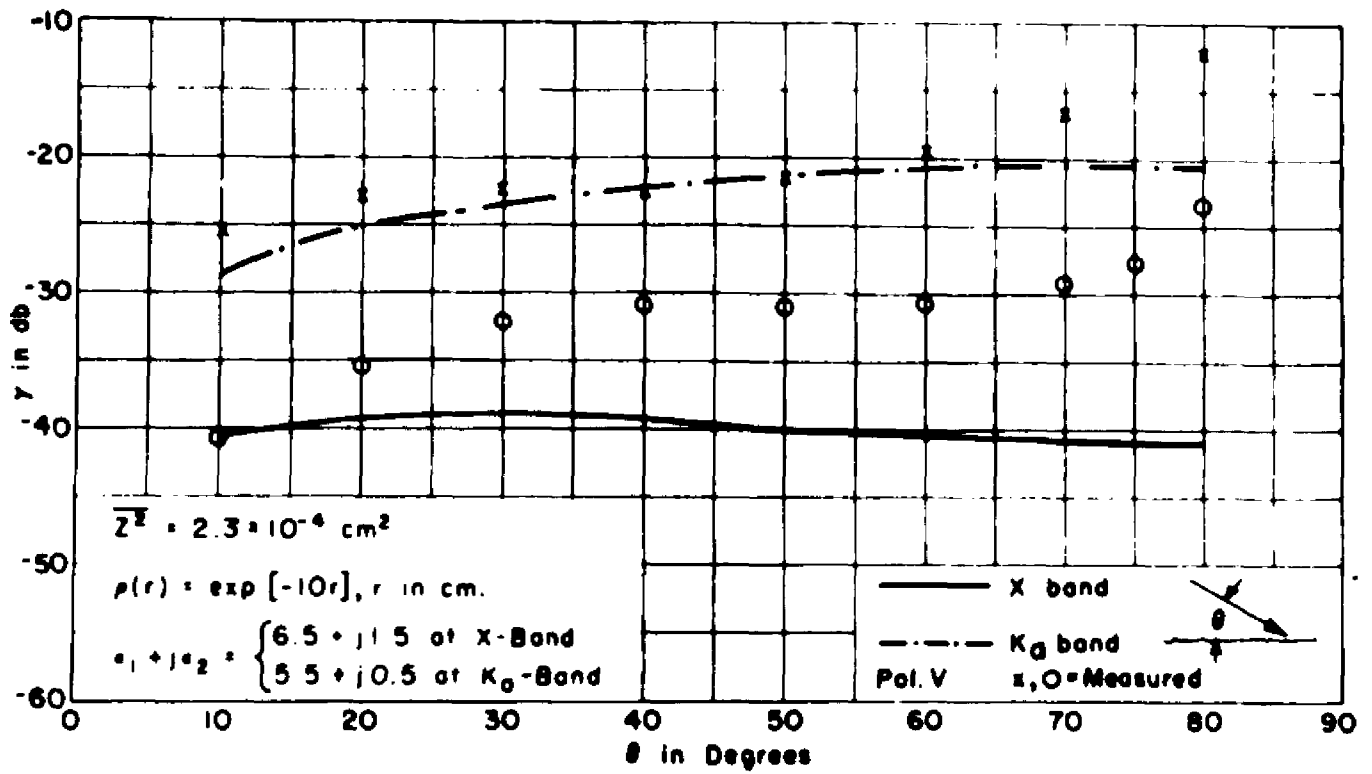


Fig. 18. Calculated and measured return from a slightly rough concrete surface (vertical polarization).

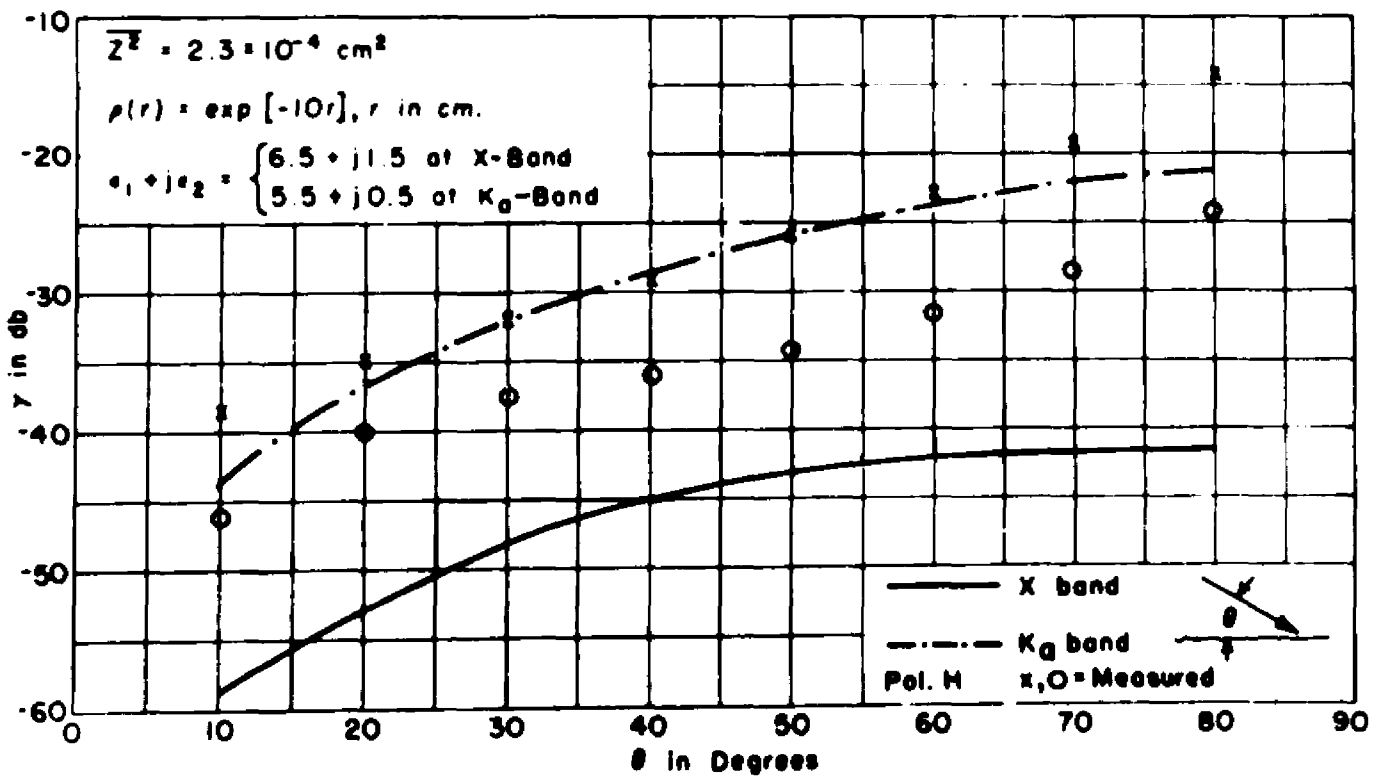


Fig. 19. Calculated and measured return from a slightly rough concrete surface (horizontal polarization).

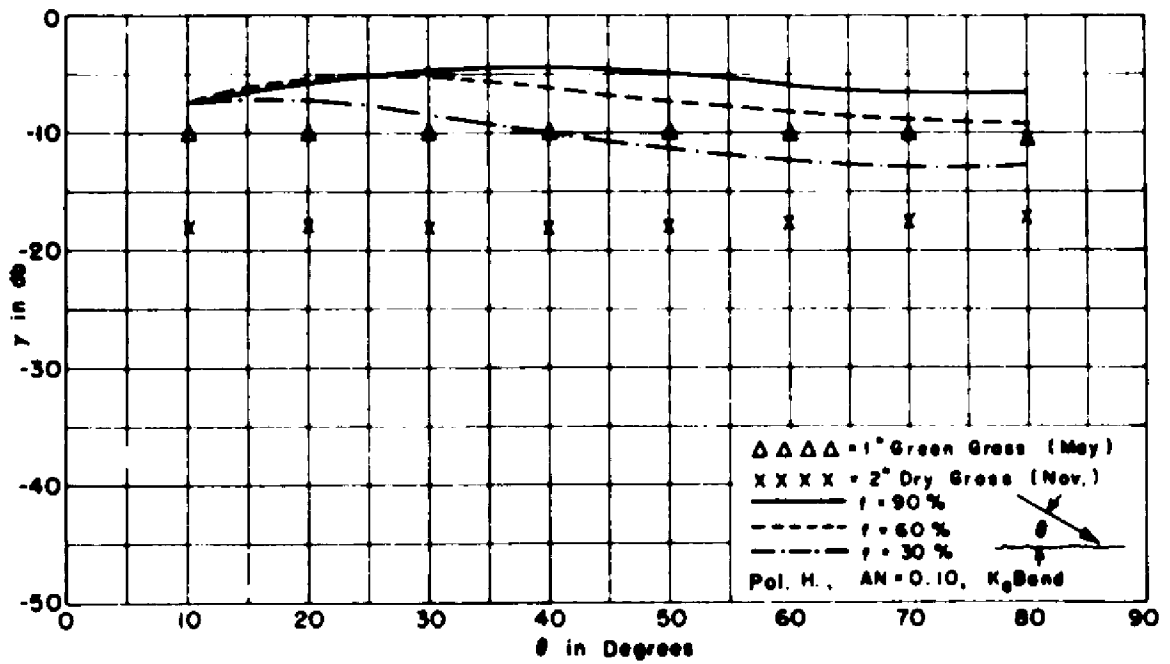


Fig. 20. Calculated and measured return from vegetation at 8.6 mm wavelength. Dependence on water content.

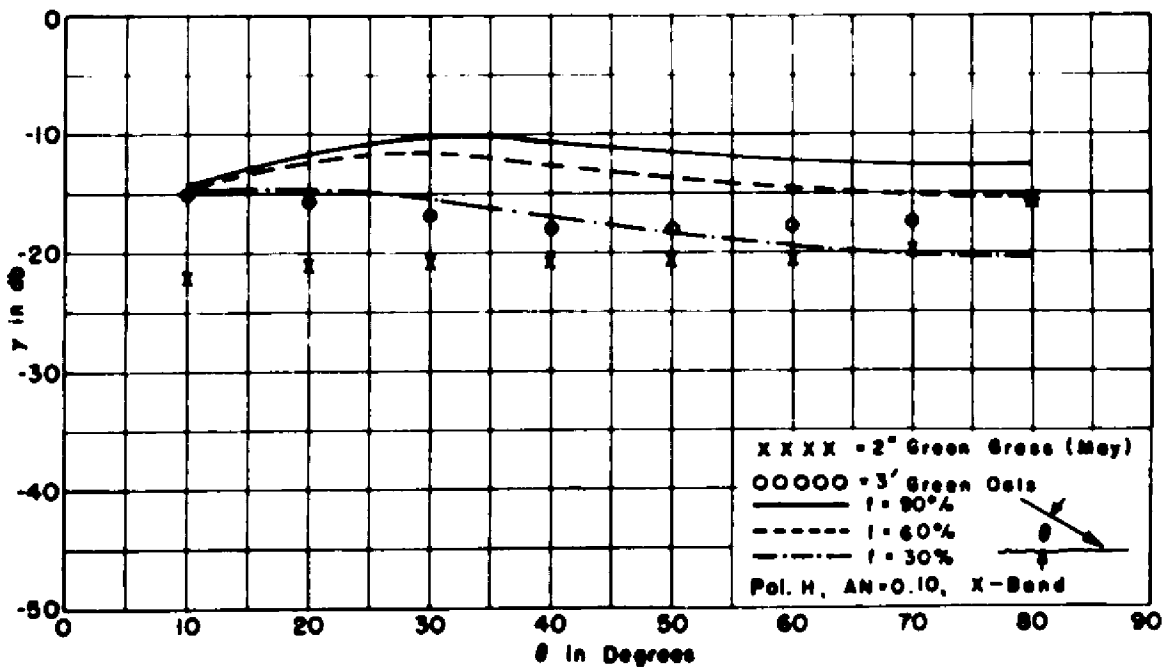


Fig. 21. Calculated and measured return from vegetation at 3 cm wavelength. Dependence on water content.

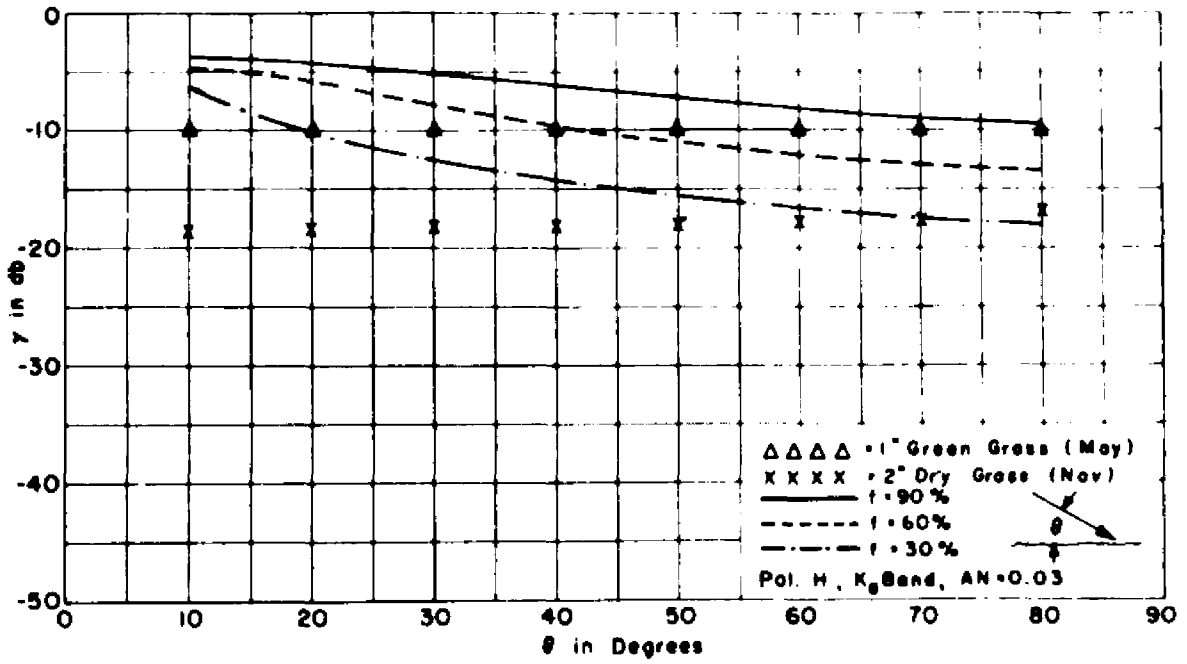


Fig. 22. Calculated and measured return from vegetation at 8.6 mm wavelength. Dependence on water content.

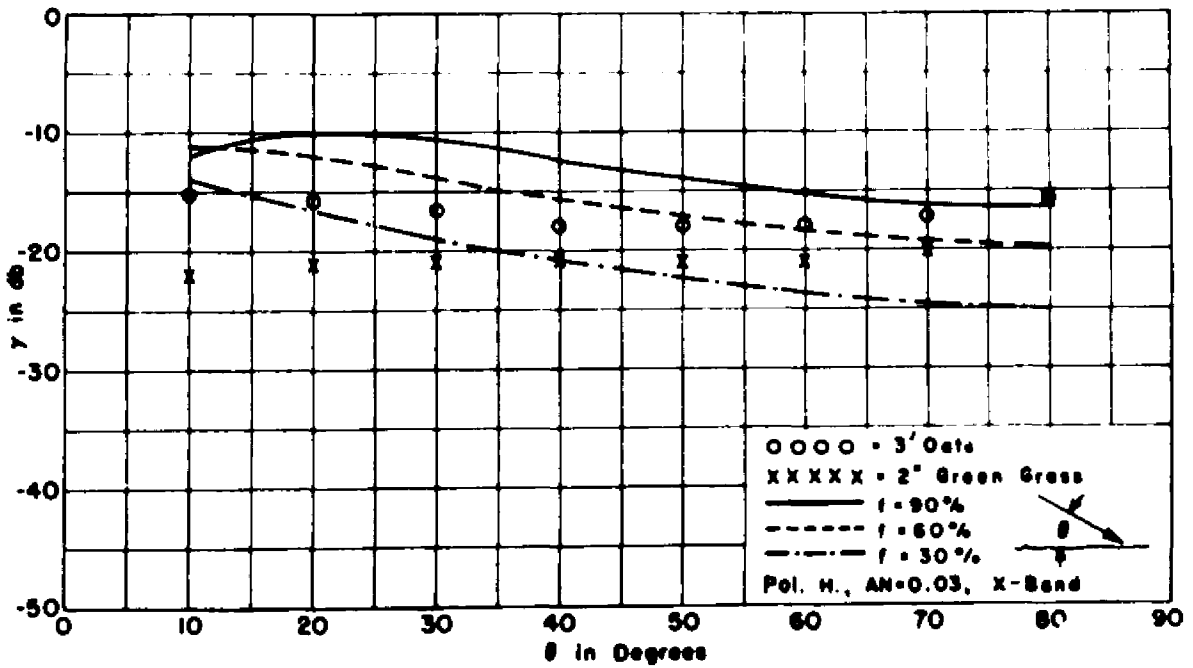


Fig. 23. Calculated and measured return from vegetation at 3 cm wavelength. Dependence on water content.

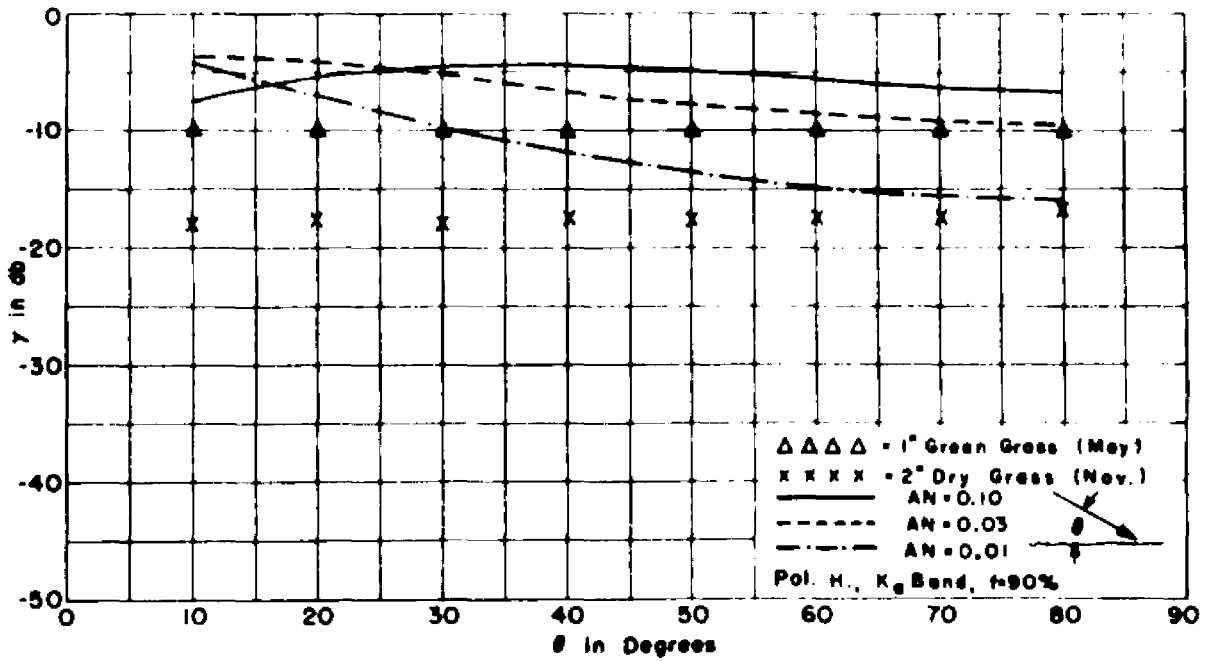


Fig. 24. Calculated and measured return from vegetation at 8.6 mm wavelength. Dependence on AN.

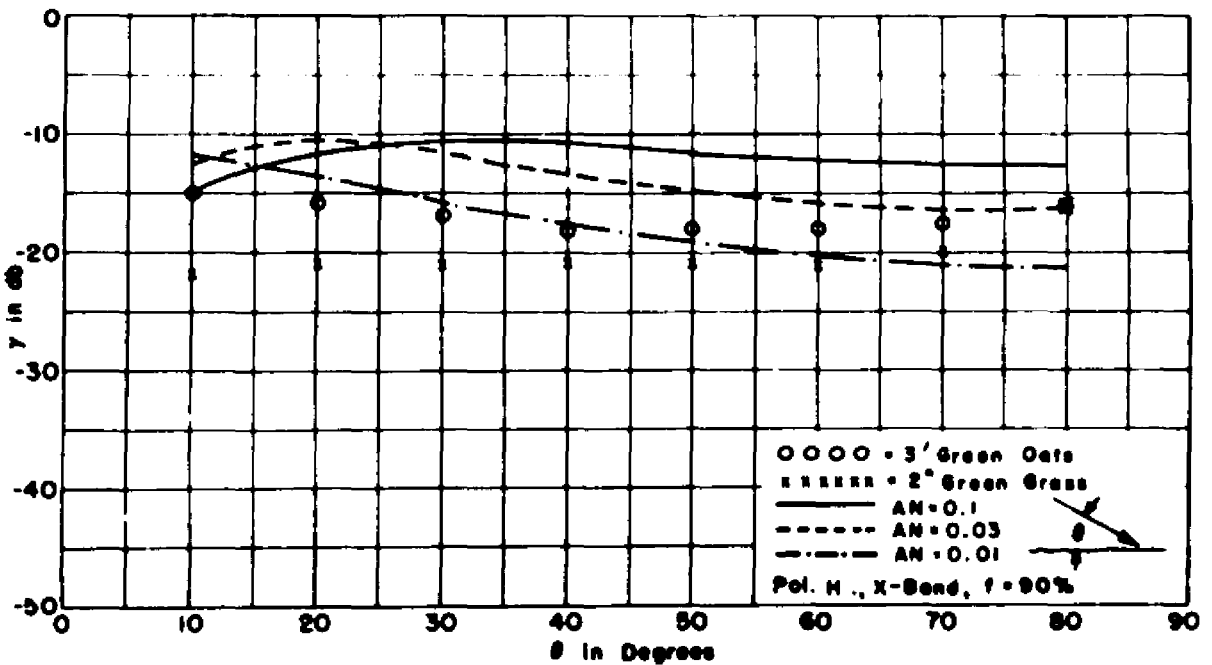


Fig. 25. Calculated and measured return from vegetation at 3 cm wavelength. Dependence on AN.



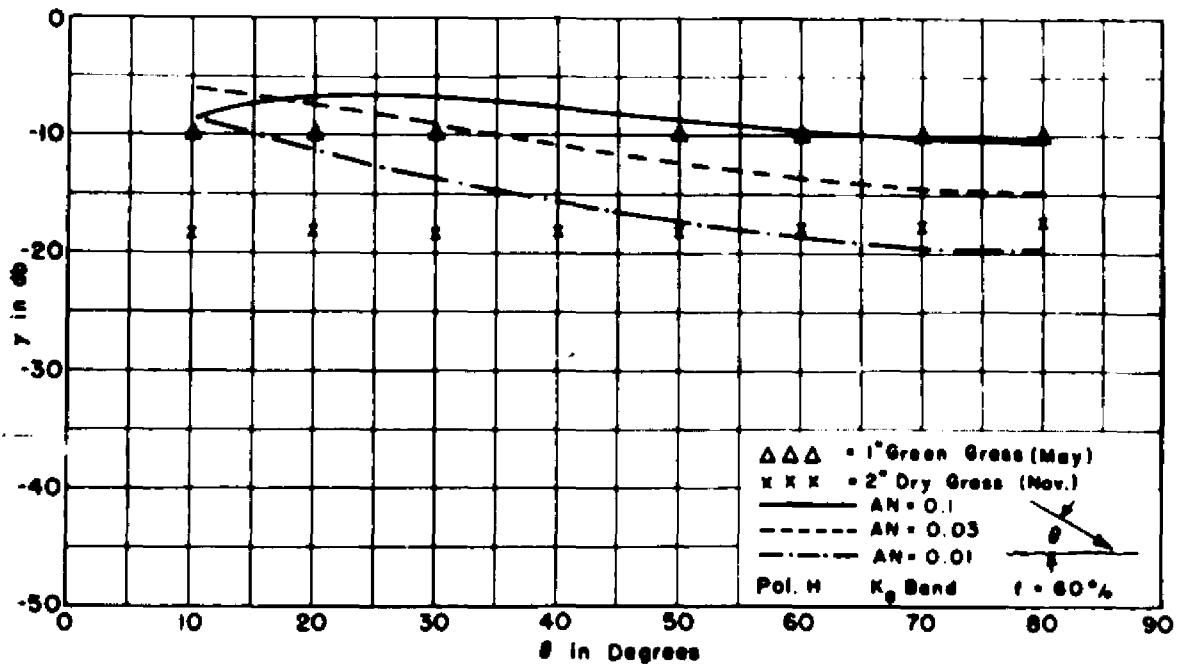


Fig. 26. Calculated and measured return from vegetation at 8.6 mm wavelength. Dependence on AN.

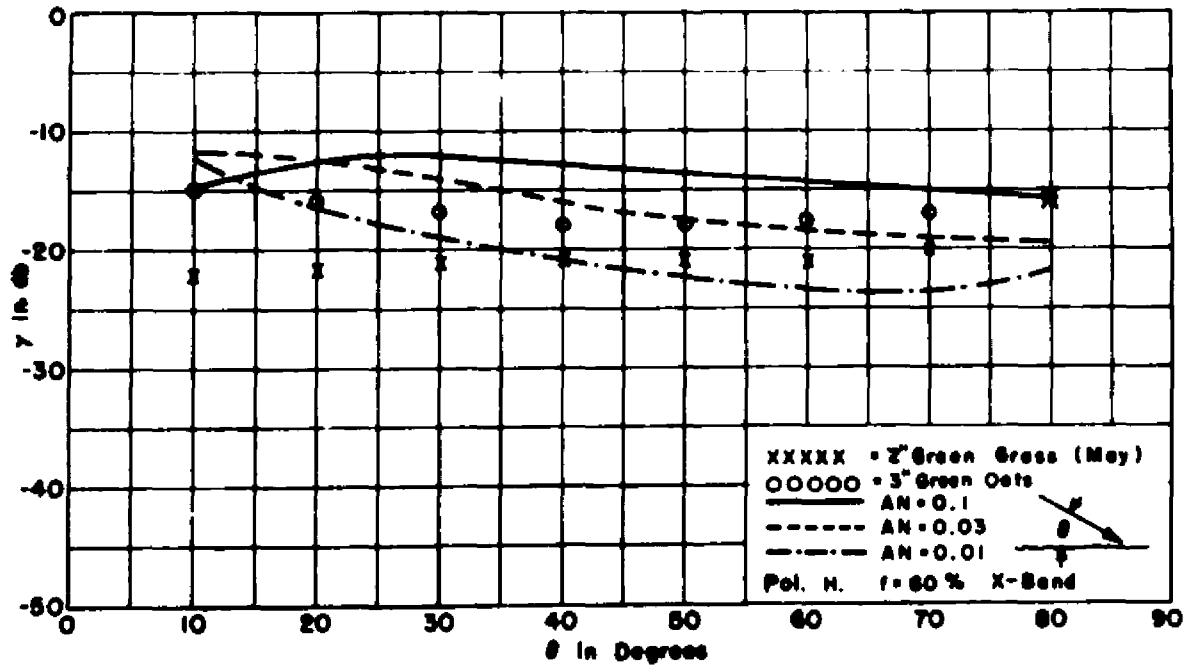
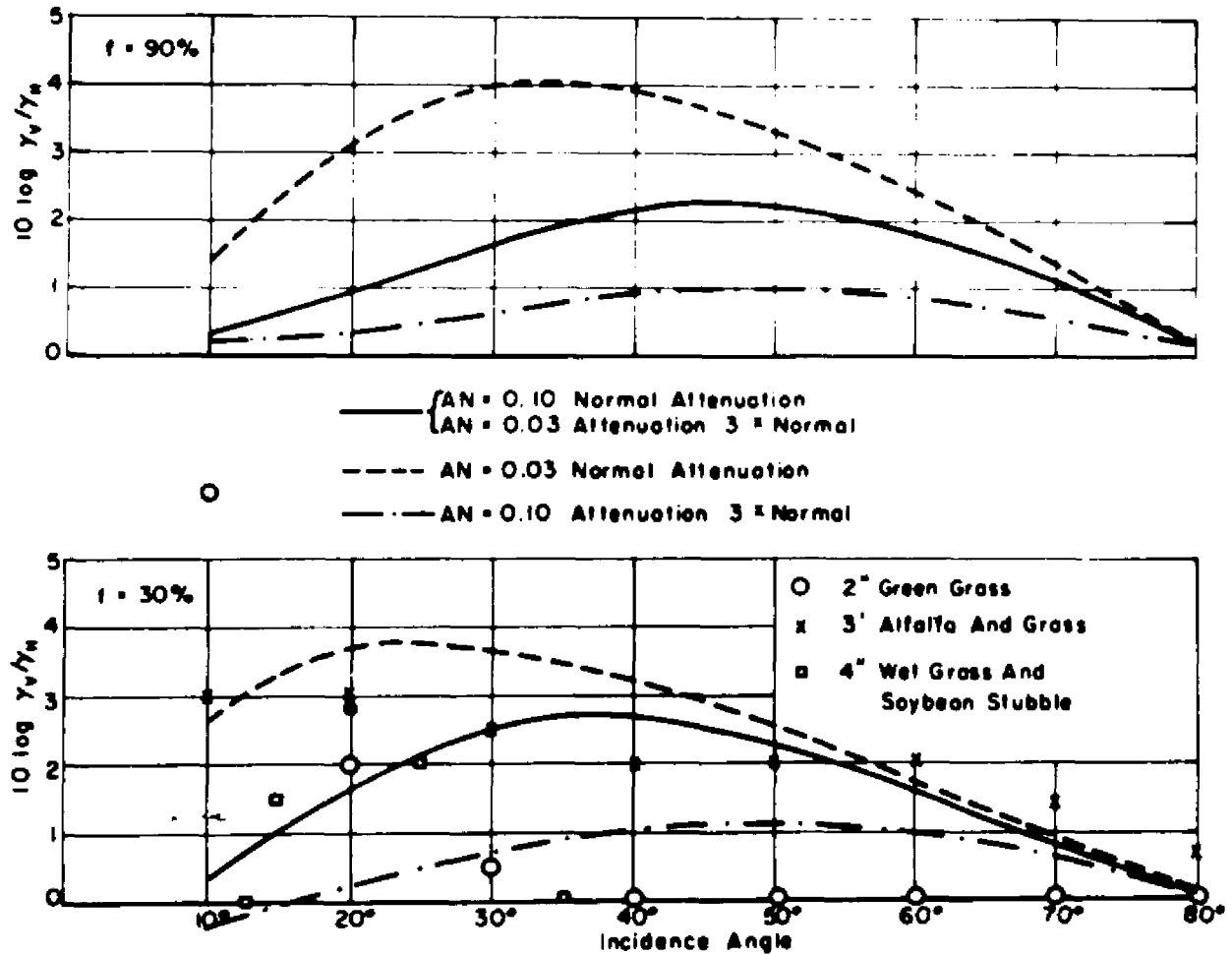
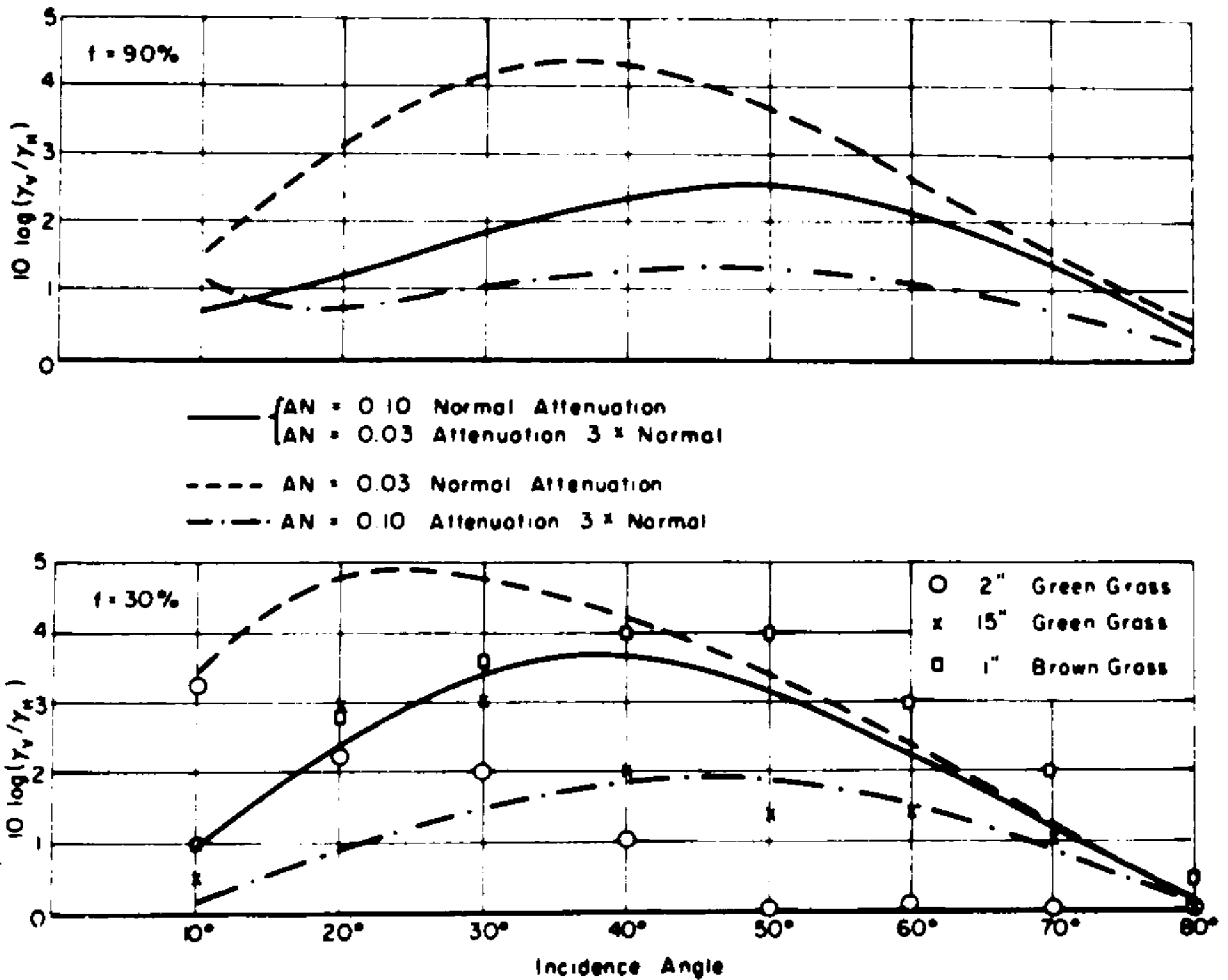


Fig. 27. Calculated and measured return from vegetation at 3 cm wavelength. Dependence on AN.



**Fig. 28. Calculated return from vegetation at  $K_a$ -band. Ratio of return for vertical polarization to return for horizontal polarization for two values of water content and various densities of vegetation.**



**Fig. 29.** Calculated return from vegetation at X-band. Ratio of return for vertical polarization to return for horizontal polarization for two values of water content and various densities of vegetation.

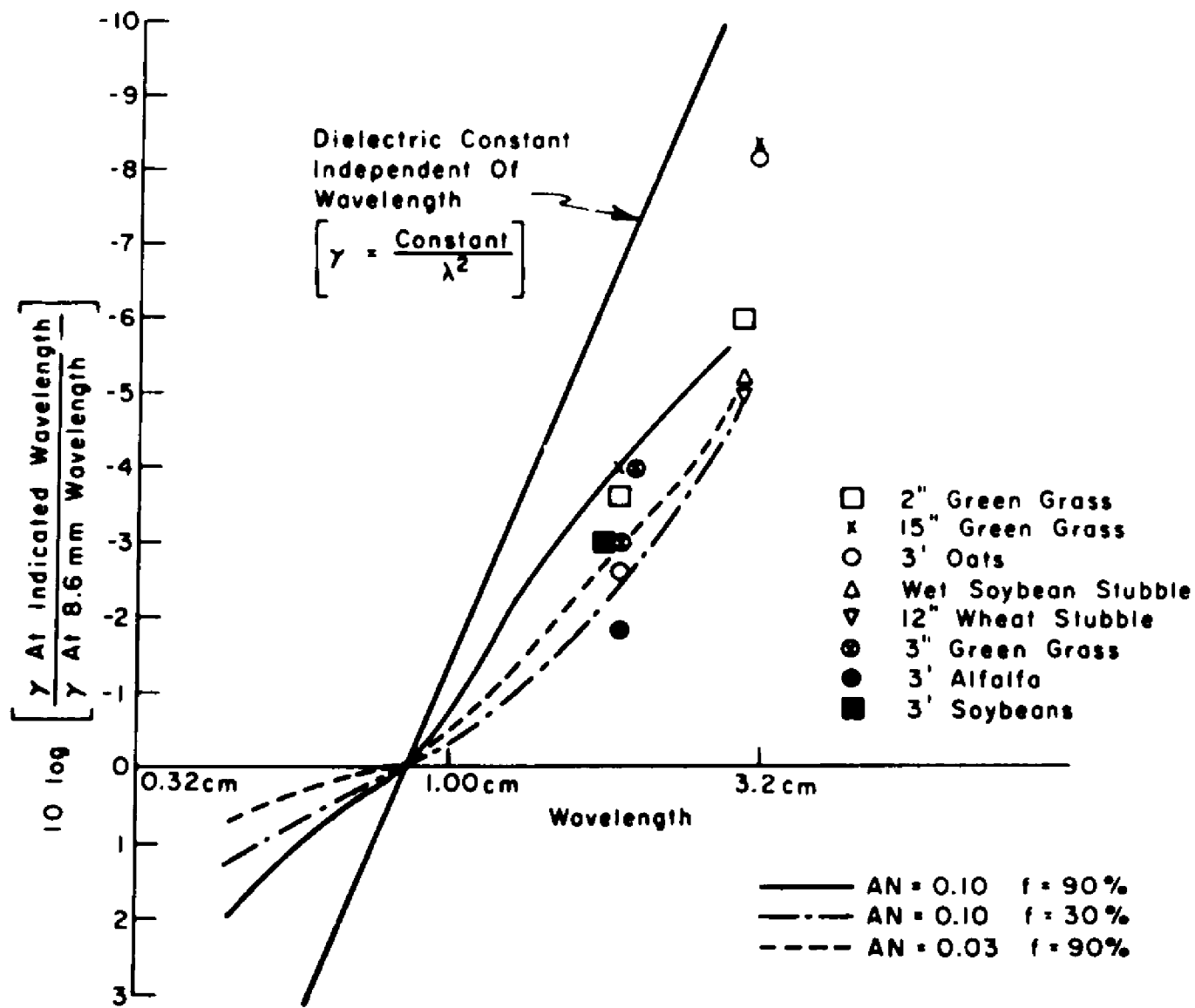


Fig. 30. Calculated and measured wavelength dependence of the return from vegetation, at 45° incidence angle.

CHAPTER IV  
APPLICATIONS TO THE RADIOMETRIC  
PROPERTIES OF TERRAIN

A. Introduction - Kirchhoff's Law

Another interesting application of the surface models developed in Chapter II is to the radiometric properties (or apparent temperatures) of natural surfaces at microwave frequencies. These have recently become of interest in connection with observations from artificial satellites, and may have some importance for an accurate determination of the heat balance of the earth. It was the intention, in formulating the complete models in Chapter II, to be able to determine these radiometric properties, in particular the emissivity, directly from the surface properties. There do exist certain special surfaces for which the emissivity may be calculated directly (for example, a perfectly flat surface of arbitrary dielectric constant). However, for non-uniform surfaces in general, it appears necessary to invoke Kirchhoff's radiation law in order to calculate the emissivity from the scattering coefficients  $\gamma$ . An understanding of this relation between the scattering coefficients and the apparent temperature of natural surfaces is particularly important at microwave frequencies. Here the scattering coefficients can be measured rather easily, whereas it may be difficult, if not impossible, to separate

the several contributions to the apparent temperature by measurement of thermal radiation alone.

Unfortunately, the usual statement of Kirchhoff's law is not adequate for the purpose. To remedy this situation, von Fragstein<sup>27</sup> has recently given a critical discussion of the form the law must take for both smooth and diffuse surfaces, and the relation between it and the reciprocity properties of the scattering coefficients. However, his discussion was for the optical case, and ignored the polarization properties of the surface. It will thus be necessary to extend his results to take account of these polarization effects, in order to provide a statement of Kirchhoff's law in its most general form.

Before carrying out the derivation it will be convenient to define the parameters that will be used to characterize the ability of a surface to emit thermal radiation.

These are, in the terminology of the review article by Rutgers,<sup>28</sup> the emission coefficients  $e_h(\theta_o\phi_o)$  and  $e_v(\theta_o\phi_o)$ . where

$$(59) \quad e_h(\theta_o\phi_o) = \frac{\left[ \begin{array}{l} \text{Power emitted with horizontal polarization by} \\ \text{unit area of surface into element of solid angle} \\ d\Omega_o \text{ in the direction } \theta_o\phi_o. \end{array} \right]}{\left[ \begin{array}{l} \text{Power emitted with horizontal polarization by} \\ \text{unit area of black body at same temperature} \\ \text{into same element of solid angle in same} \\ \text{direction.} \end{array} \right]}$$

An analogous definition holds for  $e_v(\theta_o\phi_o)$ , for vertically polarized radiation.

Throughout this chapter, it is to be understood that the thermal radiation referred to occupies a narrow band of frequencies  $\Delta f$ .

To obtain the desired relation between the emission coefficient and the absorption coefficient, defined earlier in Eq. (8), consider a surface (see Fig. 31) in temperature equilibrium with black body

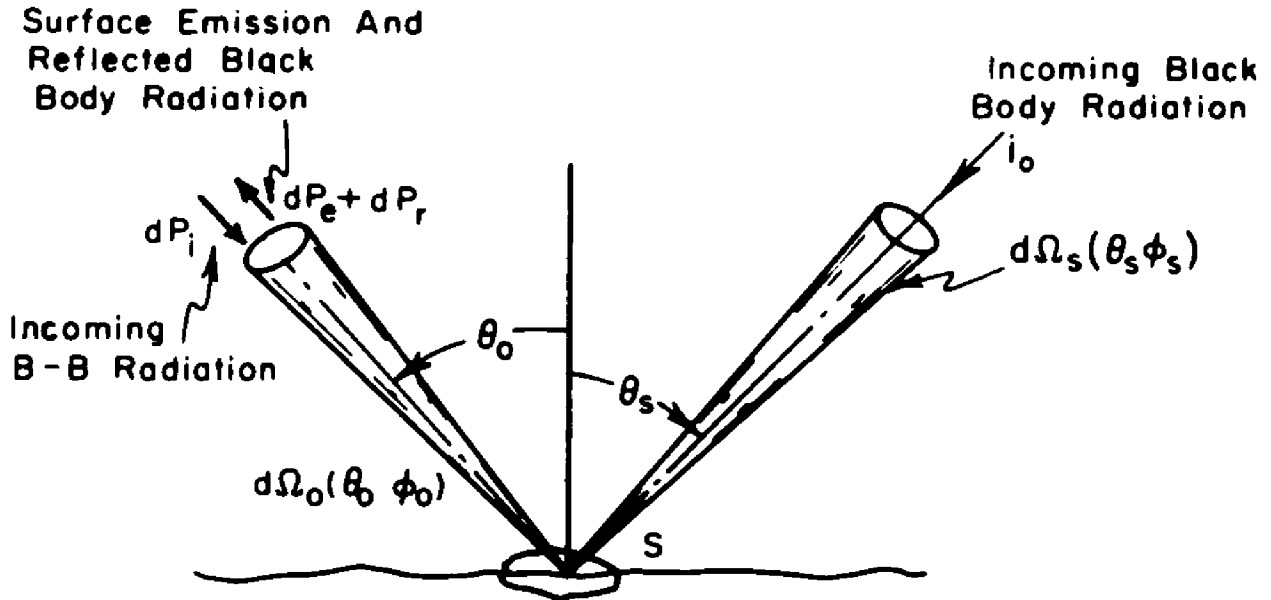


Fig. 31. Geometry for derivation of Kirchhoff's law.

radiation in the half space above it. Under this equilibrium condition, it will be assumed that just as much energy of a given polarization leaves the surface in a given direction as falls upon it from the same direction with the same polarization. To state this assumption quantitatively, let  $i_0$  be the power density per unit solid angle (watts-meter<sup>-2</sup>-steradian<sup>-1</sup>) of the black body radiation in a specific polarization state. (Thus the total power density per unit

solid angle of the black body radiation is  $2i_0$ ). Then  $i_0$  is a function of frequency and the equilibrium temperature but not of the direction or polarization of the radiation. It refers to the energy in the frequency interval  $\Delta f$ . The power  $dP_i$  incident with horizontal polarization on an element of surface of area  $S$  from a range of solid angle  $d\Omega_0$  in direction  $\theta_0\phi_0$  is

$$(60) \quad dP_i = i_0 d\Omega_0 S \cos \theta_0 .$$

The power leaving the surface is the sum of two parts, the thermal emission from the surface, and the external black body radiation reflected by the surface. The power  $dP_e$  emitted by the same element of surface into the same range of solid angle with horizontal polarization is, from the definition of emission coefficient,

$$(61) \quad dP_e = e_h(\theta_0\phi_0) i_0 d\Omega_0 S \cos \theta_0 .$$

The power reflected by the surface into  $d\Omega_0$  in the direction  $\theta_0\phi_0$  with horizontal polarization, due to black body radiation coming from the range of solid angle  $d\Omega_s$  in the direction  $\theta_s\phi_s$  is, from Eq. (2),

$$(62) \quad d^2 P_r = \underbrace{i_0 d\Omega_s S \cos \theta_s}_{\text{incident power from } \theta_s\phi_s} \underbrace{\left[ \gamma_{hh}(s, \theta) + \gamma_{vh}(s, \theta) \right]}_{\text{fraction reflected into } d\Omega_0} \frac{d\Omega_0}{4\pi} .$$



Thus the power  $dP_r$  reflected into  $d\Omega_o$  with horizontal polarization is

$$(63) \quad dP_r = \frac{i_o d\Omega_o S}{4\pi} \int [\gamma_{hh}(s, o) + \gamma_{vh}(s, o)] \cos \theta_s d\Omega_s.$$

Unless otherwise specified, integration is over the hemisphere.

Assuming the incident power of given polarization is balanced by the sum of the emitted and reflected power of the same polarization,

$$(64) \quad dP_i = dP_e + dP_r.$$

Consequently,

$$(65) \quad 1 = e_h(\theta_o \phi_o) + \frac{1}{4\pi} \int \frac{\cos \theta_s}{\cos \theta_o} [\gamma_{hh}(s, o) + \gamma_{vh}(s, o)] d\Omega_s.$$

By the reciprocity relations of Eq. (5) this becomes

$$(66) \quad 1 = e_h(\theta_o \phi_o) + \frac{1}{4\pi} \int [\gamma_{hh}(o, s) + \gamma_{hv}(o, s)] d\Omega_s.$$

The third term in Eq. (66) is just the albedo defined by Eq. (7), which is related to the absorption coefficient by Eq. (8). Thus on substituting Eqs. (7) and (8) into (66), one finds

$$(67a) \quad e_h(\theta_o \phi_o) = a_h(\theta_o \phi_o).$$

A similar relation

$$(67b) \quad e_v(\theta_o \phi_o) = a_v(\theta_o \phi_o)$$

is easily derived for vertical polarization.

Equations (67a) and (67b) constitute the desired generalization of Kirchhoff's Law, taking account of both the polarization properties of the surface and the angular dependence of the coefficients. Furthermore, through Eqs. (7) and (8), the emission coefficients can be found from the scattering coefficients  $\gamma$  of the surface.

By comparing the derivation leading to Eq. (67) with that of von Fragstein,<sup>27</sup> the different assumptions in the two derivations become clear. The latter postulated only that there was a balance between the total power incident on, emitted and reflected by the surface, whereas Eq. (64) required that each polarization state separately satisfied a power balance. On the other hand, in deriving Eq. (67), no assumptions were made about the polarization properties of the surface, whereas von Fragstein assumed, without stating the fact, that

$$(68) \quad \gamma_{hh}(o, s) + \gamma_{hv}(o, s) = \gamma_{vh}(o, s) + \gamma_{vv}(o, s) .$$

There is one other point in which the above derivation differs from the case where polarization is not taken into account. Von Fragstein pointed out that his derivation, which made use of what he referred to as the Sommerfeld-Pfrang reciprocity relation, could be reversed. That is, by assuming the validity of Kirchhoff's law, he could prove the Sommerfeld-Pfrang reciprocity relation. However the argument leading to Eq. (67) cannot be reversed to obtain

the reciprocity relations of Eq. (5). At most, it can be shown that the pairs of coefficients entering Eq. (68) satisfy a relation like Eq. (5). This is because Eq. (67) provides only two relations between the four coefficients  $\gamma$ .

### B. Apparent Surface Temperatures

In practice, real terrain surfaces are not in equilibrium with black-body radiation in the half-space above them. Thus the total radiation emanating from the surface will be different from that emitted by a black body at the same temperature. That is, the surface will have an "apparent temperature" different from its actual temperature. The concept of the apparent temperature of a surface may be defined in the following manner.

Within an enclosure whose walls are maintained at a fixed temperature  $T$ , the black-body radiation is characterized by the quantity  $i_o(T, \lambda)$ , the power density per unit solid angle of radiation of a specific polarization, with frequencies in the interval  $\Delta f$ . For sufficiently high temperatures and long wavelengths,  $i_o(T, \lambda)$  is given by the Rayleigh-Jeans approximation<sup>29</sup>

$$(69) \quad i_o(T, \lambda) = \frac{kT\Delta f}{\lambda^2} \text{ watts-meter}^{-2} \text{-steradian}^{-1}$$

where  $k$  is Boltzmann's constant. For arbitrary temperature and wavelength, the Planck<sup>31</sup> distribution law must be used.

Because of the unique relation between  $i_0$  and the temperature  $T$  of the enclosure, the radiation itself is also said to have temperature  $T$ . Consider now any arbitrary thermal radiation travelling in a specified direction with specified polarization with frequencies in the small interval  $\Delta f$ . Then the apparent temperature of this arbitrary thermal radiation is defined as the temperature of the black-body radiation which has the same power density per unit solid angle. To extend the concept to a surface, it is only necessary to postulate that the apparent temperature of a surface when viewed from some specified direction (with a detector of specified polarization) is equal to the apparent temperature of the radiation emanating from the surface in the prescribed direction with the prescribed polarization.

There are three principal contributions to the apparent temperature of natural terrain surfaces (see Fig. 32).

The first is the thermal radiation emitted by the surface. It is customary to assume that as long as the surface has a well-defined temperature ( $T_g$ ), its emission coefficient is independent of conditions external to the surface.

The second contribution to the apparent temperature is due to the reflection of the diffuse thermal radiation ( $T_h$  or  $T_v$ ) impinging on the surface from the upper hemisphere. This diffuse radiation is,

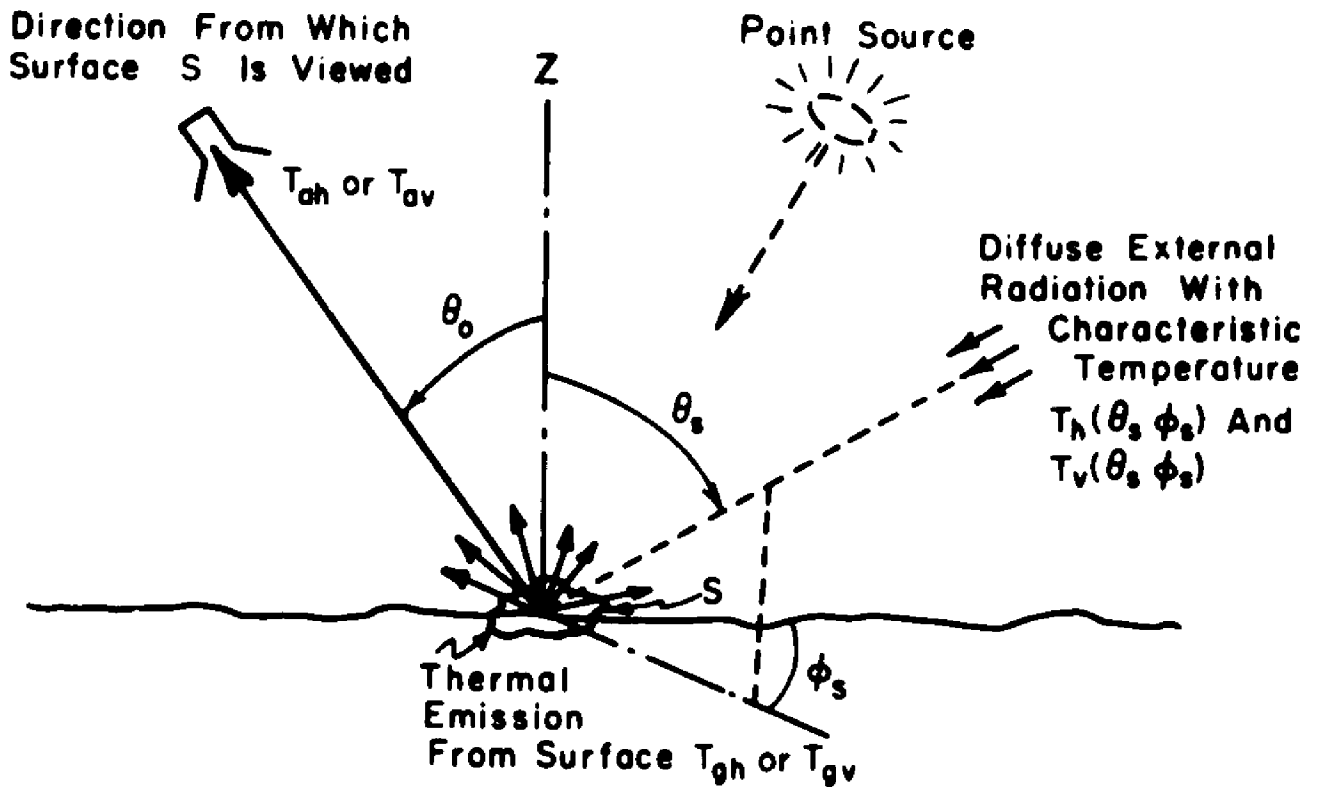


Fig. 32. Contributions to the apparent temperature of a surface, in practice, due primarily to radiation from the earth's atmosphere at microwave wavelengths shorter than 10 cm, and to extraterrestrial (or cosmic) radio noise at wavelengths longer than 100 cm.<sup>30</sup>

The third contribution to the apparent surface temperature is due to radiation from point, or quasi-point sources scattered by the surface. The most prominent of these is the sun.

The power due to these three principal contributions adds directly to give the total power emanating from the surface. Thus, for conditions under which the Rayleigh-Jeans approximation (Eq. (69)) may be used, the apparent temperature of the surface may also be expressed as a sum of contributing temperatures, viz:

$$(70) \quad T_{ah} = T_{gh} + T_{sh} + T_{ph}$$

$$T_{av} = T_{gv} + T_{sv} + T_{pv}$$

where

$T_{ah}(\theta_0\phi_0)$ ,  $T_{av}(\theta_0\phi_0)$  are the total apparent temperatures of a surface for radiation of horizontal or vertical polarization respectively, when the surface is viewed from the direction  $\theta_0, \phi_0$  (see Fig. 32).

$T_{gh}$ ,  $T_{gv}$  are the contributions to the apparent temperature due solely to the thermal radiation emitted by the surface.

$T_{sh}$ ,  $T_{sv}$  are the contributions to the apparent temperature due to the scattering of the diffuse external radiation.

$T_{ph}$ ,  $T_{pv}$  are the contributions to the apparent temperature due to the bistatic scattering of radiation from point or quasi-point sources.

The first contribution, that due to thermal emission from the ground, is easily calculated from the definition, Eq. (59), of the emission coefficient. Clearly,

$$(71) \quad T_{gh}(\theta_0\phi_0) = e_h(\theta_0\phi_0) T_g$$

$$T_{gv}(\theta_0\phi_0) = e_v(\theta_0\phi_0) T_g$$

where  $T_g$  is the actual temperature of the ground.

The second contribution, due to the external diffuse radiation may be calculated as follows. Let the apparent temperature of this radiation arriving from the direction  $\theta_s \phi_s$  be  $T_h(\theta_s \phi_s)$ ,  $T_v(\theta_s \phi_s)$  for the horizontally and vertically polarized components, respectively. Then from the definition of the scattering coefficients, Eq. (2), and the fact that the apparent temperature of radiation is assumed to be proportional to its power density/steradian, it is found that,

$$(72) \quad T_{sh}(\theta_o \phi_o) = \frac{1}{4\pi} \int \left[ T_h(\theta_s \phi_s) \gamma_{hh}(s, o) + T_v(\theta_s \phi_s) \gamma_{vh}(s, o) \right] \cdot \frac{\cos \theta_s}{\cos \theta_o} d\Omega_s .$$

From the reciprocity relations, Eq. (5), this becomes

$$(73a) \quad T_{sh}(\theta_o \phi_o) = \frac{1}{4\pi} \int \left[ T_h(s) \gamma_{hh}(o, s) + T_v(s) \gamma_{hv}(o, s) \right] d\Omega_s .$$

Similarly

$$(73b) \quad T_{sv}(\theta_o \phi_o) = \frac{1}{4\pi} \int \left[ T_v(s) \gamma_{vv}(o, s) + T_h(s) \gamma_{vh}(o, s) \right] d\Omega_s .$$

The third contribution, that due to point sources, will be discussed in the next section.

Before considering the detailed application of the foregoing results to actual terrain surfaces, it may be of interest to give formulas for the apparent temperatures of some highly idealized surface models much used in the past.<sup>28</sup>

(i) Black Body

$$e_h = e_v = 1$$

$$(74) \quad Y_{hh} = Y_{hv} = Y_{vh} = Y_{vv} = 0$$

$$T_{ah} = T_{av} = T_g .$$

The apparent temperature of a black body is equal to its actual temperature. It absorbs all radiation falling on it, and reflects none.

(ii) Gray Body

The emission coefficients for a gray body are, like those of a black body, independent of polarization and direction:

$$(75) \quad e_h(\theta_0\phi_0) = e_v(\theta_0\phi_0) = e .$$

Here  $e$  is a constant,  $e < 1$ . The scattering coefficients for a gray body have not been previously defined. However, to maintain the similarity between gray and black body radiation, it seems plausible to require the  $Y$ 's to be independent of polarization, and to follow Lambert's law. Thus

$$(76) \quad Y_{hh}(o, s) = Y_{hv}(o, s) = Y_{vh}(o, s) = Y_{vv}(o, s) = Y_g \cos \theta_s$$

where  $Y_g$  is a constant. Then the apparent temperature of a gray body is



$$(77) \quad T_{ah} = T_{av} = e T_g + \frac{\gamma_g}{4\pi} \int [T_h(s) + T_v(s)] \cos \theta_s d\Omega_s .$$

As may be seen by letting  $T_h = T_v = T_g$ , the relation between  $e$  and  $\gamma_g$  is

$$(78) \quad e = 1 - (\gamma_g/2) .$$

(iii) Flat Surface

The emission coefficients for a flat surface have long been known.<sup>31</sup> Because the reflection is specular, they may be calculated from the standard form of Kirchhoff's law, and the Fresnel coefficients. For a surface of arbitrary complex dielectric constant  $\epsilon' = \epsilon_1 - i\epsilon_2$  the apparent temperatures are

$$(79) \quad T_{ah}(\theta_0, \phi_0) = [1 - |R_h(\theta_0)|^2] T_g + |R_h(\theta_0)|^2 T_h(\theta_0, \phi_0 + \pi)$$

$$T_{av}(\theta_0, \phi_0) = [1 - |R_v(\theta_0)|^2] T_g + |R_v(\theta_0)|^2 T_v(\theta_0, \phi_0 + \pi) ,$$

where  $R_h, R_v$  are the Fresnel coefficients

$$(80) \quad R_h = \frac{\cos \theta_0 - (\epsilon' - \sin^2 \theta_0)^{\frac{1}{2}}}{\cos \theta_0 + (\epsilon' - \sin^2 \theta_0)^{\frac{1}{2}}}$$

$$R_v = \frac{\epsilon' \cos \theta_0 - (\epsilon' - \sin^2 \theta_0)^{\frac{1}{2}}}{\epsilon' \cos \theta_0 + (\epsilon' - \sin^2 \theta_0)^{\frac{1}{2}}} .$$

There is an important qualification to the foregoing discussion. The effects of atmospheric attenuation have been ignored. Consequently the apparent temperatures as calculated from the above formulas apply only near enough to the surface so that there is no appreciable attenuation between the surface and the observer at the frequency of interest. If this condition is not fulfilled, the thermal radiation due to the intervening medium must also be taken into account.

### C. Point Source Effects

In this section, the contribution of point sources to the apparent surface temperature will be calculated. This may be done most easily by the artifice of replacing the point source by an equivalent source subtending a small solid angle  $\Omega_p$ , producing radiation with  $i_p$  watts-meter<sup>-2</sup>-steradian<sup>-1</sup>. That is, if the actual point source produces radiation of intensity  $I_p$  watts-meter<sup>2</sup> at the surface, then  $I_p = i_p \Omega_p$ . Both  $I_p$  and  $i_p$  refer to radiation of specific polarization in the frequency interval  $\Delta f$ . Then from Eq. (2) the power density scattered by an element of surface  $S$  toward the observing direction  $\theta_o \phi_o$  is

$$(81) \quad I_s = [i_p \Omega_p] \gamma(s, o) \frac{S}{4\pi R^2} \cos \theta_s .$$

where  $(s)$  refers to the direction of the point source. But

$S \cos \theta_0 / 4\pi R^2$  is the solid angle subtended by  $S$  at the viewing position, so that the intensity per unit solid angle of the scattered radiation is

$$(82) \quad i_s = \frac{i_p}{S \cos \theta_0} 4\pi R^2 = \frac{i_p \Omega_p}{4\pi} \gamma(s, \theta) \frac{\cos \theta_s}{\cos \theta_0} .$$

Making use of the reciprocity relation, and taking polarization into account,

$$(83) \quad i_{sh} = \frac{(i_p \Omega_p)}{4\pi} \left[ \gamma_{hh}(o, s) + \gamma_{hv}(o, s) \right] .$$

Because of the relation Eq. (69) between  $i$  and  $T$ , the contribution of the quasipoint source to the apparent temperature becomes

$$(84) \quad T_{ph} = T_p \left( \frac{\Omega_p}{4\pi} \right) \left[ \gamma_{hh}(o, s) + \gamma_{hv}(o, s) \right]$$

where  $T_p$  is the apparent temperature of the radiation  $i_p$ . For true point sources, only the product  $T_p \Omega_p$  is known.

It may be of interest to estimate the contribution of the sun to the apparent surface temperature at microwave frequencies. At  $K_a$ -band, the apparent temperature of the sun is about  $10^4$ °K and a typical value of  $\gamma$  is 0.1. Thus  $T_{sh}$  due to the sun is about 0.01°K. It seems likely that unless great accuracy is required, the effects of the sun on apparent temperature may be ignored for diffuse surfaces.

#### D. Application to the Apparent Temperature of Some Natural Surfaces

In this section, the results of IVA and IVB will be used to estimate the apparent temperatures of two surfaces for which some measurements are available.

The first surface of interest is an asphalt roadway, the apparent temperature of which was measured<sup>36</sup> at wavelength of 4.3 mm. The measurements could be interpreted in terms of the model for a slightly rough surface developed in Chapter II. However, such a model is unnecessarily complicated for interpreting apparent temperature measurements. This is because the scattering pattern of such a surface is predominantly specular, with a reflection coefficient not very different from that for a perfectly flat surface. The diffuse part of the scattering pattern (see, e.g., Eqs. (25), (26)), though of vital importance for predicting the back scattering, contains very little power. Elementary considerations show, in fact, that the ratio of the power in the complete diffuse pattern (integrated over the hemisphere) to the power in the specular beam has an order of magnitude of  $\sqrt{2|R|^2}$  where R is the appropriate Fresnel coefficient. For the roadway surfaces presented in Figs. 10-19, this amounts to a few percent. Thus the diffuse scattering will be ignored, and the apparent temperature will be calculated from the results of IVB(iii).

To do so, it is necessary to estimate the dielectric constant of the surface, and the apparent "sky" temperatures  $T_v(\theta_0)$  and  $T_h(\theta_0)$ . At 4.3 mm wavelength, the latter is due primarily to radiation from the earth's atmosphere. A convenient formula, based on a simple model which represents the atmosphere as a uniform horizontal layer, is<sup>29, 30</sup>

$$(85) \quad T_h(\theta_0) = T_v(\theta_0) = T_a(1 - r^{\sec \theta_0})$$

where  $r$  is the fraction of power of the given wavelength transmitted through the atmosphere at normal incidence, and  $T_a$  is the temperature of the model atmosphere. Taking  $r = 0.63$ , a value appropriate to the dry air of Texas, the predictions of Eq. (85) are in fair agreement with the sky temperatures measured by Straiton.<sup>36</sup>

With this assumption about the sky temperature, the apparent temperature of a flat or slightly rough surface becomes

$$(86) \quad \begin{aligned} T_{ah}(\theta_0) &= [1 - |R_h|^2]T_g + |R_h|^2 T_a(1 - r^{\sec \theta_0}) \\ T_{vh}(\theta_0) &= [1 - |R_v|^2]T_g + |R_v|^2 T_a(1 - r^{\sec \theta_0}) . \end{aligned}$$

Using  $\epsilon' = 4$  and  $r = 0.63$ , the predictions of Eq. (86) are shown in Fig. 33. The measurements of Straiton, Britt and Tolbert<sup>36</sup> on an asphalt surface are included for comparison. It will be seen

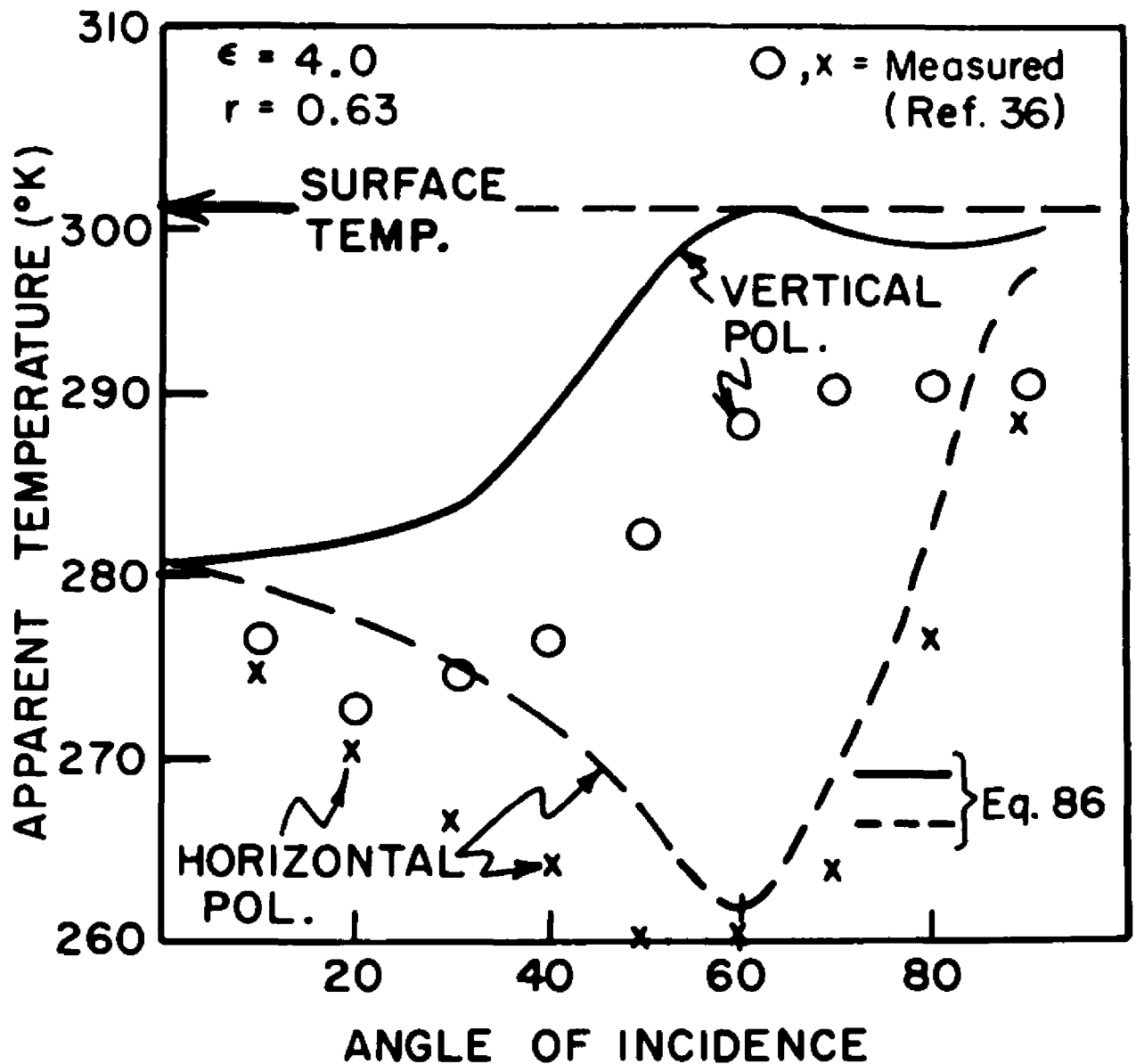


Fig. 33. Measured and calculated apparent temperature of an asphalt surface.

that apart from a systematic error of about  $10^{\circ}\text{K}$ , both the polarization dependence and the angular dependence of the measured temperatures are fairly well represented by the model.

A second surface measured by Straiton was one composed of grass and weeds, for which the lossy cylinder model of IIC should be appropriate. Again, the complexity of Eq. (41) makes it desirable

to introduce certain simplifying assumptions for a qualitative calculation. Consider first the general formula for the apparent temperature of a surface with sky temperature given by Eq. (85), viz.,

$$(87) \quad T_{ah} = T_g \left[ 1 - (4\pi)^{-1} \int \left[ \gamma_{hh}(o, s) + \gamma_{hv}(o, s) \right] d\Omega_s \right] \\ + T_a (4\pi)^{-1} \int \left[ \gamma_{hh}(o, s) + \gamma_{hv}(o, s) \right] \left[ 1 - r^{\sec \theta_s} \right] d\Omega_s ,$$

with a similar formula for vertical polarization. In the first place, measurements reported by Campbell<sup>35</sup> indicate that  $\gamma_{hv} \approx (1/4)\gamma_{hh}$  so that the term  $\gamma_{hv}$  may be dropped or accounted for by a small increase in  $\gamma_{hh}$ . Furthermore, measurements by Taylor<sup>17</sup> show that the back scattering from vegetation surfaces tends to be independent of incidence angle. Thus a plausible choice for the integrands in Eq. (87) might be either

$$(88a) \quad \gamma_{hh}^{(1)}(o, s) = \gamma_1 \quad \left[ \text{constant} \right]$$

or, secondly,

$$(88b) \quad \gamma_{hh}^{(2)}(s, o) = \gamma_2 \quad \left[ \text{constant} \right]$$

where, by Eq. (5),

$$(88c) \quad \gamma_{hh}^{(2)}(o, s) = \frac{\cos \theta_s}{\cos \theta_o} \gamma_2 .$$

Here the superscripts (1) and (2) identify the special choices of  $\gamma$ .

In order to compare the predictions of Eqs. (87) and (88) with the measurements, it is convenient to calculate  $\Delta T$ , the difference between the actual temperature and the apparent temperature of the surface. For the two special choices of  $\gamma$  given by Eq. (88), the temperature differences are

$$\Delta T_1 = T_g - T_{ah}^{(1)} = \frac{\gamma_1}{2} [T_g - T_a F_1(r)]$$

(89)

$$\Delta T_2 = T_g - T_{ah}^{(2)} = \frac{\gamma_2}{4 \cos \theta_0} [T_g - T_a F_2(r)]$$

where

$$F_1(r) = \int_0^{\pi/2} [1 - r^{\sec \theta_s}] \sin \theta_s d\theta_s$$

(90)

$$F_2(r) = 2 \int_0^{\pi/2} [1 - r^{\sec \theta_s}] \cos \theta_s \sin \theta_s d\theta_s .$$

These functions may be evaluated in terms of the exponential integral, and are plotted in Fig. 34.

Using Figs. 20 and 30, and other results of Taylor to extrapolate the back-scattering coefficient from vegetation surfaces to 4.3 mm the following values of  $\gamma_1$  and  $\gamma_2$  may be estimated:

$$\gamma_1 = \gamma_2 = 0.1 \text{ for grass and weeds - vertical polarization}$$

$$\gamma_1 = \gamma_2 = 0.126 \text{ for grass and weeds - horizontal polarization}$$



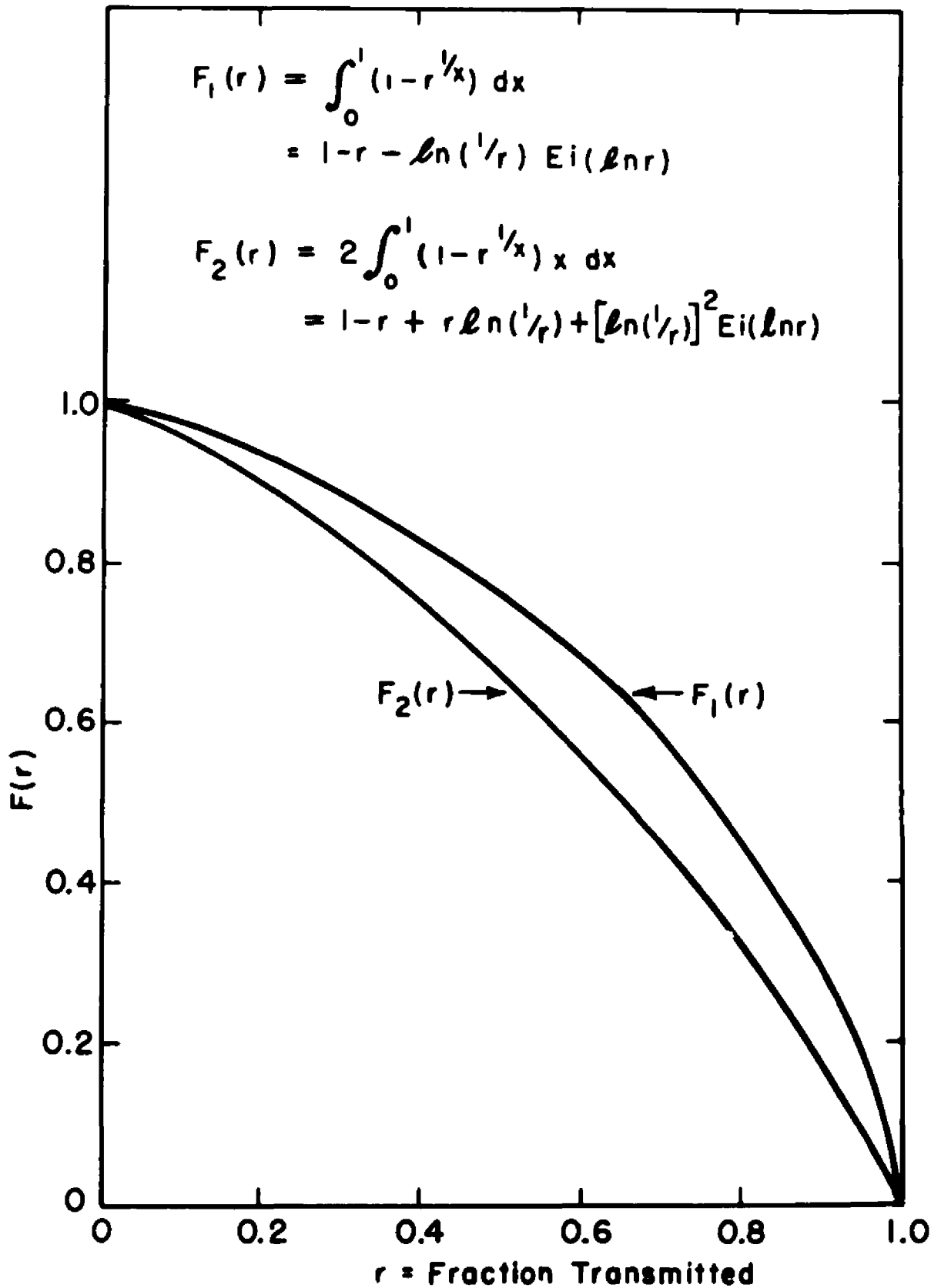


Fig. 34. The functions  $F_1(r)$  and  $F_2(r)$  vs  $r$ .

$\gamma_1 = \gamma_2 = 0.2$  for damp grass and weeds.

The second and third values are 1 db and 3 db larger than the first. With these choices of  $\gamma$ , and the value  $r = 0.63$  used previously, the predictions of  $E_{\downarrow}$  (89) are shown in Figs. 35-37. These figures also show the measured temperatures.<sup>36</sup> Again there is qualitative agreement between the measurements and the model, which could be brought into surprisingly good quantitative agreement by using the mean of  $\Delta T_1$  and  $\Delta T_2$ , i.e., by choosing

$$(91) \quad \gamma(\theta, \theta_s) = \frac{1}{2} \gamma_1 \left[ 1 + \frac{\cos \theta_s}{\cos \theta_0} \right]$$

for vegetation surfaces.

Unfortunately, there is not sufficient experimental data to check this and the previous flat surface model in the same detail as the back-scattering. Nevertheless, the qualitative features of the apparent surface temperatures for these two classes of surface can be explained by using very simple idealization of the surface models developed earlier in this report.

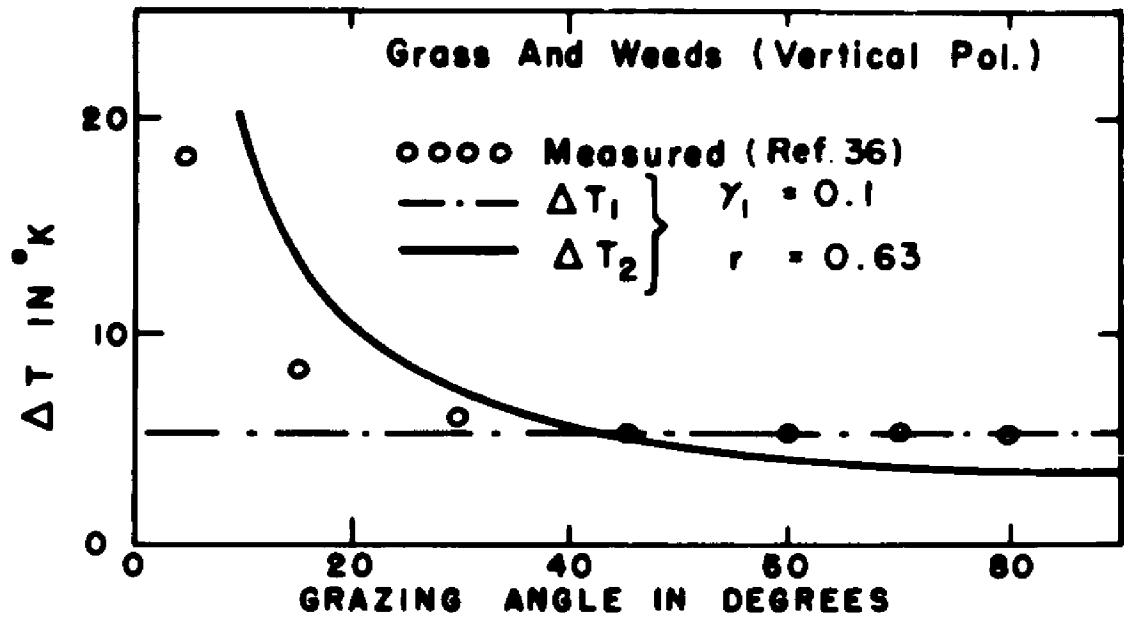


Fig. 35. Measured and calculated apparent temperature of vegetation covered surface.

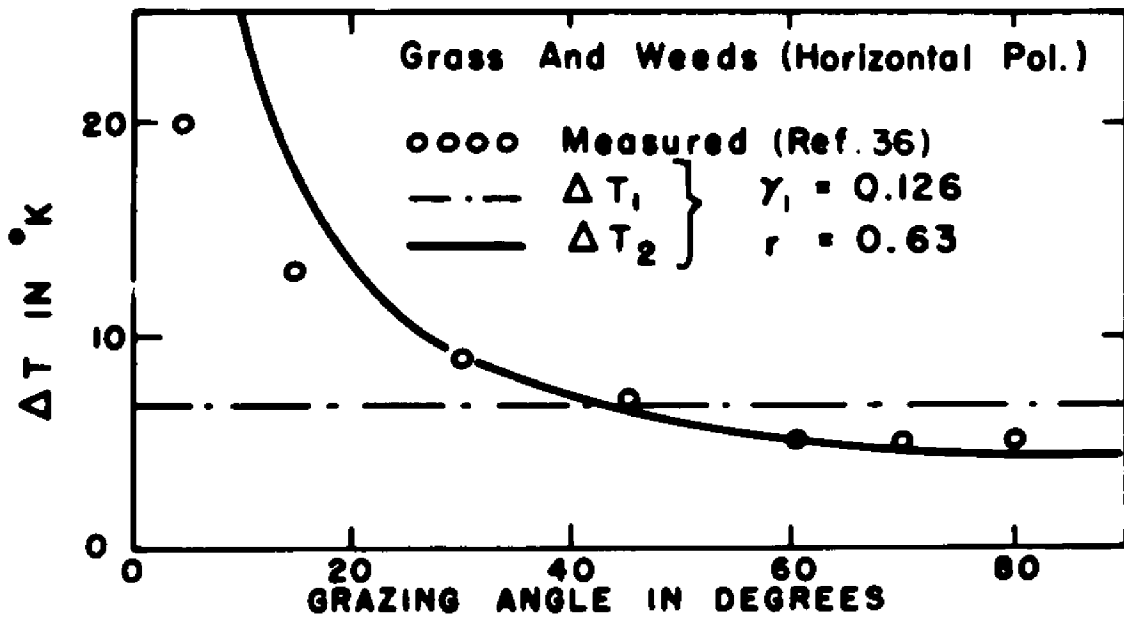


Fig. 36. Measured and calculated apparent temperature of vegetation covered surface.

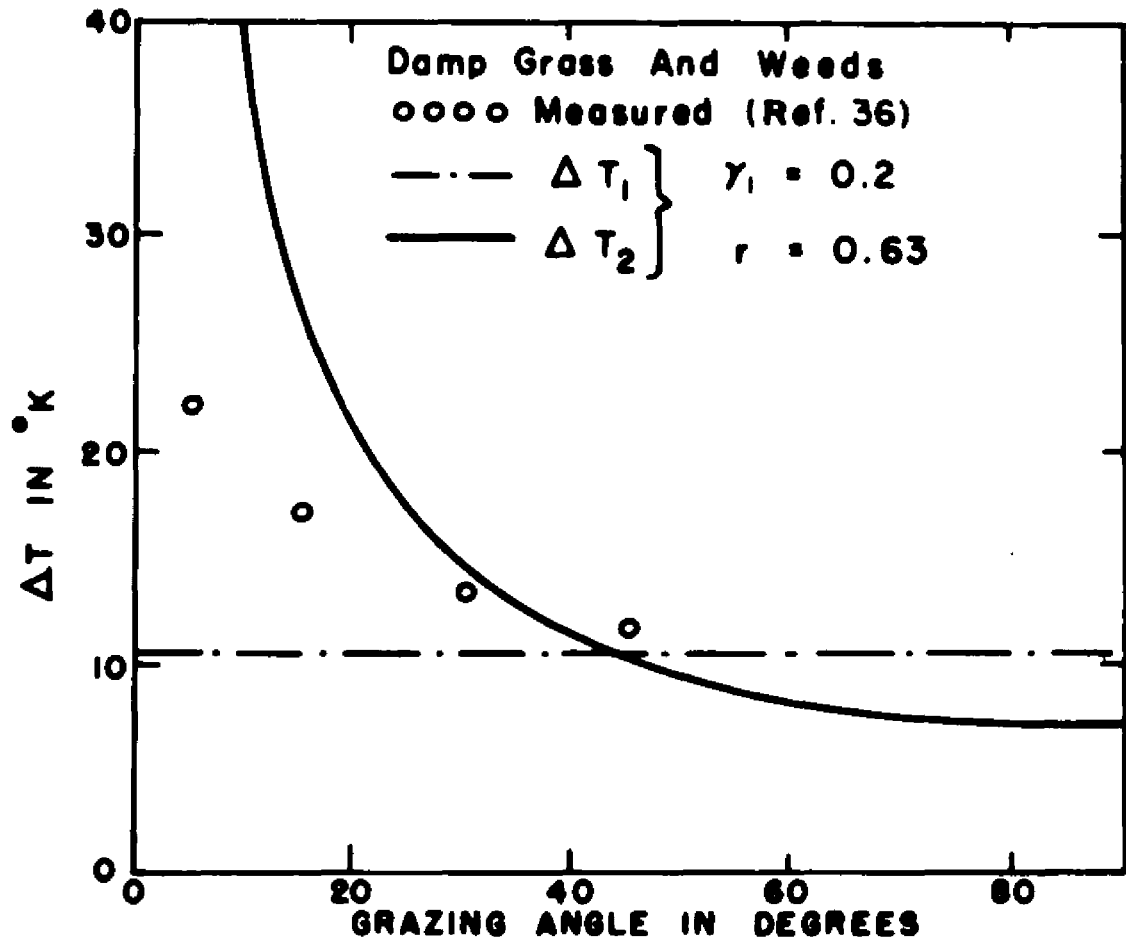


Fig. 37. Measured and calculated apparent temperature of vegetation covered surface.

## CHAPTER V CONCLUSIONS

It has been shown that the "bi-static" or "differential" scattering coefficients  $\gamma_{hh}$ , etc., may be used to determine a number of properties of the interaction of electromagnetic radiation with natural surfaces, in particular the back-scattering (radar cross-section) the albedo, and the absorption coefficient. By making use of the reciprocity relations satisfied by the scattering coefficients, it is then possible to derive Kirchhoff's radiation law in a form which accounts for the angular dependence and polarization dependence of the emission and absorption coefficients, and predicts them in terms of the  $\gamma$ 's. Thus it has been shown that once the  $\gamma$ 's are known, both the scattering and the radiometric properties of the surface may be found in terms of them. In applying the general results to actual terrain surfaces, two models have been suggested for two commonly encountered types of surface, for which the scattering coefficients have been calculated in detail. At the same time, it is shown that the models offer a convenient method for describing and classifying the surfaces in a rational and quantitative manner.

The first model, applicable to slightly rough, continuous surfaces, solves the scattering problem by perturbation methods, and gives results for the angular and polarization dependence of the back-scattering coefficients and (in idealized form) for the apparent

temperatures that are in good quantitative agreement with measurements on asphalt and concrete surfaces. One may thus infer that such surfaces are adequately represented by the model at microwave frequencies, and can be characterized by their mean square surface roughness, surface correlation function, and complex dielectric constant. The second model, proposed to represent surfaces covered with vegetation in the form of long thin lossy cylinders, solves the scattering problem in the single-scattering approximation and gives results in qualitative agreement with measurements of both the back-scattering coefficients and the apparent temperatures of actual vegetation covered surfaces. Insofar as this model is successful it implies that the surface may be described in terms of the number, size, distribution and complex dielectric constant of the individual cylinders.

## REFERENCES

1. Penndorf, R., "Luminous and Spectral Reflectance Properties as Well as Colours of Natural Objects," Geophys. Res. Paper, No. 44, AFCRC TR-56-203, February 1956.
2. Krinov, E., "Spectral Reflectance Properties of Natural Formations," (1947) Nat. Res. Council, Canada, Tech. Trans., T.T. 439, Ottawa, 1953.
3. Roll, H.U., Oberflächen-Wellen des Meeres, Handbüch der Physik, XLVIII, p. 671, Springer-Verlag, Berlin, 1957.
4. Clapp, R.E., "A Theoretical and Experimental Study of Radar Ground Return," Rad. Lab., Report No. 1024, April 10, 1946.
5. Katz, I. and Spetner, L.M., "A Functional Relationship Between Radar Cross-Section of Terrain and Depression Angle," Inst. Rad. Eng., P.G.A.P., AP-6, 310, 1958 (Abstract).
6. Katzin, M., "On the Mechanism of Radar Sea Clutter," Proc. I.R.E., 45, 44, 1957.
7. Ament, W.S., "Towards a Theory of Reflection by a Rough Surface," Proc. I.R.E., 41, 142, 1953.
8. Ament, W.S., "Forward and Back Scattering from Certain Rough Surfaces," Inst. Rad. Eng., P.G.A.P., AP-4, 369, 1956.

9. Davies, H., "The Reflection of Electromagnetic Waves from a Rough Surface," Proc. I.E.E., IV, 101, 209, 1954.
10. Carlson, I.F. and Heins, A.E., "The Reflection of Electromagnetic Waves by an Infinite Set of Plates," Quart. Appl. Math., 4, 313, 1946 and Quart. Appl. Math., 5, 82, 1947.
11. Lysanov, Y.P., "An Approximate Solution of the Problem of Scattering of Sound Waves from an Uneven Surface," Akust. Zh. 2 No. 2, p. 189, 1955 or Soviet Physics (Acoustics) Vol. 2 No. 2, 191, 1956.
12. Lysanov, Y.P., "Theory of Wave Scattering by Periodically Uneven Surfaces," Akust. Zh., 4, 3, 1958.
13. Hoffman, W.C., "Scattering of Electromagnetic Waves from a Random Surface," Quart. Appl. Math., 13, 291, 1955.
14. Twersky, V., "On the Scattering and Reflection of Electromagnetic Waves by Rough Surfaces," Inst. Rad. Eng., P.G. A.P., AP-5, 81, 1957.
15. Lysanov, Y.P., "Contribution to the Question of the Scattering of Electromagnetic Waves by Uneven Surfaces," Doklady A.N., USSR, 87, 719, 1952.
16. Rice, S.O., "Reflection of Electromagnetic Waves by Slightly Rough Surfaces," The Theory of Electromagnetic Waves (A Symposium) Interscience, 1951.



17. Taylor, R.C., "Terrain Return Measurements at X,  $K_u$ , and  $K_a$  Band," Convention Record, I.R.E. National Convention, 1959.
18. Rayleigh, Lord, The Theory of Sound, Vol. II, p. 89, Dover Publications, 1945.
19. Lax, M., "Multiple Scattering of Waves," Rev. Mod. Phys., 23, 287, 1951.
20. Silver, S. (Ed.), Microwave Antenna Theory and Design, McGraw-Hill, 1949.
21. Kerr, D.E. (Ed.), Propagation of Short Radio Waves, McGraw-Hill Book Co., Inc., New York, 1951.
22. Press, H. and Tukey, J.W., "Power Spectral Methods of Analysis and Their Application to Problems in Airplane Dynamics," Bell System Technical Monograph No. 2606 (N.A.T.O.-A.G.A.R.D. Flight Test Manual, Vol. IV, Part IVC, June 1956).
23. Walls, J.H., Houbolt, J.C. and Press, H., "Some Measurements and Power Spectra of Runway Roughness," NACA TN 3305, November 1954.
24. Hartshorn, L. and Saxton, J.A., Handbüch der Physik, Vol. XVI, p. 721, Springer Verlag, Berlin, 1958.
25. Deeg, E. and Huber, O., "Dielectric Behaviour of Various Clays in Relation to Their Water Content," Naturwiss, 42, No. 18, 507, 1955.

26. Windle, J.J. and Shaw, T.M., "Dielectric Properties of Wool-Water Systems at 3000 and 9300 Megacycles," *J. Chem. Phys.*, 22, 1952, 1954 and 25, 435, 1956.
27. Von Fragstein, G., "Über die Formulierung des Kirchhoffschen Gesetzen, und ihre Bedeutung für eine Zweckmassige Definition von Remissionzahlen," *Optik*, 12, 60, 1955.
28. Rutgers, G.A.W., Temperature Radiation of Solids, Handbüch der Physik, Vol. XXVI, 129, Springer Verlag, Berlin, 1958.
29. Pawsey, J.L. and Bracewell, R.N., Radio Astronomy, Oxford University Press, 1955.
30. Strum, P.D., "Considerations in High Sensitivity Microwave Radiometry," *Proc. I.R.E.*, 46, 43, 1958.
31. Planck, Max, Theory of Heat Radiation, (Trans. M. Masius), Blakiston, 1914.
32. Ahlgren, G.H., Forage Crops, McGraw-Hill Book Co., Inc., New York, 1949.
33. Goldstein, H., "Frequency Dependence of the Properties of Sea Echo," *Phys. Rev.*, 70, 938, 1946.
34. Sherwood, E.M. and Ginzton, E.L., "Reflection Coefficients of Irregular Terrain at 10 cm," *Proc. I.R.E.*, 43, 877, 1955.
35. Campbell, James P., "Back Scattering Characteristics of Land and Sea at X-Band," *Proc. National Conference on Airborne Electronics*, Dayton, Ohio, p. 107, 12, 13, 14 May 1958.

36. Straiton, A. W., Tolbert, C. W. and Britt, C. O., "Apparent Temperature Distributions of Some Terrestrial Materials and the Sun at 4.3 mm Wavelength," Jour. Appl. Phys., 29, 776, 1958.
37. Van de Hulst, H. C., Light Scattering by Small Particles, Wiley, 1957.
38. Maréchal, A., "La Diffusion Résiduelle des surfaces polies et des réseaux," Opt. Act. 5, 70, 1958.

APPENDIX I  
SCATTERING FROM A SLIGHTLY ROUGH SURFACE  
FOR VERTICAL POLARIZATION

In this appendix, the results of S. O. Rice<sup>16</sup> for horizontal polarization will be extended to the case of vertical polarization. The notation, except where otherwise specified, will be that of Rice's article. The equations are given the same number as the corresponding equations in the article.

If a vertically polarized incident wave is incident on a perfectly flat surface with angle of incidence  $\theta_0$  (for coordinate system, see Fig. 2), then the electric fields above and below the surface are

$$\begin{array}{l}
 (7-2) \quad \left. \begin{array}{l}
 E_x^+ = \gamma e^{-\sigma\alpha x} (e^{i\beta yz} - R e^{-i\beta yz}) \\
 E_y^+ = 0 \\
 E_z^+ = \alpha e^{-\sigma\alpha x} (e^{i\beta yz} + R e^{-i\beta yz})
 \end{array} \right\} z > 0 \\
 \\
 \left. \begin{array}{l}
 E_x^- = T \gamma' e^{-\tau\alpha' x + \tau\gamma' z} \\
 E_y^- = 0 \\
 E_z^- = \alpha' T e^{-\tau\alpha' x + \tau\gamma' z}
 \end{array} \right\} z < 0
 \end{array}$$

where, in this appendix only, T and R are the Fresnel coefficients

for vertical polarization

$$T = \frac{2\sigma/\tau}{1 + (\gamma'\sigma/\gamma\tau)} \quad R = \frac{1 - (\gamma'\sigma/\gamma\tau)}{1 + (\gamma'\sigma/\gamma\tau)} ;$$

and where

$$\begin{aligned} \gamma &= \cos \theta_0 & \alpha &= \sin \theta_0 \\ \gamma' &= (1 - \alpha'^2)^{\frac{1}{2}} & \alpha' &= (\sigma/\tau)\alpha . \end{aligned}$$

The other quantities are defined on p. 18. When the equation of the separating surface is  $z = f(x, y)$  the electric fields may be written

$$(7-3) \quad \begin{aligned} \mathbf{E}_x &= \begin{cases} \mathbf{E}_x^+ + \sum A_{mn} \mathbf{E}(m, n; z) & z > f \\ \mathbf{E}_x^- + \sum G_{mn} \mathbf{F}(m, n; z) & z < f \end{cases} \\ \mathbf{E}_y &= \begin{cases} \mathbf{E}_y^+ + \sum B_{mn} \mathbf{E}(m, n; z) & z > f \\ \mathbf{E}_y^- + \sum H_{mn} \mathbf{F}(m, n; z) & z < f \end{cases} \\ \mathbf{E}_z &= \begin{cases} \mathbf{E}_z^+ + \sum C_{mn} \mathbf{E}(m, n; z) & z > f \\ \mathbf{E}_z^- + \sum L_{mn} \mathbf{F}(m, n; z) & z < f . \end{cases} \end{aligned}$$

Here  $\mathbf{E}(m, n; z)$  (see Eq. (15)) represents a plane wave in the region above the surface and  $\mathbf{F}(m, n; z) = \exp[-ia(mx+ny) +icz]$  represents a plane wave in the region below the surface. The quantities  $a, m, n, c$ , etc. are given in Chapter II.

At the surface  $z = f$  the tangential components of the electric and magnetic fields must be continuous. That is, to  $O(f^3)$ , the four quantities

$$(7-6) \quad \begin{cases} E_x - N_x^2 E_x - N_x E_z \\ E_y - N_x N_y E_x - N_y E_z \end{cases}$$

$$(7-7) \quad \begin{cases} H_x - N_x N_y H_y - N_x H_z \\ H_y - N_y^2 H_y - N_y H_z \end{cases}$$

must be continuous. After considerable algebraic reduction, the four equations arising from these four conditions become, to  $O(f^2)$ :

$$(7-11) \quad \begin{aligned} & e^{-\sigma \alpha x} \left[ 1 - f_x^2 \right] \left[ \frac{2fU\alpha^2}{\tau} + f^2 \gamma' U \right] \\ & + f_x e^{-\sigma \alpha x} \left[ \alpha V + f^2 \alpha^3 \frac{\sigma}{\tau} U \right] \\ & + (1 - f_x^2) \left[ A_{mn} E(m, n, z) - G_{mn} F(m, n, z) \right] \\ & + f_x \left[ C_{mn} E(m, n, z) - I_{mn} F(m, n, z) \right] = 0 \\ & - f_x f_y e^{-\sigma \alpha x} \left[ \frac{2fU\alpha^2}{\tau} + f^2 \gamma' U \right] \\ & + f_y e^{-\sigma \alpha x} \left[ \alpha V + f^2 \alpha^3 \frac{\sigma}{\tau} U \right] \\ & - f_x f_y \left[ A_{mn} E(m, n, z) - G_{mn} F(m, n, z) \right] \\ & + \left[ B_{mn} E(m, n, z) - H_{mn} F(m, n, z) \right] \\ & + f_y \left[ C_{mn} E(m, n, z) - I_{mn} F(m, n, z) \right] = 0 \end{aligned}$$

$$\begin{aligned}
& -f_x f_y [e^{-\sigma \alpha x}] [2f \gamma' U + f^2 \tau U] \\
& + [ib B_{mn} - ian C_{mn}] E(m, n, z) + [ic H_{mn} + iam L_{mn}] F(m, n, z) \\
& - f_x f_y [iam C_{mn} - ib A_{mn}] E(m, n, z) + f_x f_y [ic G_{mn} + iam L_{mn}] \\
& \quad \cdot F(m, n, z) \\
& + f_x [ian A_{mn} - iam B_{mn}] E(m, n, z) - f_x [ian G_{mn} - iam H_{mn}] \\
& \quad \cdot F(m, n, z) = 0
\end{aligned}$$

$$\begin{aligned}
& (1 - f_y^2) e^{-\sigma \alpha x} [2f \gamma' U + f^2 \tau U] \\
& + (1 - f_y^2) [iam C_{mn} - ib A_{mn}] E(m, n, z) \\
& - (1 - f_y^2) (ic G_{mn} + iam L_{mn}) F(m, n, z) \\
& + f_x [ian A_{mn} - iam B_{mn}] E(m, n, z) - f_x [ian G_{mn} - iam H_{mn}] \\
& \quad \cdot F(m, n, z) = 0
\end{aligned}$$

where  $V = T(\tau/\sigma - \sigma/\tau)$  and  $U = T(\sigma^2 - \tau^2)/2$ . Expanding the coefficients as  $A'_{mn} + A^2_{mn} \dots$ , etc., utilizing (7-12) and replacing  $f \exp(-iavx)$  by its Fourier series expansion, the first order terms lead to the equations

$$\begin{aligned}
(7-13) \quad & A'_{mn} - G'_{mn} = \left[ -\frac{2U\alpha^2}{\tau} + ia\alpha V(m-\nu) \right] P(m-\nu, n) \\
& B'_{mn} - H'_{mn} = ia\alpha V P(m-\nu, n) \\
& bB'_{mn} - an C'_{mn} + c H'_{mn} + am L'_{mn} = 0 \\
& am C'_{mn} - b A'_{mn} - c G'_{mn} - am L'_{mn} = 2i U \gamma' P(m-\nu, n),
\end{aligned}$$

which, with the divergence relations

$$(7-17) \quad am A_{mn} + an B_{mn} + b C_{mn} = 0$$

$$am G_{mn} + an H_{mn} - c L_{mn} = 0,$$

provide the six equations for the six "unknowns"  $A_{mn} \dots L_{mn}$ . The solution is

$$(7-21) \quad A'_{mn} = \frac{2iUP(m-v, n)}{dD} \left[ -\gamma'(a^2 n^2 + bc) + \alpha b \frac{\tau}{\sigma} am \right]$$

$$B'_{mn} = \frac{2iUP(m-v, n)}{dD} \left[ a^2 nm \gamma' - \alpha \frac{\tau}{\sigma} ban \right]$$

$$C'_{mn} = \frac{2iUP(m-v, n)}{dD} \left[ amc \gamma' - \alpha \frac{\tau}{\sigma} (a^2 m^2 - a^2 n^2) \right]$$

$$G'_{mn} = A'_{mn} + \frac{2U\alpha}{\tau} (\alpha + i(am - av)/\sigma) P(m-v, n)$$

$$H'_{mn} = B'_{mn} + \frac{2ian\alpha U}{\sigma\tau} P(m-v, n)$$

$$L'_{mn} = \frac{am}{c} G'_{mn} + \frac{an}{c} H'_{mn} .$$



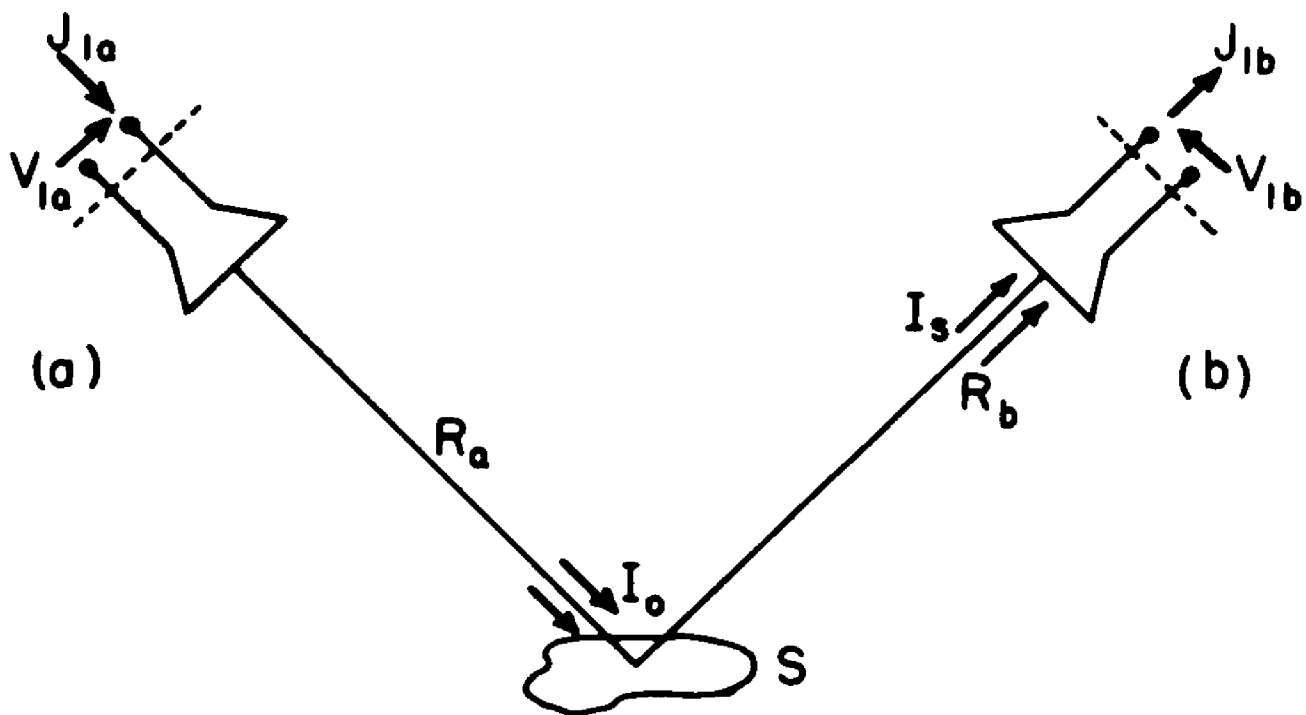
APPENDIX II  
THE RECIPROCITY RELATIONS SATISFIED  
BY THE SCATTERING COEFFICIENTS

Because of the decisive role played by the reciprocity relations, Eq. (5), in deriving Kirchhoff's law, it may be desirable to provide a more detailed proof than that given in Chapter II.

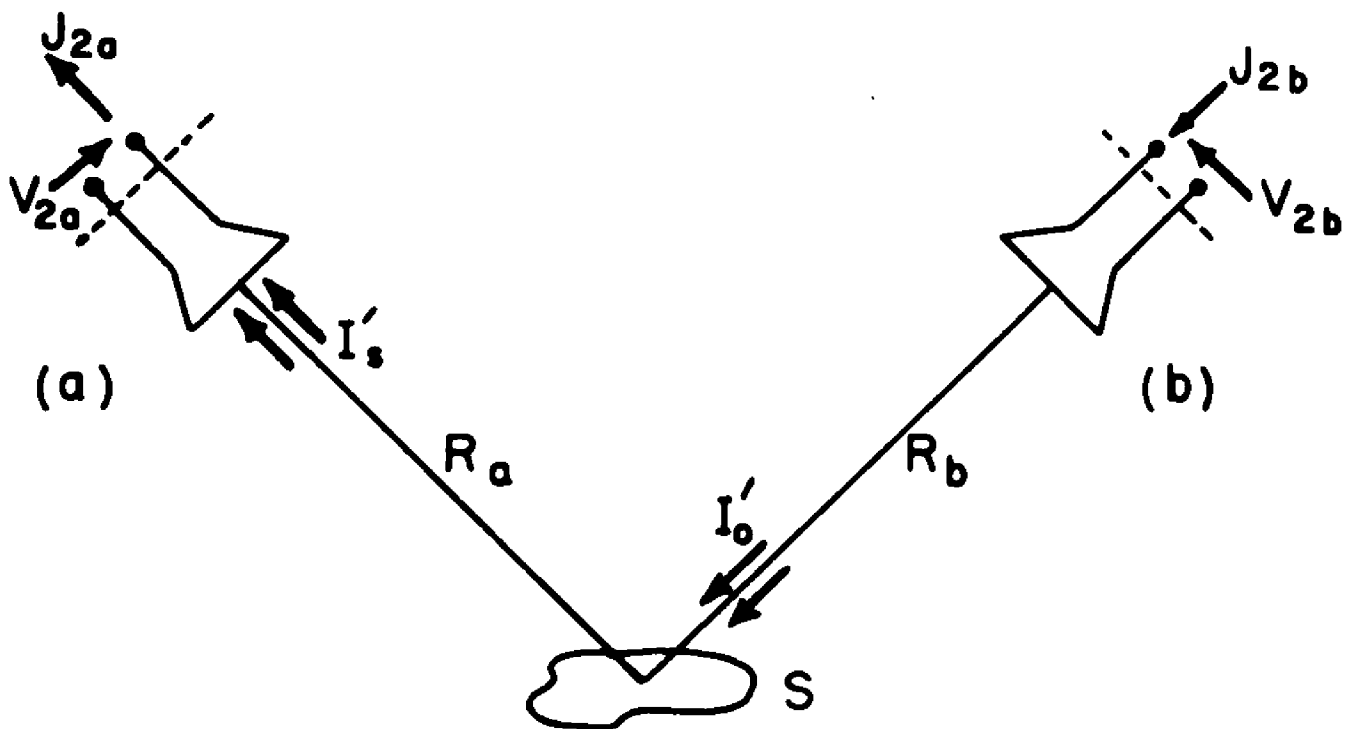
Consider two antennas, (a) and (b) (see Fig. 38) at distances  $R_a$  and  $R_b$ , respectively, from the surface element  $S$ . Suppose, for the purposes of this proof, that the antennas have the following characteristics:

- (i) The antennas are connected to transmission lines (real characteristic impedances  $Z_a$  and  $Z_b$ , respectively) matched in both directions, and supporting only one mode, so that a well defined current and voltage exist at some reference plane in each line.
- (ii) The antennas are of high gain, and are directed at  $S$ ; thus it is assumed that the only interaction between them is due to scattering from the surface  $S$ .

These two special assumptions are not necessary, but greatly simplify the following proof. For the general proof, the only requirement on the antennas is that there exist reference planes in the feed lines where the voltage and current can be defined.



Situation (1); (a) Is Transmitting



Situation (2); (b) Is Transmitting

Fig. 38. Geometry for reciprocity theorem.

Now consider the following two situations, illustrated in Fig. 38,

viz.:

- (1) A voltage  $V_{1a}$  is maintained across the reference terminals of (a) acting as a transmitter. The current at the reference terminals of (b) is measured, and found to be  $J_{1b}$ .
- (2) A voltage  $V_{2b}$  is maintained across the reference terminals of (b) acting as a transmitter. The current at the reference terminals of (a) is measured and found to be  $J_{2a}$ .

It is a consequence of the Lorentz reciprocity theorem (Reference 20, p. 59) that the above defined voltages and currents satisfy the equation

$$V_{1a}J_{2a} = V_{2b} J_{1b} .$$

This is referred to as the Rayleigh reciprocity theorem (Reference 20, p. 19). An extensive discussion of the relation between the two theorems, the proper definition of voltage and current in antenna feed lines, and the justification for representing two antennas coupled by a scatterer as a four terminal network is given in the second chapter of Reference 20. It is sufficient here to note that the scattering region  $S$  may be of any complexity, as long as the constitutive

parameters (dielectric constant, permeability, conductivity) are everywhere at most a real symmetric tensor. Thus gyrotropic media (ferrites, etc.) are not permitted. Also, because the superposition principle is used, the parameters  $\epsilon$ ,  $\mu$ ,  $g$  must be independent of field strength. Thus ferromagnetics, rectifying oxide coatings, etc. are not permitted.

The voltages and currents just defined must now be related to the power densities depicted in both Fig. 1 and Fig. 38. In situation (1), the total power radiated by (a) is just  $(2Z_a)^{-1} |V_{1a}|^2$ , so that the power density  $I_o$  at the surface S is found from

$$(2Z_a)^{-1} |V_{1a}|^2 = 4\pi R_a^2 I_o / g_a(\theta_o \phi_o)$$

where  $g_a(\theta_o \phi_o)$  is the gain of (a) in the direction of the surface. (see Reference 20, pp. 2 and 50). It is assumed that (a) is designed to produce radiation of the specific polarization of interest at S. On the other hand, the power received by (b) is  $(1/2) Z_b |J_{1b}|^2$ . Thus if  $I_s$  is the power density in the scattered wave at the aperture of (b), then

$$I_s A_b(\theta_s \phi_s) = (1/2) Z_b |J_{1b}|^2$$

where  $A_b(\theta_s \phi_s)$  is the receiving aperture of (b) in the scattering direction (see Reference 20, pp. 3 and 50). It is assumed that (b) is designed to receive the polarization of interest.

In situation (2), the power density  $I'_0$  at the surface S, and  $I'_s$  at the aperture of the receiver (a), may be found similarly,

$$(2Z_b)^{-1} |V_{2b}|^2 = 4\pi R_b^2 I'_0 / g_b(\theta_s \phi_s)$$

$$(1/2) Z_a |J_{2a}|^2 = A_a(\theta_0 \phi_0) I'_s .$$

Now it is also a consequence of the Lorentz reciprocity theorem (applied to isolated antennas, without the scatterer) that the gain of an antenna in a given direction for radiation of a specific polarization is related to its receiving aperture for radiation from the same direction with the same polarization by the following equation,

$$\frac{g_a(\theta_0 \phi_0)}{A_a(\theta_0 \phi_0)} = \frac{g_b(\theta_s \phi_s)}{A_b(\theta_s \phi_s)} = \frac{4\pi}{\lambda^2} .$$

This is known as the antenna pattern reciprocity theorem, and is proved on p. 51 of Reference 20.

When the relations between voltage, current and power density are substituted into the Rayleigh reciprocity theorem, it is found that

$$R_a^2 \frac{I_0}{I_s} \frac{A_a(\theta_0 \phi_0)}{g_a(\theta_0 \phi_0)} = R_b^2 \frac{I'_0}{I'_s} \frac{A_b(\theta_s \phi_s)}{g_b(\theta_s \phi_s)} .$$

Thus using the antenna pattern reciprocity theorem, there results

$$R_a^2 (I_0/I_s) = R_b^2 (I'_0/I'_s) .$$

If it is assumed that  $R_a = R_b$ , and that (a) and (b) are identical (except for polarization), so that  $I_o = I_o'$ , then  $I_s = I_s'$ . This is just the relation required on p. 9 to prove the reciprocity relations for the scattering coefficients.

## AUTOBIOGRAPHY

I, William Heller Peake, was born on the tenth of June, 1926, in Binghamton, New York. I received the Bachelor of Science degree from the Massachusetts Institute of Technology in 1946, and the Master of Arts degree from Columbia University in 1951. Since 1952 I have been employed at the Antenna Laboratory in the Department of Electrical Engineering of The Ohio State University.